VNIVERSITAT DE VALÈNCIA

Doctorado en Biomedicina y Biotecnología
Departamento de Bioquímica i Biologia Molecular

BÚSQUEDA Y CARACTERIZACIÓN DE SUSTRATOS FISIOLÓGICOS DE MALINA, LA E3-UBIQUITIN LIGASA IMPLICADA EN LA ENFERMEDAD DE LAFORA

Doctoranda:
Lorena Kumarasinghe

Directores:
Pascual Sanz Bigorra
Mª Adelaida García Gimeno

Mayo, 2023

Doctorado en Biomedicina y Biotecnología
Departamento de Bioquímica i Biologia Molecular

BÚSQUEDA Y CARACTERIZACIÓN DE SUSTRATOS FISIOLÓGICOS DE MALINA, LA E3-UBIQUITIN LIGASA IMPLICADA EN LA ENFERMEDAD DE LAFORA

Memoria presentada por
Lorena Kumarasinghe
Para optar al grado de Doctora

Dirigida por:
Pascual Sanz Bigorra
Mª Adelaida García Gimeno

Valencia, 31 Mayo, 2023

GOBIERNO DE ESPAÑA MINISTERIO DE CIENCIA E INNOVACIÓN

CSIC
CONSEJO SUPERIOR DE INVESTIGACIONES CIENTÍFICAS
INSTITUTO DE BIOMEDICINA DE VALENCIA (IBV)

VNIVERSITAT DE VALÈNCIA

D. Pascual Sanz Bigorra, Doctor en Farmacia, Profesor de Investigación del Consejo Superior de Investigaciones Científicas (CSIC), en el Instituto de Biomedicina de Valencia, y miembro del Centro de Investigación Biomédica en Red de Enfermedades Raras (CIBERER), Instituto de Salud Carlos III.

Dña. Mª Adelaida García Gimeno, Doctora en Farmacia, Profesora Titular de la Universitat Politècnica de València.

CERTIFICAN

Que Dña. Lorena Kumarasinghe, con un "Master of Science on Experimental Therapeutics" por la Universidad de Oxford (Reino Unido) y con la Licenciatura en "Biotecnología de la Salud" por la Universidad Federico II de Nápoles (Italia), con NIE Y7689688C, ha realizado, bajo nuestra dirección, el trabajo de tesis doctoral que lleva por título "**Búsqueda y caracterización de sustratos fisiológicos de malina, la E3-ubiquitin ligasa implicada en la enfermedad de Lafora"** en el laboratorio de Señalización por Nutrientes del Instituto de Biomedicina de Valencia, CSIC.

Que entendemos que el trabajo reúne los requisitos para ser susceptible de defensa ante el tribunal apropiado, por reflejar adecuadamente el estado del conocimiento y discutir apropiadamente el contenido y las implicaciones del trabajo realizado y porque las conclusiones recogen un avance suficiente en el campo objeto de estudio como para hacer al candidato merecedor del doctorado. Además, el trabajo ha generado ya tres publicaciones en revistas internacionales del primer cuartil, siendo la candidata primera autora en dos de ellas.

Y para que conste a los efectos oportunos, los directores y el tutor de la Tesis firman el presente certificado en Valencia a 22 de Mayo de 2023

SANZ BIGORRA PASCUAL FELIPE - DNI 19835103H

Firmado digitalmente por SANZ BIGORRA PASCUAL FELIPE - DNI 19835103H
Nombre de reconocimiento (DN): c=ES, o=CONSEJO SUPERIOR DE INVESTIGACIONES CIENTIFICAS, ou=CERTIFICADO ELECTRONICO DE EMPLEADO PUBLICO, ou=IBV, ou=19835103, serialNumber=IDCES-19835103H, sn=SANZ BIGORRA, givenName=PASCUAL FELIPE, cn=SANZ BIGORRA PASCUAL FELIPE - DNI 19835103H
Fecha: 2023.05.19 17:59:54 +02'00'

Fdo. Pascual Sanz Bigorra
sanz@ibv.csic.es

Firmado por JOSE ENRIQUE PEREZ ORTIN - NIF:***7571** el día 25/05/2023 con un certificado emitido por ACCVCA-120

Fdo. José Enrique Perez Ortín
Catedrático Universitat València
Dept. Bioquímica i Biologia Molecular
jose.e.perez@uv.es

GARCIA GIMENO MARIA ADELAIDA - 24330557F

Firmado digitalmente por GARCIA GIMENO MARIA ADELAIDA - 24330557F
Nombre de reconocimiento (DN): c=ES, serialNumber=IDCES-24330557F, givenName=MARIA ADELAIDA, sn=GARCIA GIMENO, cn=GARCIA GIMENO MARIA ADELAIDA - 24330557F
Fecha: 2023.05.19 18:05:20 +02'00'

Fdo. Mª Adelaida García Gimeno
magar27m@btc.upv.es

Este proyecto ha recibido financiación del Programa de Investigación e Innovación Horizonte 2020 de la Unión Europea bajo el acuerdo de subvención **Marie Skłodowska-Curie** No 813599, convocatoria H2020-MSCA-ITN-2018 - Innovative Training Networks 2018 del **TRIM-NET** A training network in drug discovery targeting TRIM ubiquitin ligases.

También ha recibido financiación del proyecto PID2020-112972RB-I00 titulado "Estudio de la relación entre neuroinflamación y epilepsia: el caso de le enfermedad de Lafora", del Programa RETOS del Ministerio de Ciencia e Innovación.

Las titulaciones de Dña. Lorena Kumarasinghe han recibido la correspondiente homologación por parte del Ministerio de Universidades con fecha 12 de Mayo de 2023.

Con el fin de cumplir con la normativa para tesis redactada en lenguas diferentes a las oficiales de la Universidad de Valencia, se ha incluido al final de la memoria un Anexo 2 con un resumen amplio redactado en castellano en el que figuran los objetivos, la metodología y las conclusiones de la tesis.

En el Anexo 3 se indican las publicaciones asociadas a esta Tesis.

To my Family

Acknowledgements

I would like to sincerely thank Professor Pascual Sanz for having me as a PhD student and giving me the opportunity to carry out this work in his research group. It was an experience of great scientific growth for me. He supported me in every phase of the project with great seriousness and critical sense and I will always be grateful for this. I thank him for teaching me to be objective with my work, when necessary, without ever turning off my enthusiasm. In the same way I would like to thank Professor Mª Adelaida García Gimeno for teaching me to consider multiple points of view and for teaching me to look at things in the bigger picture. Thank you for teaching me how important it is not to take anything for granted but always try to delve into the details. It will be something I will always treasure in the future. I want to thank both of you for teaching me so much and always supporting me. You will remain great mentors for me, and I hope to make you scientifically proud one day.

Next, I would like to thank my tutor Professor Jose Enrique Perez Ortin for always being there when it was necessary and for clarifying any doubts. I am grateful for his care in monitoring and following-up my doctoral project. I thank him for being so helpful and patient over time.

A heartfelt thanks goes to the evaluators of my doctoral thesis, for the care with which they examined the work.

My sincere thanks go especially to the collaborators Dr Ugo Mayor and Dr Juamna Ramirez thanks to whom we lit the fuse to undertake this project in a spirit of teamwork and great scientific support. It was very exciting and rewarding to work together and this too marked a precious moment of growth for me as a scientist. I would also like to thank Dr Jose Luis Zugaza to host me at his laboratory in Bilbao. The stay marked an important moment in the development of the project, and I also thank Dr Francisco Llavero for his precious teachings.

I am also immensely grateful to have had the opportunity to be part of the TRIM Network funded by the European Union's Horizon 2020 Research and Innovation Program under the Marie Skłodowska-Curie grant. It was an immense opportunity to be part of the network and to have had so many privileges to be a PhD student supported by such a program. I got to meet many people and build relationships that go beyond science with the other PhD students in the network.

I would like to thank the research institute “Instituto de Biomedicina de Valencia” that hosted me during my PhD. I have met people who are always available and always ready to help in times of need. I have always breathed in a

very scientific climate with broad horizons. It has been an enormous growth to listen to and draw from scientific worlds far from one's own. I have always found a way to learn a lot thanks to the scientific sharing that I have always found in many people. It was an environment in which I felt at ease and in which I always went with great happiness.

I would like to sincerely thank the present and past members of the group: Angela, Belen, Dani, Eva, Laura, Mireia, Rosa and Teresa. I couldn't ask for a better group to embark on the arduous PhD journey. I want to thank you from the bottom of my heart for making me feel good every single day. Your smiles have always comforted me and made me feel so much human warmth. I also thank you for all the teachings, advice and help that have facilitated my doctoral journey. Thank you for teaching me to enjoy the moments with the celebrations, it's something I will try to keep in mind and do in the future as well. I will always carry you in my heart. Thanks for everything! I feel lucky to have been with you.

Finally, I would like to thank all my family for being there in the most difficult moments and for rejoicing in the happy moments. I thank them for all the sacrifices they have made for me since I was born. I hope I can always make you proud. I thank Antonio for all the love and patience he has shown all these years. Thank you for always supporting me to keep going and never give up.

Table of Content

Abbreviations

ACID	Acid-rich region
AD	Alzheimer's disease
ALS	Amyotrophic Lateral Sclerosis
ARI-1	Ariadne-1
ARF	ADP-ribosylation factor family domain
BAG	Bcl2-associated athano-gene
BROMO	Bromodomain
CBM	Carbohydrate-binding module
CHIP	Carboxyl terminus of Hsc70-interacting protein
CHX	Cycloheximide
CR	Charger linker domain
CTD	C-Terminal Domain
dbcAMP	dibutyryl-cAMP
DH	Dbl homology
DMEM	Dulbecco's modified Eagle medium
DSP	Dual specificity phosphatase
DTT	Dithiothreitol
DUB	Deubiquitinating enzyme
EPM2A	Gene A of Progressive Myoclonus Epilepsy
EPM2B	Gene B of Progressive Myoclonus Epilepsy
FBS	Fetal bovine serum
FNIII	Fibronectin type III repeat
FTD	Frontotemporal dementia
GEF	Guanine-nucleotide exchange factor
GLUT	Glucose transporter
GPCR	G-protein-coupled receptors
GST	Glutathione-S-Transferase
GST-RBD-PAK1	GST fusion protein containing the Rac1 binding domain of PAK1
HCC	Hepatocellular carcinoma
HCD	High-energy collision dissociation
HD	Huntington disease
HEK293	Human embryonic kidney
HIP	Hsp70 interacting protein

HOP/STIP1	Hsp90-Hsp70 organizing protein
HRP	Horseradish peroxidase
HSE	Heat shock elements
HSF	Heat shock factor
HSP90AA1	Heat shock protein 90 alpha family class A member 1
HSP90AB1	Heat shock protein 90 alpha family class B member 1
HSPs	Heat shock protein
iDHPH	isolated DH/PH
IP4P	Inositol polyphosphate 4-phosphatase
LBs	Lafora bodies
LD	Lafora disease
LFQ	Label-free quantification
MATH	Meprin and TRAF-homology domain
MD	Middle Domain
MS	Mass Spectrometer
NHLRC1	NHL Repeat Containing E3 Ubiquitin Protein Ligase 1
NSF	N-ethylmaleimide sensitive factor
NTD	N-Terminal Domain
OXPHOS	Mitochondrial Oxidative Phosphorylation System
PAGE	Polyacrylamide gel electrophoresis
PBS	Phosphate buffered saline
PD	Parkinson's disease
PH	Pleckstrin homology
PIP3	Phosphatidyl inositol-3, 4, 5 triphosphate
PKA	cAMP-dependent kinase
PME	Progressive myoclonus Epilepsy
PMSF	Phenylmethylsulfonyl fluoride
PP1	Protein phosphatase 1
PRDM8	PR domain zinc finger protein 8
PREX1	Phosphatidylinositol 3,4,5-trisphosphate-dependent Rac exchanger 1 protein
PTM	Post-translational modifications
RBD	Rac Binding Domain
SDS	Sodium Dodecyl Sulfate
TRIM	Tripartite motif family

SUMMARY

Summary

Lafora disease (LD) is a rare genetic disease that mainly affects adolescents and belongs to the group of diseases known as Progressive Myoclonus Epilepsies (PMEs). It is a fatal form of progressive myoclonus epilepsy and has an incidence of less than 4 cases in a million people worldwide. LD is caused by the accumulation of aberrant glycogen-like inclusions known as Lafora bodies (LBs), which are present in several tissues but are predominantly found in the brain. These LBs are insoluble and their aggregation leads to cellular toxicity, generating several progressive neurological symptoms, including difficult-to-control seizures, myoclonus, ataxia, dementia, and other symptoms. There is currently no definitive cure for LD, and treatment is mainly symptomatic and supportive, focusing on controlling seizures and managing other symptoms as they arise. The disease is caused by mutations that fall onto genes that codify for two different proteins: Laforin and Malin. These proteins have different functions but work in complex with each other.

My Ph.D. studies focused especially on Malin, known to be an E3 ubiquitin ligase which plays a major role in a process called ubiquitination. Therefore, Malin's activity makes LD a disease connected to the ubiquitin system. Several substrates of Malin have been identified to date, including those involved in the accumulation of polyglucosans, impairment in the degradation processes at the level of the proteasome and autophagy, alteration of glutamatergic transmission and mitochondrial dysfunction. However, many molecular mechanisms leading to these conditions need further elucidation. The hunt for novel substrates could help to identify previously unidentified dysfunctions of Lafora disease and to gain a better understanding of the aforementioned pathophysiological alterations. A proteomic analysis using the bioUb strategy identified 88 differentially ubiquitinated potential candidates involved in protein folding, heat shock response, and regulation of

mitochondrial function. Two proteins, P-Rex1 and Hsp90α, were chosen for further study due to their high ubiquitination rate and/or unique peptide number in the proteomic analysis. In this thesis, evidence will be reported in demonstrating how the first substrate is related to LD. We have validated the Malin-dependent ubiquitination of P-Rex1 and have focused on the effect of Malin on the function of P-Rex1 as a guanine-nucleotide exchange factor (GEF) in activating Rac1 GTPase and in increasing glucose uptake. The analysis conducted upon this substrate sets the genesis of the delineation of a molecular pathway that leads to altered glucose uptake, which could be one of the origins of the accumulation of the polyglucosans present in the disease.

Experiments conducted for Hsp90α have validated it as a substrate of Malin, not only when it is overexpressed but also at endogenous level and, further on, we have hypothesized how it could possibly be related to the disease.

RESUMEN

Resumen

La enfermedad de Lafora es una rara enfermedad genética que afecta principalmente a los adolescentes y pertenece al grupo de enfermedades conocidas como Epilepsias Mioclónicas Progresivas (PME). Es una forma fatal de epilepsia mioclónica progresiva y tiene una incidencia de menos de 4 casos en un millón de personas en todo el mundo. La LD es causada por la acumulación de inclusiones aberrantes similares al glucógeno conocidas como cuerpos de Lafora (LB), que están presentes en varios tejidos pero se encuentran predominantemente en el cerebro. Estos LB son insolubles y su agregación conduce a la toxicidad celular, generando varios síntomas neurológicos progresivos, que incluyen convulsiones de difícil control, mioclonías, ataxia, demencia y otros síntomas. Actualmente no existe una cura definitiva para la LD, y el tratamiento es principalmente sintomático y de apoyo, centrándose en controlar las convulsiones y manejar otros síntomas a medida que surgen. La enfermedad es causada por mutaciones en genes que codifican para dos proteínas diferentes: Laforin y Malin. Estas proteínas tienen diferentes funciones pero trabajan en forma compleja entre sí.

Durante el doctorado, los estudios se centraron especialmente en Malina, conocida por ser una ubiquitina ligasa E3 que desempeña un papel importante en un proceso llamado ubiquitinación. Por lo tanto, la actividad de Malina convierte la enfermedad de Lafora en una enfermedad relacionada con el sistema de ubiquitinación. Se han identificado varios sustratos de Malina hasta ahora, incluidos los implicados en la acumulación de poliglucosanos, deterioro en los procesos de degradación a nivel del proteasoma y autofagia, alteración de la transmisión glutamatérgica y disfunción mitocondrial. Sin embargo, muchos mecanismos moleculares que conducen a estas condiciones necesitan mayor aclaración. La búsqueda de nuevos sustratos podría ayudar a identificar disfunciones de la enfermedad de Lafora no identificadas previamente y a una mayor comprensión de las alteraciones fisiopatológicas descritas anteriormente.

Un análisis proteómico utilizando la estrategia bioUb identificó 88 candidatos potenciales diferencialmente ubiquitinados involucrados en el plegamiento de proteínas, la respuesta al choque térmico y la regulación de la función mitocondrial. Se eligieron dos proteínas, P-Rex1 y Hsp90α, para su posterior estudio debido a su alta tasa de ubiquitinación y número de péptido único en el análisis proteómico. En esta tesis, se reportarán evidencias para demostrar cómo el primer sustrato se relaciona con la enfermedad de Lafora. Se ha validado la ubiquitinación de P-Rex1 dependiente de Malina y hemos estudiado como esta modificación altera la actividad de P-Rex1 como factor intercambiador de nucleótidos de guanina (GEF) sobre la GTPasa Rac1 y en la toma de glucosa. El análisis realizado sobre este sustrato establece la génesis de una vía molecular que conduce a la alteración de la captación de glucosa, lo que podría ser uno de los orígenes de la acumulación de los poliglucosanos presentes en la enfermedad.

Los experimentos realizados para Hsp90α la han validado como sustrato de Malina y, hemos hipotetizado cómo podría estar relacionada con la enfermedad.

RESUM

Resum

La malaltia de Lafora és una malaltia genètica minoritària que afecta principalment els adolescents i pertany al grup de malalties conegudes com a Epilèpsies Mioclòniques Progressives (EMP). És una forma fatal d'epilèpsia mioclònica progressiva i té una incidència de menys de 4 casos per cada milió de persones a tot el món. La malaltia de Lafora es causa per l'acumulació d'inclusions aberrants similars al glucogen conegudes com a cossos de Lafora, presents en diversos teixits, però predominantment al cervell. Aquests són insolubles i la seua agregació condueix a la toxicitat cel·lular, generant diversos símptomes neurològics progressius, que inclouen convulsions de difícil control, mioclònies, atàxia, demència i altres símptomes. Actualment no existeix una cura definitiva per a la malaltia de Lafora, i el tractament és principalment simptomàtic i de suport, centrant-se en controlar les convulsions i altres símptomes a mesura que sorgeixen. La malaltia és causada per mutacions en gens que codifiquen dos proteïnes diferents: Laforina i Malina. Aquestes proteïnes tenen diferents funcions però treballen de forma complexa entre si.

Durant el meu doctorat, els estudis es van centrar especialment en Malina, coneguda per ser una ubiquitina ligasa E3 que exerceix un paper important en un procés anomenat ubiquitinació. Per tant, l'activitat de Malina converteix la malaltia de Lafora en una malaltia relacionada amb el sistema d'ubiquitinació. Fins al moment s'han identificat diversos substrats de Malina, estant implicats en l'acumulació de poliglucosans, la deterioració en els processos de degradació a nivell del proteasoma i autofàgia, l'alteració de la transmissió glutamatèrgica i la disfunció mitocondrial. No obstant això, molts mecanismes moleculars que condueixen a aquestes condicions necessiten un major coneixement. La cerca de nous substrats podria ajudar a identificar disfuncions de malalties no identificades prèviament i una millor comprensió de les alteracions fisiopatològiques anteriors. Un anàlisi proteòmic utilitzant l'estratègia bioUb va identificar 88 candidats potencials diferencialment

ubiquitinats involucrats en el plegament de proteïnes, la resposta al xoc tèrmic i la regulació de la funció mitocondrial. Es van triar dos proteïnes, P-Rex1 i Hsp90α, per al seu posterior estudi degut a la seua alta taxa d'ubiquitinació i el número de pèptid únic en l'anàlisi proteòmic. En aquesta tesi, es reportaran evidències que demostren com el primer substrat es relaciona amb la malaltia de Lafora. S'ha validat la ubiquitinación de P-Rex1 dependent de Malina i hem estudiat com aquesta modificació altera l'activitat de P-Rex1 com a factor intercanviador de nucleòtids de guanina (GEF) sobre la GTPasa Rac1 i en la captasió de glucosa. L'anàlisi realitzat sobre aquest substrat estableix la gènesi d'una via molecular que condueix a l'alteració de la captació de glucosa, la qual cosa podria ser un dels orígens de l'acumulació dels poliglucosans presents en la malaltia.

Els experiments realitzats per a Hsp90α en el següent treball validen aquesta proteïna com a substrat de Malina. En un futur, intentarem descriure com podria estar relacionada amb la malaltia

INTRODUCTION

Introduction

Lafora Disease

Background and Clinical features

Lafora disease (LD, OMIM#254780) is a rare genetic disease whose incidence is estimated to be less than 4 cases in a million people worldwide (Turnbull, Tiberia et al. 2016, Orsini, Valetto et al. 2019, Pondrelli, Muccioli et al. 2021). It is a fatal form of progressive myoclonus epilepsy and belongs to the group of diseases known as Progressive Myoclonus Epilepsies (PMEs) (Kalviainen 2015). It mainly affects adolescents but can occur at any age (Monaghan and Delanty 2010). The disease is more common in people of Mediterranean and Indian ancestry, but it has been reported in people from a variety of ethnic backgrounds especially in places where there is a high rate of consanguinity (Genton 2007, Turnbull, Tiberia et al. 2016).

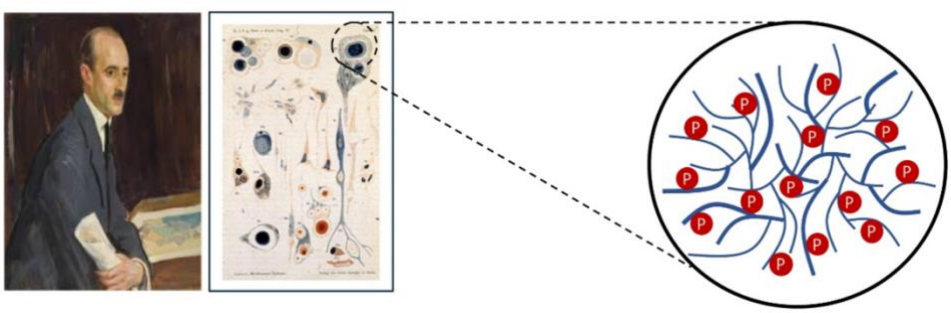

Fig. 1: In 1911, the Spanish neurologist Dr. Gonzalo Rodriguez Lafora described polyglucosan bodies in the perikaryon of neurons in the cerebral cortex, thalamus, globus pallidus, and substantia nigra of affected patients. Lafora bodies are the result of the aggregation of long, unbranched, hyperphosphorylated and insoluble forms of glycogen. The left panel shows a painting of Dr. Lafora displayed at Prado Museum (Díez, José Luis (dir.), *Pintura del Siglo XIX en el Museo del Prado: catálogo general*, Museo Nacional del Prado, Madrid, 2015, pp. 198. Madrid). The middle panel shows a copy of the original paintings of neurons from affected patients. The right panel shows a cartoon of the hyperphosphorylated aberrant glycogen present in Lafora bodies.

The origin of the name of the disease is given by its discoverer, the neurologist Dr Gonzalo Rodriguez Lafora who, in 1911, described for the first time the presence of accumulations of "amyloid bodies" (Fig. 1) in neural tissues and other tissue biopsies from a patient who died of an epileptic condition (Lafora and Glueck 1911). These bodies assumed the name of Lafora bodies (LBs). The characteristic Lafora bodies, found in Lafora patients, are present along several tissues but are predominant especially in the brain (Sakai, Austin et al. 1970). These LBs are glycogen-like inclusions also known as polyglucosans which constitute the hallmark of the disease. This abnormal form of glycogen that accumulates is insoluble and its aggregation leads to cellular toxicity generating several progressive neurological symptoms. These characteristic symptoms of LD can vary in severity and onset from person to person and include epilepsy, usually difficult to control with medication and can be either generalized or focal; myoclonus with sudden and involuntary muscle jerks that can affect different parts of the body; ataxia that can affect walking, balance, and fine motor skills; and dementia due to progressive damage of the brain caused by Lafora bodies and subsequently leading to a decline in cognitive function, memory loss, and behavioral changes. Beyond these, there are other symptoms such as visual hallucinations, macular degeneration, speech difficulties, dysphagia, muscle weakness, tremors, depression and anxiety, and liver or cardiac failure that may occur. From the onset of the first symptoms patients have a median life expectancy of 11 years (Turnbull, Girard et al. 2012, Turnbull, Tiberia et al. 2016, Pondrelli, Muccioli et al. 2021). Because of its rarity and the variability in onset and severity, Lafora disease can be challenging to diagnose, and there may be cases that go undiagnosed or misdiagnosed.

Therapy management

There is currently no definitive cure for Lafora disease, and treatment is mainly symptomatic and supportive, focusing on controlling seizures and

managing other symptoms as they arise. However, after some time, patients develop resistance towards the use of anti-seizure medications (Garcia-Gimeno, Knecht et al. 2018). The role of glycogen synthase, the enzyme involved in the synthesis of glycogen, has been the subject of numerous studies with the goal of developing a new therapy. In Lafora disease models, numerous studies have demonstrated how a decrease in glycogen synthesis can reduce the production of polyglucosans (Turnbull, DePaoli-Roach et al. 2011, Pederson, Turnbull et al. 2013, Turnbull, Epp et al. 2014). The observed outcomes compelled the researchers to create novel approaches, such as the use of antisense oligonucleotides, that can reduce glycogen synthase expression (Ahonen, Nitschke et al. 2021), or the development of novel compounds that can directly digest and, therefore, reduce Lafora bodies (Brewer and Gentry 2019).

Genes

Lafora disease happens when mutations occur along two different genes, *EPM2A* (6q24) or *EPM2B/NHLRC1* (6p22.3). In general, a mutation on the *EPM2A* gene, which codes for the glucan phosphatase Laforin, causes LD in approximately 44% of the cases (Minassian, Lee et al. 1998, Serratosa, Gomez-Garre et al. 1999, Romá-Mateo, Moreno et al. 2011, Pondrelli, Muccioli et al. 2021), while a mutation on the *EPM2B/NHLRC1* gene, which codes for the RING-type E3-ubiquitin ligase Malin, causes LD in approximately 56% of cases (Chan, Young et al. 2003, Turnbull, Tiberia et al. 2016, Pondrelli, Muccioli et al. 2021). Because the two proteins, Laforin and Malin, function as a coordinated complex, mutations on either of the two genes disrupt the balanced system. This explains why individuals with mutations in either *EPM2A* or *EPM2B/NHLRC1* exhibit similar pathological phenotypes and why mutations affecting the interaction between the two proteins can result in disease (Gentry, Worby et al. 2005, Solaz-Fuster, Gimeno-Alcañiz et al. 2008, Romá-Mateo, Moreno et al. 2011, Rubio-Villena, Garcia-Gimeno et al. 2013,

Garcia-Gimeno, Knecht et al. 2018). A database is available that collects all genetic modifications: http://projects.tcag.ca/lafora/.

A new type of early-onset LD has been tentatively linked to a third gene, *PRDM8* (PR domain zinc finger protein 8) (4q21.21), by researchers (Turnbull, Girard et al. 2012). However, no further research has confirmed its role to date.

Laforin

Despite having higher levels of expression in the brain, skeletal muscle, heart, and liver, Laforin is ubiquitously expressed in all tissues (Serratosa, Gomez-Garre et al. 1999). The cerebellum, hippocampus, frontal cortex, and olfactory bulb of the brain exhibit the highest levels of Laforin expression (Ganesh, Agarwala et al. 2001, Dubey and Ganesh 2008). Laforin is a 331 amino acid bi-modular protein (Fig. 2) with an amino-terminal carbohydrate binding module (CBM, residues 1–124), that allows the protein to bind glycogen and LBs, and a carboxy-terminal dual specificity phosphatase domain (DSP, residues 157–326), which mediates glycogen's dephosphorylation. There is also a minor isoform of 317 amino acids that lacks phosphatase activity and localizes to the cytoplasm and nucleus (Dubey and Ganesh 2008, Gentry, Romá-Mateo et al. 2013).

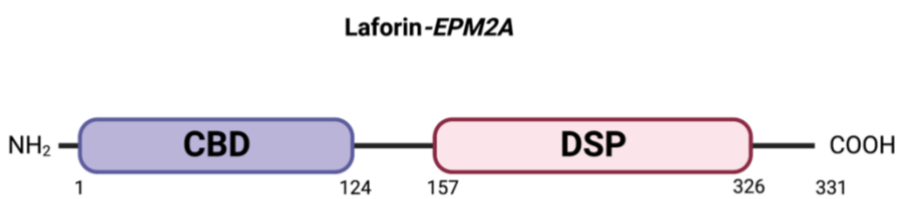

Fig. 2: Laforin. Laforin glucan phosphatase is characterized by the presence of two domains: an amino-terminal carbohydrate-binding module (CBM) followed by a dual specificity phosphatase (DSP) domain. Created with BioRender.com

Laforin plays a critical role in regulating glycogen metabolism in the body, particularly in the process of glycogen synthesis and degradation. Laforin helps removing excess phosphate groups from glycogen to favor its degradation by glycogen degradative enzymes. Without a proper dephosphorylation of the sugar, glycogen can accumulate as insoluble aggregates leading to Lafora disease. Studies conducted with the objective of analyzing LD patient mutations have described how these can disrupt the functionality of the protein (Raththagala, Brewer et al. 2015). In mice lacking endogenous Laforin but overexpressing the C266S mutated form of the protein, affecting the catalytic phosphatase domain, leads to the inability of Laforin in hydrolyzing phosphate from glycogen, confirming that the glucan phosphatase activity of the protein is an essential requirement in the dephosphorylation of the sugar (Tagliabracci, Turnbull et al. 2007, Raththagala, Brewer et al. 2015, Romá-Mateo, Raththagala et al. 2016).

Malin

The brain, cerebellum, spinal cord, medulla, heart, liver, skeletal muscle, and pancreas all express Malin. No reports of the endogenous form of Malin being localized have been published yet. Since there isn't a good antibody to detect endogenous Malin at the subcellular level, several researchers have only been able to detect Malin at the cytoplasmic, nuclear and endoplasmic reticulum levels by overexpressing fluorescent proteins that have been tagged with Malin (Sengupta, Badhwar et al. 2011, Romá-Mateo, Sanz et al. 2012).

Malin is a RING type E3 ubiquitin ligase and participates in the last step of the ubiquitination process. Ubiquitination is a post-translational modification of a protein that covalently binds to ubiquitin. It is catalyzed by three enzymes, E1, E2, and E3 (Hershko and Ciechanover 1998), which form isopeptide (lysine), thioester (cysteine), ester (serine and threonine), and peptide (N-

terminus) bonds. The addition of one ubiquitin results in monoubiquitination of the target protein, but if repeated a certain number of times, a polyubiquitinated chain of ubiquitin can grow on the target protein (Komander and Rape 2012, Zheng and Shabek 2017). The type of chain that is formed, its length, and the type of residue of the target on which this chain grows will influence the path that the target substrate must take (Mallette and Richard 2012).

Malin protein, also defined as a TRIM-like E3 ubiquitin ligase (Romá-Mateo, Moreno et al. 2011, Kumarasinghe, Xiong et al. 2021), has 395 aminoacidic residues.

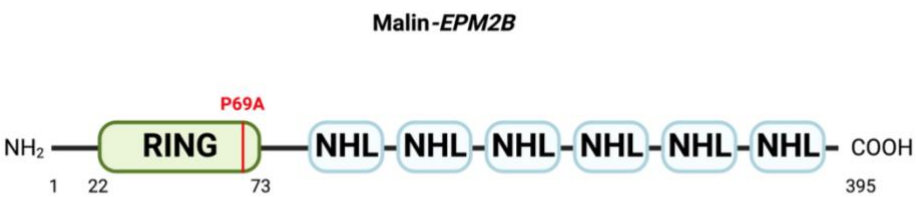

Fig. 3: Malin. Malin is characterized by the Really Interesting New Gene (RING) finger domain, which possesses the ubiquitin ligase activity (or where catalytic activity takes place) and 6 NHL repeats. Both domains are involved in protein-protein interactions. In patients, P69A is the most recurrent mutation found along *EPM2B* gene. Created with BioRender.com

Malin functions similarly to TRIM proteins but differs from them structurally. TRIM proteins belong to the RING–B-Box–Coiled-coil (RBCC) family and are made of proteins that have a RING finger, and one or two B-box motifs followed by a coiled-coil domain. The RING finger and B-box domains are involved in protein-protein interactions. At the level of the C-terminus, TRIM proteins may have different domains: COS domain, fibronectin type III repeat (FNIII), PRY domain, SPRY domain, acid-rich region (ACID), filamin-type IG domain (FIL), NHL domain, PHD domain, bromodomain (BROMO),

Meprin and TRAF-homology domain (MATH), ADP-ribosylation factor family domain (ARF), and transmembrane region I (Slack and Ruvkun 1998).

Unlike TRIM proteins, Malin lacks the B-box and coiled-coil domains and has only the RING finger domain followed by six NHL domains (also present in NCL1, HT2A, and LIN-41 proteins) located in its C-terminus (Fig. 3). NHL domains are known to be involved in protein-protein interactions (Gentry, Worby et al. 2005).

About 90 different mutations along *EPM2B* have been linked to LD (Singh and Ganesh 2009). Malin's enzymatic activity or its interactions with other proteins may be affected by such mutations. On the RING motif of Malin, P69A mutation is the most frequent one recognized in patients, which renders Malin catalytically inactive. Interestingly, the D146N mutation abolishes the interaction with Laforin while leaving Malin's ubiquitinating activity unaffected. This mutation prevents the formation of a Laforin-Malin functional complex, which results in an abnormal buildup of glycogen (Solaz-Fuster, Gimeno-Alcañiz et al. 2008, Couarch, Vernia et al. 2011).

Laforin-Malin complex

Laforin and Malin are two proteins that have different functions but can work in complex with each other. It seems that they both need each other to function properly. It could be that Malin's E3 ubiquitin ligase activity uses the adapter protein Laforin to target specific proteins for ubiquitination (Gentry, Romá-Mateo et al. 2013, Garcia-Gimeno, Knecht et al. 2018) but further investigations are necessary to confirm it. In addition, Malin can auto-ubiquitinate itself and promote its own degradation. In this scenario the action of Laforin seems necessary to prevent the auto-degradation of the Malin to keep its cellular levels stable (Gentry, Romá-Mateo et al. 2013, Mittal, Upadhyay et al. 2015, Garcia-Gimeno, Knecht et al. 2018).

On the contrary Laforin requires Malin for its degradation. As a matter of fact, Laforin is a substrate of Malin. Lafora patients with mutations occurring

on Malin have shown a lack of polyubiquitination and degradation of Laforin. This suggests a role of Malin in the regulation of Laforin in terms of protein concentration through polyubiquitination-dependent degradation (Gentry, Worby et al. 2005, Romá-Mateo, Sanz et al. 2012).

Pathophysiological features of Lafora disease

Given the activity of Malin, LD can be viewed as a disease connected to the ubiquitin system (Garcia-Gimeno, Knecht et al. 2018). Several substrates of Malin have been identified to date (Solaz-Fuster, Gimeno-Alcañiz et al. 2008, Moreno, Towler et al. 2010, Sharma, Mulherkar et al. 2012, Rubio-Villena, Garcia-Gimeno et al. 2013, Sanchez-Martin, Romá-Mateo et al. 2015, Viana, Lujan et al. 2015, Perez-Jimenez, Viana et al. 2020, Sanchez-Martin, Lahuerta et al. 2020), and their identification has helped in defining some of the pathophysiological characteristics (Fig. 4) of the disease that have been previously described. These features include accumulation of polyglucosans (Cheng, Zhang et al. 2007, Solaz-Fuster, Gimeno-Alcaniz et al. 2008, Rubio-Villena, Garcia-Gimeno et al. 2013); an increase in glucose uptake (Singh, Singh et al. 2012); impairment in the degradation processes at the level of the proteasome and autophagy (Aguado, Sarkar et al. 2010, Puri and Ganesh 2012, Sanchez-Martin, Lahuerta et al. 2020); alteration of glutamatergic transmission (Munoz-Ballester, Berthier et al. 2016, Perez-Jimenez, Viana et al. 2020); mitochondrial dysfunction (Romá-Mateo, Aguado et al. 2015, Lahuerta, Aguado et al. 2018); and neuroinflammation (Lopez-Gonzalez, Viana et al. 2017, Lahuerta, Gonzalez et al. 2020, Rubio, Viana et al. 2023).

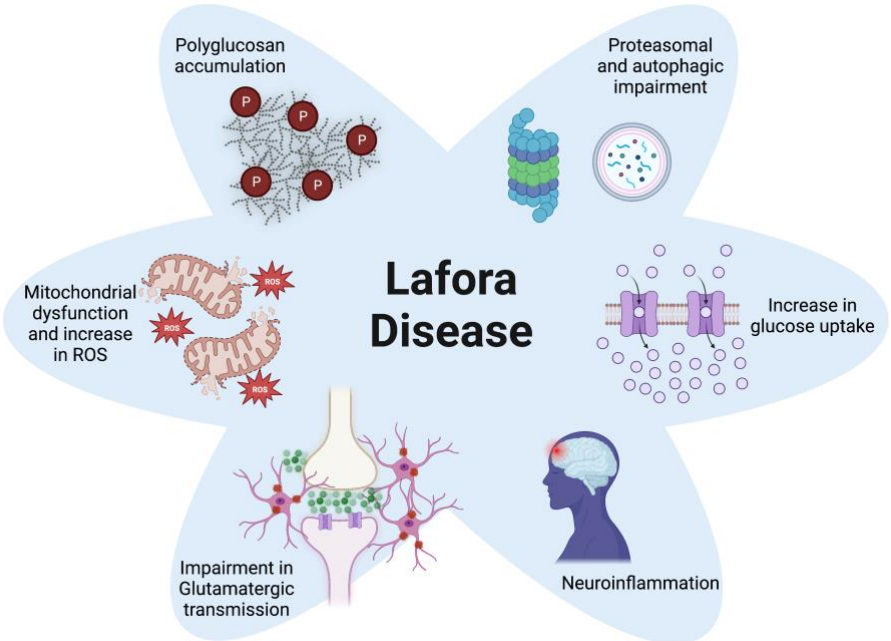

Fig. 4: Dysfunctions associated to LD. Lafora disease is altered in the formation and accumulation of Lafora bodies, alteration of proteostasis, increase in glucose uptake, increase in neuroinflammation, impaired glutamatergic transmission and mitochondrial dysfunction with increase in oxidative stress. Created with BioRender.com

Although these dysfunctions have been described, many molecular mechanisms leading to these conditions need further elucidation. The hunt for novel substrates could undoubtedly be beneficial for several reasons, including the identification of previously unidentified disease dysfunctions and a better understanding of the above pathophysiological alterations.

Discovery of new substrates

Typical techniques used to identify most of the potential Malin substrates relay on protein-protein interaction assays such as Co-Immunoprecipitation, yeast two-hybrid, etc (Garcia-Gimeno, Knecht et al. 2018). The substrates discovered so far are listed in Table 1.

Protein	Substrate/Interactor	Outcome	Reference
LAFORIN	substrate	polyubiquitination and degradation	(Gentry, Worby et al. 2005)
DISHEVELLED2	substrate	K48 and K63 ubiquitination and degradation	(Sharma, Mulherkar et al. 2012)
GLYCOGEN SYNTHASE	substrate	ubiquitination and proteasome-dependent degradation	(Vilchez, Ros et al. 2007)
NNAT (neuronatin)	interactor	ubiquitination and proteasomal degradation and regulation of glycogen synthesis	(Sharma, Rao et al. 2011)
GL	substrate	ubiquitination and inhibition of glycogen accumulation	(Worby, Gentry et al. 2008)
R6	substrate	ubiquitination and inhibition of glycogen accumulation	(Worby, Gentry et al. 2008) (Rubio-Villena, Garcia-Gimeno et al. 2013)
R5/PTG	substrate	ubiquitination and inhibition of glycogen accumulation	(Solaz-Fuster, Gimeno-Alcañiz et al. 2008) (Vilchez, Ros et al. 2007) (Worby, Gentry et al. 2008)
CHIP	interactor	regulation of the activity of transcription factor HSF1	(Sengupta, Badhwar et al. 2011)
AGL	substrate	regulation by ubiquitination	(Cheng, Zhang et al. 2007)
PRDM8	interactor	nuclear interaction	(Turnbull, Girard et al. 2012)
UBE2D1	interactor	E2 enzyme of ubiquitination process	(Gentry, Worby et al. 2005)
UBE2E1	interactor	E2 enzyme of ubiquitination process	(Gentry, Worby et al. 2005)
UBE2H	interactor	E2 enzyme of ubiquitination process	(Gentry, Worby et al. 2005)
UBE2N	interactor	E2 enzyme of ubiquitination process	(Sanchez-Martin, Roma-Mateo et al. 2015)
UBE2D3	interactor	E2 enzyme of ubiquitination process	(Gentry, Worby et al. 2005), (Sharma, Mulherkar et al. 2012)
PYRUVATE KINASE M1,M2	substrate	ubiquitination and nuclear translocation only of PKM2	(Viana, Lujan et al. 2015)
AMPK subunit alfa and beta	substrate	K63 linked polyubiquitination	(Moreno, Towler et al. 2010)
p62	substrate	target substrates for autophagic degradation upon ubiquitination	(Sanchez-Martin, Roma-Mateo et al. 2015)
BECLIN, VPS34, VPS15, ATG14L, UVRAG	substrates	impairment of the maturation of autophagosomes	(Sanchez-Martin, Lahuerta et al. 2020)
EAAT2	substrate	localization of GLT1 at the plasma membrane	(Perez-Jimenez, Viana et al. 2020)
alfa arrestin1, beta arrestin	interactors	stability of GLT1	(Perez-Jimenez, Viana et al. 2020)

Table 1: List of substrates and interactors of Malin. The outcome of the modification is indicated.

The novel substrates discovered and described in this thesis were obtained through an unbiased alternative strategy (Franco, Seyfried et al. 2011) that relies on the ubiquitination activity of Malin E3-ubiquitin ligase. This

alternative approach was chosen in order to be able to identify any unidentified targets of the ubiquitin pathway. Numerous cellular processes involve the posttranslational modification of proteins by ubiquitin. The ubiquitin pathway is crucial for the growth and function of the brain, and disruption of it is linked to a number of neurodegenerative diseases, such as Parkinson's and Alzheimer's diseases. For this reason, it's critical to be able to identify new targets in order to more thoroughly investigate these diseases, as in our case, Lafora disease. Franco et al, adopted a strategy to find ubiquitinated proteins that can exploit the ubiquitination activity of E3 ligases rather than using the more conventional techniques (Franco, Seyfried et al. 2011). Although effective, proteins identified using traditional methods that rely on the capacity of proteins to interact with one another still require validation because it cannot be assumed that a protein identified in this way is always a substrate of an E3 ligase. In addition, there is a chance that many candidates will drop out and go undetected if this type of analysis is used, which could also result in false negatives. The strategy adopted by Franco et al. (Franco, Seyfried et al. 2011) partially have similar issues that result to be less critical but more credible since the strategy exploits the ubiquitination activity that occurs naturally *in vivo* inside cells. Not to mention the fact that this type of strategy allowed to discover novel substrates also in highly challenging cell types such as neurons, which had been difficult to analyze until then.

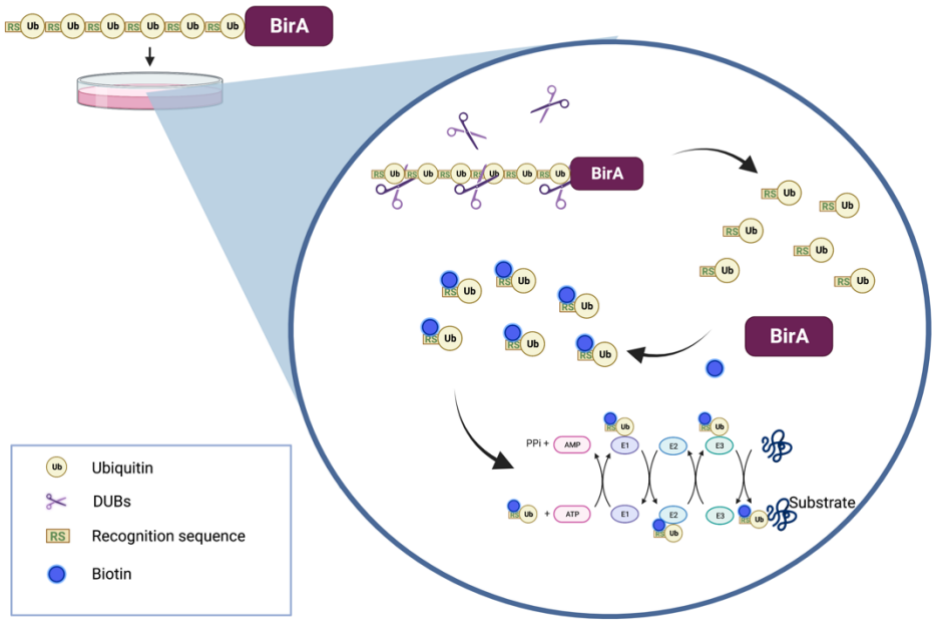

Fig. 5: The *E. coli* biotin ligase (BirA) and six copies of ubiquitin tagged with biotinylation target motifs. When expressed in cells, the polyubiquitin is cleaved by the deubiquitinating enzymes (DUBs). Each ubiquitin is then biotinylated, and endogenous ubiquitin ligases (E1, E2 & E3) will introduce the biotinylated ubiquitins on protein-substrates. Avidin-conjugated beads will be used to isolate biotinylated and ubiquitinated proteins. Created with BioRender.com

The method (Fig. 5) relies on the *in vivo* biotinylation of ubiquitin, which is accomplished by ectopically expressing the *Escherichia coli* BirA enzyme to attach a biotin molecule to a particular BirA recognition sequence (Beckett, Kovaleva et al. 1999, de Boer, Rodriguez et al. 2003) added at the N terminus of each ubiquitin chain. Franco et al., (Franco, Seyfried et al. 2011) took advantage of the processing ability of endogenous DUBs to digest a linear polypeptide precursor containing six copies of the tagged ubiquitin and the BirA enzyme. The BirA enzyme will be released by the action of the DUBs and will biotinylate the ubiquitin chains tagged with BirA recognition sequence. The

biotinylated ubiquitins will be incorporated, together with other ubiquitin moieties present inside the cellular microenvironment, in the endogenous ubiquitination process. The E1, E2 and E3 ubiquitin conjugating enzymes will add the biotinylated ubiquitins into their substrates. In this way, the authors were able to isolate and enrich the neuronal ubiquitinated proteins from a multicellular organism to levels not previously gained by any other method because of the potency and specificity of the avidin-biotin interaction. As a result, they were able to determine whether a neuronal protein was mono- or polyubiquitinated by Western blotting and to identify it by mass spectrometry. Because this was accomplished without the use of proteasome inhibitors, physiological levels of ubiquitination were noted.

The application of this strategy has also given other groups (Lectez, Migotti et al. 2014, Ramirez, Martinez et al. 2015, Martinez, Lectez et al. 2017, Pirone, Xolalpa et al. 2017, Ramirez, Lectez et al. 2018, Elu, Osinalde et al. 2019) the incentive to use it when looking for new substrates. For example, Ramirez et al. applied the following strategy in 2021 to discover new substrates for the E3 ubiquitin ligase Ariadne-1 (Ari-1). Ari-1 is crucial for neuronal development, but its neuronal substrates weren't yet discovered. They employed the *in vivo* ubiquitin biotinylation strategy combined with quantitative proteomics of *Drosophila* heads to look for potential Ari-1 substrates. A significant change of at least two-fold increase in ubiquitination and the identification of at least two unique peptides led them to identify 16 candidates. The homologue of the N-ethylmaleimide sensitive factor (NSF), which is involved in neurotransmitter release, was found among these candidates. Thanks to this discovery and subsequent validation of the candidate they were able to offer major insights on the mechanism of NSF activity in the synaptic cleft via Ari-1-dependent ubiquitination (Ramirez, Morales et al. 2021).

In a similar manner, we have also employed this method to search for new substrates of Malin E3 ubiquitin ligase. Thanks also to a close collaboration with Ramirez and Mayor themselves, in this thesis I will explain how we

exploited the bioUb strategy (Martinez, Lectez et al. 2017, Ramirez, Lectez et al. 2018) and how we managed to obtain a set of proteins whose ubiquitination was found to be increased in cells expressing Malin wild type in comparison to cells expressing an inactive form of Malin (P69A). Subsequently, among the several candidates obtained, we validated P-Rex1 and Hsp90α as novel substrates of Malin. In addition, for the former, we managed to describe the biological relevance that followed its ubiquitination by Malin giving major insights on the altered pathological feature of glucose uptake of LD, while for the latter, at present, we are only able to give a future perspective on what could be its implication in LD based on the known literature and preliminary data obtained so far.

P-Rex1

P-Rex1 (PIP_3-dependent Rac exchanger 1), together with P-Rex2, is one of the guanine-nucleotide exchange factors (GEFs) for Rac family of small G proteins that include Rac1, Rac2, Rac3 and RhoG, a branch of the Rho family. P-Rex1 and P-Rex2 belong to the P-Rex family and are Dbl-type Rac-GEFs. The Rac family small G proteins, known also as Rac-GTPases, are involved in many essential cell functions and responses (Hall 1998, Wennerberg, Rossman et al. 2005) and their activation can be promoted by two types of GEFs that differ for the structure of their catalytic domain: the Dbl and the DOCK type Rac-GEFs (Welch 2015). When the Rac-GEFs mediate the activation of the small G proteins, these go across a change in their conformation in such a way that they are able subsequently to interact with downstream targets and promote different cellular responses. The change in the conformation (Fig. 6B) of the Rac-GTPases happen when Rac-GEFs can favor the release of GDP from Rac proteins (GDP-bound inactive state) enabling free GTPs in the cell to bind to them. P-Rex family members are not the only Dbl-type Rac-GEFs; there are

also other types that differ due to their structure and regulation (Rossman, Der et al. 2005, Vigil, Cherfils et al. 2010).

The P-Rex proteins are majorly associated with cancer progression but there are also emerging roles in metabolic diseases (Welch 2015).

Genes and proteins

The two P-Rex genes' coding sequences are 49% identical (Donald, Hill et al. 2004). In humans, the P-Rex1 gene (*PREX1*; NM 020820) is situated on chromosome 20 (20q13.13), close to a region linked to type 2 diabetes, and the P-Rex2 gene (*PREX2*; NM 024870) is situated on chromosome 8 (8q13.2), close to a region linked to aggressive cancers and metastasis. P-Rex1 (185 kDa, 1659 amino acids; NP 065871) is encoded by *PREX1*, and P-Rex2 (183 kDa, 1606 amino acids; NP 079146) and P-Rex2b (112 kDa, 979 amino; NP 079446), which lacks the C-terminal half, are encoded by *PREX2* (Fig. 6A)

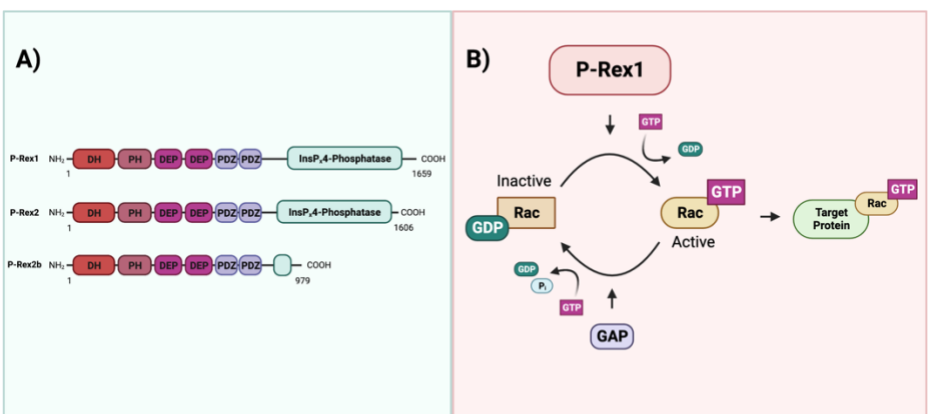

Fig. 6: P-Rex1 domains and Rac1 activation. (**A**) Domain structure. P-Rex1 and P-Rex2 are typical Dbl-type Rho-GEFs and have identical domain structure. The N-terminal Dbl homology (DH) domain, which confers Rac-GEF activity, is followed by a PH domain which binds PIP_3, followed by 2 DEP and 2 PDZ protein interaction domains and weak homology over their C-terminal half to inositol polyphosphate 4-phosphatase (IP4P) which harbours no phosphatase activity. P-Rex2b is a splice variant of P-Rex2. (**B**) The Rac-GEF activity of P-Rex family proteins promotes the release of GDP from Rac (Rac1, Rac2, Rac3, RhoG), allowing excess free cellular GTP to bind, and thus induces the active conformation of Rac which is able to engage downstream targets and stimulate cell responses. Created with BioRender.com

Regarding their proteins structure, P-Rex1 and P-Rex2 share 56% of identity in their aminoacidic sequence. As is typical for Dbl-type Rho-GEFs, (Fig. 6A) they are composed of an N-terminal pleckstrin homology (PH) domain that confers their Rac-GEF catalytic activity, two DEP protein interaction domains, and weak homology to inositol polyphosphate 4-phosphatase (IP4P) over their C-terminal half. P-Rex proteins don't seem to contain any catalytic phosphatase activity, even though the IP4P domain has the minimal number of residues needed for phosphatase activity (Welch, Coadwell et al. 2002, Rynkiewicz, Liu et al. 2012).

Cell and tissue distribution

When it comes to P-Rex1 expression at the cellular and tissue level, neutrophils (Welch, Coadwell et al. 2002, Hill and Welch 2006) are the cell type that expresses it the most. Other peripheral blood leukocytes, like macrophages (Wang, Dong et al. 2008), as well as platelets (Aslan, Spencer et al. 2011, Qian, Le Breton et al. 2012), endothelial cells (Carretero-Ortega, Walsh et al. 2010), and neurons (Yoshizawa, Kawauchi et al. 2005), also express P-Rex1 strongly. P-Rex1 has a high level of tissue expression throughout the brain, but it is expressed, among other tissues, at a lower level in the bone marrow, thymus, spleen, lymph nodes, and lung (Welch, Coadwell et al. 2002, Yoshizawa, Kawauchi et al. 2005).

Rac-GEFs must be localized to the membrane in order for Rac proteins to be activated at cellular membranes. P-Rex1 and P-Rex2 in basal cells, however, are primarily cytosolic like the majority of Rac-GEFs, and cell stimulation is necessary for their membrane translocation.(Welch, Coadwell et al. 2002, Donald, Hill et al. 2004, Yoshizawa, Kawauchi et al. 2005).

Rac family Substrates

All Rac-like Rho family small G proteins, including the widely expressed Rac1, haematopoietic Rac2, neuronal Rac3, and the more distantly related widely expressed RhoG, as well as some that are Cdc42-like (Cdc42 and TC10, but not TCL), can be activated *in vitro* by full-length P-Rex1 or the isolated DH/PH domain tandem (iDHPH), but none that are Rho-like (RhoA, RhoB or RhoC) (Jaiswal, Dvorsky et al. 2013). P-Rex1 activates Rac1, Rac2, Rac3, and RhoG *in vivo*, but Cdc42 does not appear to be activated. Depending on the cell type and upstream signal, P-Rex1 can activate one or more isoforms of Rac *in vivo*. P-Rex1 preferentially activates Rac2 upon G-protein-coupled receptors (GPCR) stimulation (Dong, Mo et al. 2005, Welch, Condliffe et al. 2005) but Rac1 upon E-selectin engagement in mouse neutrophils, where endogenous Rac1 and Rac2 play non-redundant roles in ROS formation, cell spreading and motility (Herter, Rossaint et al. 2013). In contrast, P-Rex1 activates Rac1 upon GPCR stimulation in macrophages, which also express Rac1 and Rac2. Rac1 and Rac3 are meant to have non-redundant roles in neuritogenesis (de Curtis 2008). Different studies show that P-Rex1 can activate either isoform in NGF-stimulated neuronal PC12 cells (Yoshizawa, Kawauchi et al. 2005, Waters, Astle et al. 2008). However, P-Rex1 activity toward Rac3 has to date only been investigated using overexpressed Rac protein and therefore requires confirmation.

P-Rex1 activation and inhibition

Full length P-Rex proteins have low basal activity, and this is very typical for Rac-GEFs. However, the combination of signals that activate P-Rex proteins is unique to this Rac-GEF family. In the case of P-Rex1, both PIP_3 (Phosphatidyl inositol 3,4,5 triphosphate) and Gβγ can stimulate the GEF in a synergistic fashion (Welch, Coadwell et al. 2002, Urano, Nakata et al. 2008). P-Rex1 can also be activated by protein phosphatase 1α (PP1α). Endogenously, P-Rex1 and PP1α interact constitutively, and the binding happens through the

RVxF motif in the IP4P domain of P-Rex1. In HEK-293 cells, P-Rex1 dependent Rac activity was stimulated by coexpression of PP1α and required an intact RVxF. To a lesser extent, the closely related PP1α isoform PP1β could mediate P-Rex1 dependent Rac activity too (Barber, Hendrickx et al. 2012). On the contrary, the activity of P-Rex1 via PIP_3 and Gβγ can be blocked by cAMP-dependent kinase (PKA) (Mayeenuddin and Garrison 2006, Urano, Nakata et al. 2008). However, the effects of PKA on endogenous P-Rex1 need further investigation.

Known interactors of P-Rex1

Remarkably few P-Rex binding proteins have been discovered to date, and of those, only mTOR and PTEN have been demonstrated to directly bind P-Rex proteins. However, several new interactions in cells have been discovered such as Ephrin-B1, a ligand of the RTK EphB which controls neuronal migration and axonal guidance (Dimidschstein, Passante et al. 2013), EHBP1, an adaptor protein involved in GLUT4 trafficking (Guilherme, Soriano et al. 2004), and others (Welch 2015).

Insulin Resistance and type 2 Diabetes

P-Rex1 has a role in tumoral growth of different types of cancers such as melanoma and breast and prostate cancer. Interestingly, evidence show that P-Rex1 has an alternative role in insulin signaling and has been associated to type 2 diabetes (Lewis, Palmer et al. 2010, Balamatsias, Kong et al. 2011, Montero, Seoane et al. 2013). P-Rex1 dependent insulin signaling seems to be entirely mediated through its Rac-GEF activity.

In 3T3-L1 adipocytes, where P-Rex1 is endogenously expressed, P-Rex1 siRNA inhibits the uptake of glucose by these cells in response to insulin. This might be caused by the effect of P-Rex1 on the trafficking of glucose transporter GLUT4. Co-expression of P-Rex1 with a GLUT4-tagged form in 3T3-L1 adipocytes showed that P-Rex1 promotes the insulin-stimulated plasma

membrane localization of the transporter. Parallel to this, a dominant-negative Rac1 mutant prevented P-Rex1-dependent GLUT4 membrane localization, indicating that P-Rex1 mediates GLUT4 trafficking via Rac (Balamatsias, Kong et al. 2011).

Hsp90α

Hsp90α, together with Hsp90β, are the two major isoforms of the 90 kDa Heat shock protein Hsp90. Hsp90 is defined as a molecular chaperone and is a highly abundant protein and constitutes around the 1-2% of cellular protein content in eukaryotic cells (Scheibel, Weikl et al. 1998). Besides Hsp90α and Hsp90β, a report described the existence of an additional isoform Hsp90N (Grammatikakis, Vultur et al. 2002) to the Hsp90 family. The proteins that belong to the Hsp90 family are highly conserved and involved in many cellular processes. They are distributed in several cellular compartments and are essential for cellular homeostasis. In general, molecular chaperones, such as Hsp90, are essential for the stability, folding and activation of a wide range of client proteins (Wandinger, Richter et al. 2008, Schopf, Biebl et al. 2017). Therefore, alterations at the levels of these molecular chaperones could lead to the development and progression of cancer and neurodegenerative diseases (Lackie, Maciejewski et al. 2017).

Genes and proteins

Hsp90α is encoded by the gene *HSP90AA1* and is located on chromosome 14 (14q32–33) while Hsp90β is encoded by *HSP90AB1* and is located on chromosome 6 (6p21) (Sreedhar, Kalmar et al. 2004). Hsp90α is recognized to be the inducible form while Hsp90β is the constitutive form (Csermely, Schnaider et al. 1998). Moreover, these two isoforms are most likely to be product of gene duplication (Gupta 1995), and therefore have high homology and share approximately 85% of sequence identity (Johnson 2012, Hoter, El-Sabban et al. 2018). However the comparison of their protein

sequence revealed the presence of specific regions that vary among them, and this allowed to suggest that Hsp90α and Hsp90β can also mediate diversified functions (Sreedhar, Kalmar et al. 2004). The two isoforms are majorly cytosolic but, under normal conditions, 5-10% of total Hsp90 is also present in the nucleus and tends to increase under stress conditions (Csermely, Schnaider et al. 1998, Galigniana, Echeverria et al. 2010). Analogues of Hsp90 are meant to be found in alternative places inside the cells. Grp94 and Hsp75/TRAP1 are found at the endoplasmic reticulum and mitochondrial matrix, respectively (Hoter, El-Sabban et al. 2018).

Structure of Hsp90 isoforms

The N-terminal domain (NTD), C-terminal domain (CTD), and middle domain (MD) are the three main conserved domains that make up the overall molecular structure of Hsp90 homologues (Csermely, Schnaider et al. 1998, Sreedhar, Kalmar et al. 2004, Jackson 2013).

Fig. 7: Hsp90 isoforms and domains. Hsp90 has different domains. The N-Terminal Domain (NTD) domain contains an ATP binding motif that is required for Hsp90 ATPase activity necessary for the chaperone cycle and binding of client proteins. The Charged Linker Region (CR) that is highly charged and has variable length and amino acid composition. This region seems to increase the flexibility and dynamicity of the chaperone. The Middle Domain (MD) modulates the Hsp90 function by binding the γ-phosphate of ATP specified for the NTD thus modulating its ATPase activity. Additionally, several studies demonstrated that this domain is implicated in binding co-chaperones like Aha1 and interacting with client proteins. The C-Terminal Domain (CTD) responsible for the homodimerization of the chaperone and binding of different client proteins. In addition, this domain contains the existence of the MEEVD peptide sequence which binds the TPR-domain (tetratricopeptide-containing repeats) containing co-chaperones like HOP and immunophilins. Created with BioRender.com

The NTD and the MD are connected in eukaryotes by a variable charger linker domain (CR) (Tsutsumi, Mollapour et al. 2012). Each domain (Fig. 7) in the Hsp90 structure carries out a particular task. The NTD is known as the nucleotide-binding site because it binds to ATP. Depending on the Hsp90 isoform and its cellular location—either in the cytoplasm or the ER—the CTD, which is responsible for protein dimerization, contains either the special motifs MEEVD or KDEL. Despite having a divergent sequence among many eukaryotic organisms, it was discovered that the charged linker domain is crucial for the flexibility, interaction, and function of chaperones (Tsutsumi, Mollapour et al. 2012).

Expression of Hsp90 by transcriptional regulation

Heat shock factors (HSFs) are a subset of specialized stress-related transcription factors that typically regulate the expression of HSPs. When activated, HSFs bind to the heat shock element (HSE) of a specific location in the HSP promoter region and RNA polymerase is stimulated to act on the HSP gene's coding region (Csermely, Schnaider et al. 1998). Studies propose that HSF1 is rendered inactive through Hsp90 and Hsp70 binding. However, stress conditions promote the dissociation of HSF1 from the HSPs and translocate to the nucleus to promote HSP transcription when chaperone function is required (Voellmy and Boellmann 2007).

Post-translational modifications of Hsp90

For proteostasis to be maintained, to carry out a range of typical cellular processes, and to preserve tissue and organismal health, it is critical to tightly regulate Hsp90 chaperone function and the downstream activities of its client proteins. The chaperone cycle, a series of Hsp90 conformational changes, and an ATPase activity that is connected to its chaperone function are all features of Hsp90 (Schopf, Biebl et al. 2017). Hsp90's post-translational modifications

(PTMs) and a group of proteins collectively known as co-chaperones control and regulate the activity of the chaperone protein to meet the needs of the cell and the client proteins (Rohl, Rohrberg et al. 2013, Zierer, Rubbelke et al. 2016, Cox and Johnson 2018).

The effects of post-translational modifications on the chaperone function of Hsp90 have been studied, and it has been discovered that these modifications affect the ATPase activity, co-chaperone and client binding, client maturation, subcellular localization and degradation. (Cloutier and Coulombe 2013, Backe, Sager et al. 2020). The accessibility of the binding sites is modified by posttranslational modification of Hsp90 isoforms, which affects their chaperone function (Schopf, Biebl et al. 2017). Phosphorylation, acetylation, SUMOylation, methylation, ubiquitination, and S-nitrosylation are among the PTMs that the cytoplasmic isoforms of Hsp90 go through (Mollapour and Neckers 2012, Zuehlke, Beebe et al. 2015, Backe, Sager et al. 2020).

In relation to the subject covered in the thesis, I would like to deepen on the modifications made on Hsp90 through ubiquitination by different E3-ligases. Ubiquitination of Hsp90 happens at numerous lysine residues (Akimov, Barrio-Hernandez et al. 2018). Hsp90 is ubiquitinated and degraded by HECT domain E3 ubiquitin protein ligase (Hectd1) and, as described in cranial mesenchyme cells, mutations occurring on Hectd1 led to increased Hsp90α secretion and Hsp90-dependent migration (Sarkar and Zohn 2012). Another player involved in Hsp90's ubiquitination is carboxyl terminus of Hsc70-interacting protein (CHIP). In particular, Hsp90β was found to be degraded as a result of CHIP ubiquitinating it on 13 lysine residues (Kundrat and Regan 2010, Kundrat and Regan 2010). Phosphorylation of Hsp90α at positions T725 and S726 as well as S718 reduced interaction with CHIP, highlighting the interplay between Hsp90 phosphorylation and ubiquitination (Muller, Ruckova et al. 2013). Finally, it has been described that FXBL6 E3-ligase promotes K63-dependent ubiquitination of the chaperone to avoid its degradation, and this

leads to a stabilized activation of c-MYC. The activated c-MYC, in turn, will directly bind to the promoter region of FBXL6 to induce its mRNA expression. In this scenario, Hsp90 seems to function as an onco-protein that is involved in the correct assembly, folding and degradation of its client protein c-MYC. In this regard, hepatocellular carcinoma (HCC) samples report high levels of FXBL6. Inhibition of this E3 ubiquitin ligase might represent an effective therapeutic strategy for HCC treatment (Shi, Feng et al. 2020). To date, Hectd1, CHIP and FXBL6 seem to be the only E3 ubiquitin ligases that mediate ubiquitination of Hsp90.

Mechanism of action of Hsp90: ATPase activity

Dimerization is necessary for Hsp90 to function properly under physiological conditions (Prodromou 2016). The ATPase activity of Hsp90 and cycling between the closed and open states (Fig. 8) are the fundamental conditions of its mechanism of action (Rowlands, McAndrew et al. 2010). All Hsp90 isoforms, including those found in the cytoplasm, ER, and mitochondria, act similarly in terms of conformational changes after nucleotide binding despite being located in various parts of the cell (Wandinger, Richter et al. 2008). As previously mentioned, Hsp90 is a flexible homo-dimer made up of monomers that have the NTD, MD, and CTD structural domains. In the ATP binding cleft in the NTD of Hsp90, ATP is bound, causing a series of conformational events. The translocation of a brief N-domain fragment (ATP-lid) over the binding pocket and subsequent attachment to the corresponding N-domain of the other homo-dimer leads to a final product (Hoter, El-Sabban et al. 2018).

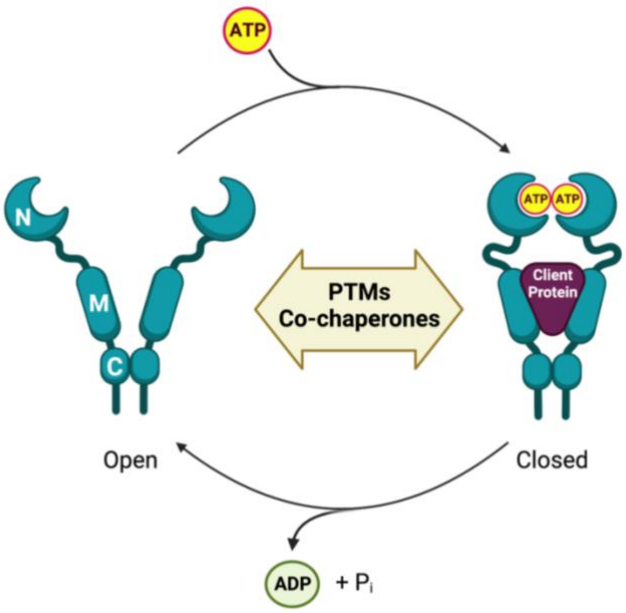

Fig. 8: Dimerization, open and closed state of Hsp90. Hsp90 begins its chaperone cycle in an open conformation that is dimerized only at the C-domain. ATP binding and an ordered series of conformational changes allow it to adopt a closed conformation, which is N-terminally dimerized. Upon ATP hydrolysis, Hsp90 returns to the open conformation and is ready to begin another chaperone cycle. This allows for the activation of client proteins. This cycle is tightly regulated by co-chaperone proteins as well as PTMs, and Hsp90 inhibitors can also modulate the chaperone cycle. Created with BioRender.com

Co-chaperones and client proteins

Hsp90 interact with many proteins that can be or co-chaperones or client proteins. Co-chaperones are basically molecules that help other chaperone proteins, such as Hsp90, in performing their function and in getting regulated in some way. Among the different co-chaperones we can find Hsp40, Hsp70,

HOP/Stip1 (Hsp90-Hsp70 organizing protein), CHIP and many others. Hsp40 and Hsp70, as co-chaperones, help stabilize and deliver client proteins to Hsp90 (Walter and Buchner 2002). HOP/Stip1 mediates the interaction between Hsp70 and Hsp90 (Baindur-Hudson, Edkins et al. 2015, Bhattacharya, Weidenauer et al. 2020). Unfolded client proteins can be degraded by CHIP as a co-chaperone of Hsp90 (Muller, Ruckova et al. 2013).

Client proteins are basically substrates recognized to be interacting partners of Hsp90 through non-covalent binding. Numerous cellular pathways are affected by the wide variety of client proteins that Hsp90 have (Wayne, Mishra et al. 2011, Karagoz and Rudiger 2015). The website held by Dr. Didier Picard, at http://www.picard.ch/downloads/Hsp90interactors.pdf, gathers the list of co-chaperones and client proteins of Hsp90. Interestingly, among this list Malin (*NHLRC1)* is defined as a client protein.

The role of Hsp90 in the chaperone cycle of protein folding

A complex procedure known as the Hsp90 chaperone cycle allows members of the Hsp90 family to carry out their function of folding client proteins. Co-chaperones, partner proteins, and immunophilins are some of the molecules that must work together for the Hsp90 chaperone machinery to function effectively. These molecules act in a precise and dynamic manner to aid in efficient protein folding by Hsp90. (Li, Soroka et al. 2012).

Protein folding in constantly switched on to maintain protein homeostasis in the cellular environment and to prevent potential aggregation (Fig. 9). Hsp70 binds to misfolded protein/nascent polypeptide in an ATP- and Hsp40-dependent reaction. The Hsp70/Hsp40/ADP complex can be stabilized by the binding of HIP (Hsp70 interacting protein) or dissociated by the interaction of BAG (Bcl2-associated athano-gene) homologues, which stimulate the exchange of ATP for ADP and polypeptide release (Walter and Buchner 2002, Chaudhury, Welch et al. 2006). Before taking any further action, Hsp90

binds the misfolded protein/nascent polypeptide that is housed within the Hsp70/Hsp40 protein complex.

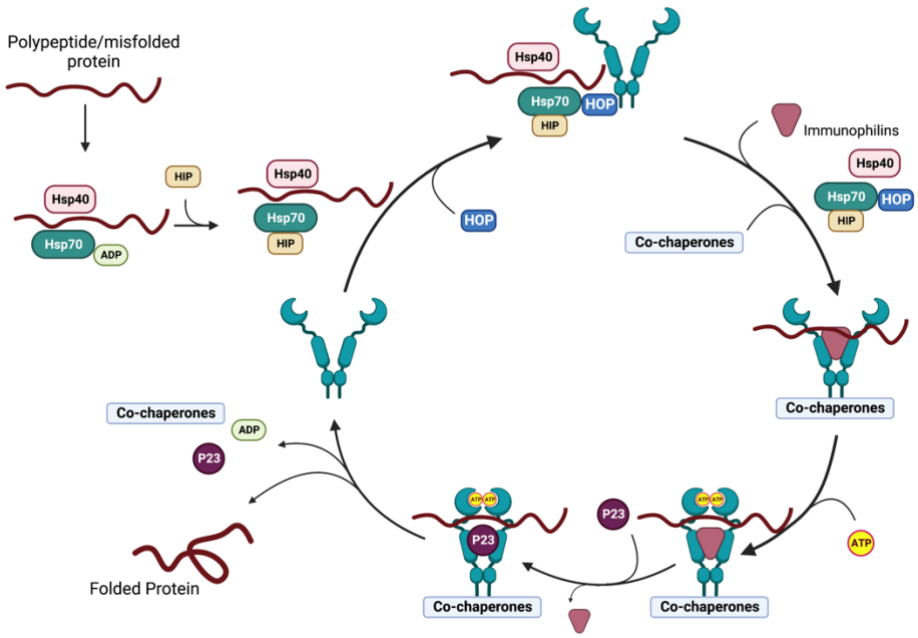

Fig. 9: The chaperone cycle. This cycle mediated by chaperones regulates protein homeostasis and prevents potential aggregation. In the presence of a misfolded protein/nascent polypeptide, Hsp70/Hsp40/ADP complex come into play and binds the aforementioned. The complex can be stabilized by the binding of HIP (Hsp70 interacting protein). Hsp90 binds the misfolded protein/nascent polypeptide harbored by the Hsp70/Hsp40 protein complex. The interaction between Hsp90 and Hsp70 is favored by the adaptor protein HOP/Stip1. While the misfolded protein/nascent polypeptide is loaded on Hsp90, additional co-chaperones and immunophilins come to the scene to promote the formation of a heteroprotein complex. At the same time, Hsp70, HIP, and HOP are released and Hsp90 goes from an open to a closed state by the binding of ATP to the NTD of Hsp90 in the heteroprotein complex. When other co-chaperones, such as p23, enter the cycle they bind to the middle domain and lead to a

series of effects: release of immunophilins and co-chaperones, induction of ATP hydrolysis, and folding of the bound misfolded protein/nascent polypeptide. Created with BioRender.com

The adaptor protein HOP/Stip1 facilitates the interaction between Hsp90 and Hsp70 (Murphy, Kanelakis et al. 2001, Muller, Ruckova et al. 2013, Baindur-Hudson, Edkins et al. 2015, Bhattacharya, Weidenauer et al. 2020). While the misfolded protein/nascent polypeptide is being loaded, additional co-chaperones and immunophilins, such as FKBP51 and FKBP52, are added to the Hsp90 homodimer to create an activated heteroprotein complex. Simultaneously, release of Hsp70, HIP, and HOP occurs. The "open state" of Hsp90 is changed to its "closed state" by the binding of ATP to the NTD of Hsp90 in the heteroprotein complex (Prodromou, Panaretou et al. 2000). At this stage, other co-chaperones such as p23 and Aha1 (activator of Hsp90 ATPase homologue 1) enter in the cycle. Aha1 binding to the MD of Hsp90 promotes the release of Immunophilins and co-chaperones, induces ATP hydrolysis, and supports the folding of the bound client (Felts and Toft 2003, Ali, Roe et al. 2006, Wolmarans, Lee et al. 2016).

Hsp90-CHIP mediated protein quality control

CHIP presents three domains: the TPR domain which interacts with chaperones Hsp70 and Hsp90; a coiled-coil domain involved in CHIP dimerization; and a U-box domain which connects to an E2 ubiquitin-conjugating enzyme and, in turn, ubiquitinates Hsp70- and Hsp90-bound client proteins and targets them to the proteasome for degradation (Shiber and Ravid 2014).

Hsp70 is very well conserved and has functions in protein folding and disaggregation (Mayer and Bukau 2005). Hsp70 has a substrate-binding domain (Hsp70SBD; 25 kDa) that recognizes the client protein and traps it while the nucleotide-binding domain (Hsp70NBD; 45 kDa) controls opening and closing

of the Hsp70SBD. The two domains are connected by a very flexible, well-conserved linker. Under stress conditions, CHIP overexpression mediates the proteasomal degradation of several substrates (Quintana-Gallardo, Martin-Benito et al. 2019).

Once formed, the Hsp70:substrate complex requires interaction with CHIP to mediate substrate ubiquitination. Following this, the co-chaperone Bag1 binds to the Hsp70:substrate and will link the complex to the proteasome (Fang, Li et al. 2013).

In a similar way, Hsp90 can direct its bound clients to degradation under certain stress conditions or in the presence of certain inhibitors such as geldanamycin (GA). Although no physical linker has been identified in this instance between the Hsp90:client protein complex and the proteasome, the addition of CHIP to the Hsp90:substrate complex causes a similar reaction to GA treatment, encouraging proteasomal degradation of the client protein (Connell, Ballinger et al. 2001, Quintana-Gallardo, Martin-Benito et al. 2019).

Chaperone machinery in neurodegenerative diseases

Numerous pathological conditions, such as cancer, neurodegenerative diseases, infectious diseases, and others, are influenced by alterations occurring on the normal functions of HSPs, including Hsp90.

The accumulation and aggregation of misfolded proteins within almost all cellular compartments is one of the main effects of neurodegenerative diseases. In a variety of neurodegenerative diseases, including Alzheimer's disease (AD), Parkinson's disease (PD), Amyotrophic Lateral Sclerosis (ALS), frontotemporal dementia (FTD), and human prion disease (HD), protein misfolding can result in the formation of aggregates (Knowles, Vendruscolo et al. 2014). Deposits can be amorphous, but soluble to some extent, or fibrillar and insoluble. Each disease's predominant protein, such as β-amyloid, tau, huntingtin, α-synuclein, or prion protein, makes up most of these deposits,

which are frequently unique to each disease (Chiti and Dobson 2006, Goedert, Klug et al. 2006, Goedert and Spillantini 2006, Han, Kato et al. 2012).

In PD, for example, Hsp90, Hsp70, Hsp60, Hsp40, and Hsp27 were shown to be localized within Lewy bodies and this evidenced the involvement of the molecular chaperones in the disease (Uryu, Richter-Landsberg et al. 2006). In the scenario of AD, HSPs and their co-chaperones, such as Hsp27, Hsp70, CHIP, and αB crystalline, can recognize hyperphosphorylated tau species in order to repair malignant tau or move forward with its recycling (Dou, Netzer et al. 2003, Petrucelli, Dickson et al. 2004, Shimura, Miura-Shimura et al. 2004, Luo, Dou et al. 2007). The atypically large substrate-binding site on Hsp90, which is relatively open and accessible to clients like tau, allows Hsp70 and Hsp90 to bind to the intrinsically unstructured tau at the same time. In fact, it seems that Hsp90 has a role in protecting hyperphosphorylated tau from degradation and this is correlated with studies that show that inhibitors of Hsp90 decrease levels of phosphorylated tau (Dickey, Ash et al. 2006, Dickey, Dunmore et al. 2006). In addition to this, the formation of CHIP complexes with phosphorylated tau (p-tau) was increased when Hsp90 was inhibited, and CHIP specifically destroyed these p-tau species, effectively preventing p-tau aggregation. P-tau and neurofibrillary tangles, which are collections of hyperphosphorylated tau, are also strongly co-localized with CHIP. These results suggest that CHIP, particularly because of its activity as a ubiquitin enzyme, is a promising candidate for modulating tau activity in neurodegenerative tauopathies (Dickey, Kamal et al. 2007).

In the context of diseases, molecular chaperones are also found in polyglucosan inclusions (Thomsen, Malfatti et al. 2022). In the study of Thomsen et al., quantitative analyses were conducted to identify the principal protein components of polyglucosan bodies in polyglucosan body myopathy type 1 (PGBM1), a disease that causes muscle weakness and cardiomyopathy and that sometimes is associated to severe immune system dysregulation and auto-inflammation. By analyzing the content of the polyglucosans, several

proteins associated to protein quality control were found and among these Hsp90α and Hsp90β were recognized (Thomsen, Malfatti et al. 2022). This might indicate that also in other types of polyglucosan storage diseases, such as Lafora disease, aggregation of protein associated to quality control may occur.

Lafora disease and HSPs

In order to find other potential roles for Malin, studies on the pathology of LD looked into the alteration of processes unrelated to glycogen metabolism. Many studies support the concept that Malin and Laforin, by forming a complex with Hsp70, may contribute to protein clearance, limiting harmful circumstances caused by misfolded protein buildup (Garyali, Siwach et al. 2009).

Moreover, during heat stress, Laforin and Malin create a complex with CHIP, a U-box E3 ligase, and a cochaperone that translocates to the nucleus to regulate the activation of heat shock factor 1 (HSF1). HSF1 protects the cell from heat-shock-induced death by binding to and activating heat-shock elements found in the promoter region of genes producing heat shock proteins. The Laforin-Malin complex translocates into the nucleus in response to temperature stress, requiring both CHIP and HSF1 (Sengupta, Badhwar et al. 2011). The Laforin-Malin complex regulates HSF1 transcriptional activity once within the nucleus. The nuclear translocation of Laforin and CHIP is blocked in the absence of Malin, and the heat shock response is thereby abrogated (Rao, Sharma et al. 2010). So far, research suggests that several clinical symptoms of LD may be caused by a malfunction in the HSF1-mediated stress response pathway (Sengupta, Badhwar et al. 2011).

OBJECTIVES

Objectives

The objectives of this thesis can be summarized in the following points.

1. Search and discovery of possible new candidate-substrates of Malin E3-ubiquitin ligase through a technique that exploits its ubiquitination activity.
2. Validate P-Rex1 as a substrate of Malin and delineate its ubiquitination effect.
3. Validate Hsp90 as a substrate of Malin and outline its ubiquitination effect.

MATERIALS AND METHODS

Materials and Methods

Mammalian cell culture

Human embryonic kidney cells (HEK293) (HPA Culture Collection#851820602) were used for transfection experiments. Cells were grown in Dulbecco's modified Eagle medium (DMEM) (Lonza. Barcelona. Spain), supplemented with 10% inactivated fetal bovine serum (FBS) (Invitrogen. Madrid. Spain), 1% L-glutamine, 100 units/ml penicillin, and 100 μg/ml streptomycin in a humidified atmosphere at 37°C and 5% (vol/vol) of CO_2.

Preparation of mouse primary astrocytes

Malin knockout mice (*Epm2b*-/-) (Criado, Aguado et al. 2012) were obtained on a pure B6 background by backcrossing more than 10 generations with corresponding C57BL/6JRccHsd mice (WT) from Harlan laboratories. Mice were maintained at the IBV-CSIC facility on a 12 light/dark cycle with food and water ad libitum. This study was carried out in strict accordance with the recommendations in the Guide for the Care and Use of Laboratory Animals of the Consejo Superior de Investigaciones Cientificas (CSIC, Spain) and approved by the Consellería de Agricultura, Medio Ambiente, Cambio Climático y Desarrollo Rural from the Generalitat Valenciana. All mouse procedures were approved by the animal committee of the Instituto de Biomedicina de Valencia-CSIC [Permit Number: IBV-51, 2019/VSC/PEA/0271]. All efforts were made to minimize animal suffering. Mouse primary astrocytes from control and *Epm2b*-/- mice (Lahuerta, Gonzalez et al. 2020) were obtained from P0 to P1 mice. Cortices, including the hippocampus, were dissected, the meninges were removed, and the tissues were homogenized using the Neural Tissue Dissociation kit and the GentleMACS dissociator from Mylteny Biotec (Madrid. Spain). Once obtained, microglia contamination was removed using CD11b Microbeads in a magnetic field

(Mylteny Biotec. Madrid. Spain). Cells were grown in Dulbecco's modified Eagle medium (Lonza. Barcelona. Spain) containing 20% of inactivated FBS, supplemented with 1% L-glutamine, 7.5 mM glucose, 100 units/ml penicillin, and 100 µg/ml streptomycin, in a humidified atmosphere at 37°C with 5% of CO_2. After 48 h, FBS was reduced to 10%. For the following 10 days, 0.25 mM dibutyryl-cAMP (dbcAMP) (D0627, Sigma-Aldrich) was added to the cultures to favor astrocytes' maturation. At the end of the maturation process, primary astrocytes were grown for a further 48 h in the absence of dbcAMP to avoid any undesired effect deriving from the compound (Magistretti, Manthorpe et al. 1983, Hertz, Peng et al. 1998, Muller, Fox et al. 2014).

Plasmid constructs

The following plasmids were described in reference (Sanchez-Martin, Romá-Mateo et al. 2015): pFLAG-Laforin, pECFP-Laforin, pEGFP-Malin, and pFLAG-Malin. Plasmid pFLAG-Malin P69A was described in reference (Couarch, Vernia et al. 2011); Dr. Atanasio Pandiella (CIC-Salamanca) kindly provided plasmid Myc-P-Rex1; plasmid pCMV-6xHisUbiq was generously provided by Dr. Manuel Rodríguez (Proteomics Unit. CIC-bioGUNE, Bizkaia, Spain) and plasmids pCMV-6xHis-Ubiq-K48R and pCMV-6xHis-Ubiq-K63R were a generous gift of Dr. Ch. Blattner (Institute of Toxicology and Genetics. Karlsruhe Institute of Technology, Karlsruhe, Germany). Plasmid pCEFL-AU5-Rac1 was provided by Dr. Jose Luis Zugaza (Achucarro Basque Center for Neuroscience. Leioa, Bizkaia, Spain). The GST fusion protein containing the Rac1 binding domain of PAK1 (GST-RBD-PAK1) was obtained as described in (Arrizabalaga, Lacerda et al. 2012). pCAG-(bioUb)x6-BirA plasmid was described in (Ramirez, Prieto et al. 2021). mCherry Hsp90α was purchased from Addgene (#108222). pEGFP-C1-Hsp90α was cloned using pEGFP-C1 and mCherry Hsp90α. pEGFP-C1-Hsp90α was cloned through digestion of mCherry Hsp90α (*BamH1*) and subcloned the Hsp90α ORF fragment in pEGFP-C1 (*BamH1*) vector purchased from Clontech (#6084-1).

Biotin pulldown

For the analysis of differentially ubiquitinated Malin substrates, we applied the ^{bio}Ub strategy described in previous reports (Lectez, Migotti et al. 2014, Ramirez, Martinez et al. 2015, Martinez, Lectez et al. 2017, Pirone, Xolalpa et al. 2017, Ramirez, Lectez et al. 2018, Elu, Osinalde et al. 2019, Ramirez, Morales et al. 2021). Briefly, 13.5 x 10^6 cells were seeded in three independent 150 mm dishes for each experimental condition (WT and Malin-P69A). After 48 h, cells were transfected with either FLAG-Malin or FLAG-Malin P69A and the pCAG-(bioUb)x6-BirA plasmid (Franco, Seyfried et al. 2011, Elu, Lectez et al. 2020), a construct expressing a precursor polypeptide composed of six biotinylatable versions of ubiquitin, conjugated to BirA, the *E. coli* biotin ligase enzyme, using lipofectamine 3000 reagent (Invitrogen. Madrid, Spain), according to the manufacturer's instructions, and supplemented with 50 µM biotin solution. The ^{bio}Ub construct (^{bio}Ub-BirA) gets digested in the cells by the endogenous deubiquitinating enzymes (DUBs) leading to the release of BirA and bio-Ub. Then, BirA recognizes the short specific N-terminal sequence of each modified ubiquitin and biotinylates it, generating biotin-tagged-ubiquitins. This reaction is executed very efficiently with minor off-targets. The biotin-tagged-ubiquitins are then incorporated into the cascade of the ubiquitination process to modify the corresponding proteins (Fig. 10A). The next day, cells were harvested and lysed with 2.5 ml of a solution containing 8 M urea, 1 % SDS, 50 mM N-ethylmaleimide (Sigma-Aldrich), and a complete protease inhibitor cocktail (Roche Diagnostics, Barcelona, Spain). Lysates were then passed through a 20G needle 10 times and applied to a PD10 desalting column (GE Healthcare. Barcelona, Spain), previously equilibrated with 25 ml of 3 M urea, 1 M NaCl, 0.25% SDS, and 50 mM N-ethylmaleimide. Recovered eluates were incubated with 150 µl of NeutrAvidin agarose beads suspension (Thermo Fisher Scientific, Waltham, MA. USA), and gentle rolling for 40 min at room temperature and 2 h at 4ºC. Afterward, beads were washed with the following solutions: twice with 8 M urea and 0.25 % SDS, thrice with 6 M

guanidine-HCl, once with 6.4 M urea, 1 M NaCl and 0.2 % SDS, thrice with 4 M urea, 1 M NaCl, 10 % isopropanol, 10 % ethanol, and 0.2 % SDS, once again with 8 M urea and 0.25 % SDS, once with 8 M urea and 1 % SDS, and thrice with 2 % SDS. All the solutions were prepared in PBS. Ubiquitinated material was then eluted with 80 µl of elution buffer (250 mM Tris-HCl, pH 7.5, 40% glycerol, 4% SDS, 0.2% bromophenol blue, and 100 mM DTT) boiling them at 95ºC for 5 min. Samples were subjected to final centrifugation at 16.000 x *g* in a Vivaclear Mini 0.8 µm PES-micro-centrifuge unit (Sartorius. Madrid, Spain) to discard the NeutrAvidin resin used. A similar amount of total ubiquitinated material was recovered in cells transfected with FLAG-Malin or FLAG-Malin P69A (Fig. 10B).

Liquid chromatography with tandem mass spectrometry (LC-MS/MS)

Eluates from biotin pull-down assays were resolved by SDS-PAGE using 4–12% Bolt Bis-Tris Plus pre-cast gels (Invitrogen. Carlsbad. CA. USA) and visualized with GelCode Blue Stain reagent following manufacturer's instructions (Thermo Fisher Scientific, Waltham, MA. USA). After the exclusion of avidin monomers and dimers, each lane was cut into four slices and subjected to in-gel digestion as described previously (Osinalde, Sanchez-Quiles et al. 2015, Ramirez, Prieto et al. 2021).

Mass spectrometry analyses were performed at the Proteomics Core Facility-SGIKER [University of Basque Country (UPV/EHU), Lioa, Spain). It was carried out on an EASY-nLC 1200 liquid chromatography system interfaced via a nanospray flex ion source with Q Exactive HF-X (Thermo Fisher Scientific. Waltham. MA. USA). Peptides were loaded onto an Acclaim PepMap100 pre-column (75 mm × 2 cm. Thermo Fisher Scientific. Waltham. MA. USA) connected to an Acclaim PepMap RSLC (50 mm × 25 cm Thermo Fisher Scientific. Waltham. MA. USA) analytical column. Peptides were eluted from the columns using a two-step gradient of 2.4 to 24% (90 min) and 24 to

32% (2 min) acetonitrile in 0.1% of formic acid at a flow rate of 300 nL min^{-1} over 92 min. The mass spectrometers were operated in positive ion mode. Full MS scans were acquired from m/z 375 to 1850 with a resolution of 60.000 at m/z 200. The 10 most intense ions were fragmented by high-energy collision dissociation (HCD) with a normalized collision energy of 28 and MS/MS spectra were recorded with a resolution of 15.000 at m/z 200. The maximum injection time was 50 ms for the survey and 100 ms for MS/MS scans, whereas AGC target values of 3×10^6 and 1×10^5 were used for the survey and MS/MS scans, respectively. To avoid repeat sequencing of peptides, dynamic exclusion was applied for 20 s. Singly charged ions or ions with unassigned charge states were also excluded from MS/MS. Data were acquired using Xcalibur software (Thermo Fisher Scientific. Waltham. MA. USA).

Data Processing and Bioinformatics Analysis

Acquired raw data files were processed with the MaxQuant (Cox and Mann 2008) software (versions 1.5.3.17 and 1.6.0.16) using the internal search engine Andromeda and searched against the UniProtKB database restricted to Homo sapiens (20,187 entries), as described in (Ramirez, Prieto et al. 2021). Spectra originated from the different slices corresponding to the same biological sample were combined. Carbamidomethylation © was set as fixed modification, whereas Met oxidation, protein N-terminal acetylation, and Lys GlyGly (not C-term) were defined as variable modifications. Mass tolerance was set to 8 and 20 ppm at the MS and MS/MS level, respectively; except in the analysis of the TOF data for which the values of 0.006 Da and 40 ppm were used, respectively. Enzyme specificity was set to trypsin, allowing for cleavage N-terminal to Pro and between Asp and Pro with a maximum of two missed cleavages. Match between runs option was enabled with 1.5 min match time window and 20 min alignment window to match identification across samples. The minimum peptide length was set to seven amino acids. The false discovery rate for peptides and proteins was set to 1%. Normalized spectral protein label-free

quantification (LFQ) intensities were calculated using the MaxLFQ algorithm. To further clarify, the following default parameters from MaxQuant were used: Decoy mode, revert; PSM FDR, 0.01; Protein FDR, 0.01; Site FDR, 0.01. MaxQuant output data was then analyzed with Perseus software (version 1.6.0.7) (Tyanova, Temu et al. 2016), and statistically significant differences in protein abundance were determined by a two-tailed Student's t-test.

Analysis of protein ubiquitination

The method described in (Kaiser and Tagwerker 2005) was used to study the ubiquitination of P-Rex1. For this purpose, HEK293 cells were transfected with the plasmids indicated in each experiment using X-treme GENE HP transfection reagent according to the manufacturer's protocol (Roche Diagnostics, Barcelona, Spain). After 24-36 h of transfection, cells were lysed using a 25-gauge needle in buffer A (6 M guanidinium-HCl, 0.1 M sodium phosphate, 0.1 M Tris-HCl pH 8.0) to inhibit the action of endogenous deubiquitinases. Protein extracts were clarified after centrifugation (12.000 × g 15 min) and protein concentration was measured through the Bradford technique. 1.5 mg of protein were incubated with 150 µl of a TALON cobalt resin (Clontech. Barcelona. Spain) equilibrated in buffer B containing 10 mM imidazole, 6 M guanidinium-HCl, 0.1 M sodium phosphate, 0.1 M Tris-HCl pH 8.0. To purify His-tagged proteins, incubation was carried out for 2 h at room temperature on a rocking platform. Then, the resin was washed with 1 mL of buffer B and four times with buffer C (buffer B, but with 8 M urea instead of 6 M guanidinium-HCl). Bound proteins were boiled at 95°C for 5 min in 50 µl of 2×Laemmli's sample buffer and analyzed by Western blotting using the appropriate antibodies. To determine the topology of the ubiquitin chains, when indicated, plasmids pCMV-6xHis-Ubiq-K48R and pCMV-6xHis-Ubiq-K63R were used in the assay instead of pCMV-6xHis-Ubiq wild type.

GFP-trap analysis of protein-protein interactions

HEK293 cells were transfected with specific constructs of Laforin, Malin, and the protein of interest. Cells were washed twice with cold phosphate-buffered saline (PBS) and scraped on ice in lysis buffer [10 mM Tris–HCl pH 7.5, 150 mM NaCl, 0.5 mM EDTA, 0.5% (v/v) Nonidet P-40, complete protease inhibitor cocktail (Roche Diagnostics. Barcelona. Spain), 1 mM PMSF, 2.5 mM NaF, 0.5 mM $NaVO_4$, and 2.5 mM $Na_4P_2O_7$]. The lysates were collected in an Eppendorf tube and further lysis was performed using a 25-gauge needle. Cell lysates were then centrifuged at 13.000 × g for 10 min at 4°C. Supernatants (1.5 mg of total protein, measured through the Bradford technique) were incubated with Chromotek GFP-trap beads (Chromotek, Planegg-Martinsried, Germany) for 30 min on a rocking platform at 4°C. Beads were washed two times with 1 mL of lysis buffer and one time with the lysis buffer containing 300 mM NaCl. Bound proteins were boiled at 95°C for 5 min in 30 µl of 2×Laemmli's sample buffer. The GFP- and CFP-fused proteins were pelleted and visualized by immunoblotting using specific antibodies. As a negative control, a construct expressing CFP or GFP proteins (plasmid pECFP-N1 and pEGFP-N1, respectively), was used to confirm the specificity of the interaction.

Western blot analyses

30 µg of total protein from the soluble fraction of cell lysates were analyzed by SDS-PAGE and proteins were transferred to PVDF membranes (Millipore. Madrid. Spain). Membranes were blocked with 5% (w/v) non-fat milk in Tris-buffered saline Tween20 buffer [TBS-T: 50 mM Tris-HCl pH 7.4, 150 mM NaCl, 0.1% (v/v) Tween20] for 1 h at room temperature and incubated overnight at 4°C with the corresponding primary antibodies: rabbit anti-P-Rex1 (13168. Cell Signaling Technology, Barcelona, Spain), mouse anti-P-Rex1 (ab264535. Abcam, Madrid, Spain), mouse anti-Flag (F3165. Sigma-Aldrich, Madrid, Spain), rabbit anti-GFP (210-PS-1GFP. Inmunokontackt, Madrid, Spain), mouse anti-Rac1 (05-389. Millipore; Madrid, Spain), rabbit anti-Pygm

(ab81901. Abcam. Madrid, Spain), rabbit anti-Pygb (ab154969. Abcam. Madrid, Spain), rabbit anti-GLUT1 (PA1-46152. Invitrogen. Madrid, Spain), goat anti-biotin-HRP-conjugated antibody (#7075. Cell Signaling Technology, Barcelona, Spain), mouse anti-Na+/K+-ATPase (ab7671. Abcam. Madrid, Spain), rabbit anti-Hsp90 (4874. Cell Signaling Technology, Barcelona, Spain), mouse anti-Hsp90α (ab79849. Abcam, Madrid, Spain), mouse anti-Hsp90β (ab53497. Abcam, Madrid, Spain), mouse anti-Gapdh (sc-32233. Santa Cruz Biotechnologies, Madrid, Spain), mouse anti-Tubulin (T6199. Sigma-Aldrich, Madrid, Spain), and rabbit anti-Actin (A2066. Sigma-Aldrich, Madrid, Spain), were used as loading controls. After washing, membranes were incubated with the corresponding HRP-conjugated secondary antibodies for 1 hat room temperature. Signals were visualized using Lumi-Light Western Blotting Substrate (Roche Applied Science. Barcelona. Spain) or ECL Prime Western Blotting Detection Reagent (GE Healthcare. Barcelona. Spain) and analyzed by chemiluminescence using the FujiLAS400 (GE Healthcare, Barcelona, Spain) image reader. Quantification of the protein bands was carried out using the software Image Studio version 5.2 (LI-COR Biosciences, Germany).

Analysis of the Degradation Rate of P-Rex1

Mouse primary astrocytes from *Epm2b-/-* and control mice were treated with 70 μM cycloheximide (CHX; Sigma-Aldrich, Madrid, Spain) for the indicated times (from 0 to 24 h). Cells were lysed in cold cell lysis buffer [10 mM Tris pH 7.6, 150 mM NaCl, 1% Nonidet P-40, 10 mM $MgCl_2$, 1mM PMSF, complete protease inhibitor cocktail (Roche Diagnostics. Barcelona. Spain)], using a 25-gauge needle. Cell lysates were centrifuged at 13.500 rpm for 10 min at 4°C. 25 μg of cell extracts (measured by the Bradford technique) were analyzed by Western blotting using anti-P-Rex1 antibody. The same extracts were analyzed using anti-Tubulin antibody as a loading control.

Rac1 activation assay

Rac1 pulldown assay was performed using the GST-RBD-PAK1 fusion protein described above. 50 μg of this fusion protein were coupled to glutathione-sepharose beads for 1 h at 4°C. HEK293 cells were transfected the day before with the plasmids indicated in the experiment. HEK293 cells were lysed in cold cell lysis buffer [10 mM Tris-HCl pH 7.6; 150 mM NaCl, 1% Nonidet P-40, 10 mM $MgCl_2$, 1mM PMSF, and complete protease inhibitor cocktail (Roche Diagnostics. Barcelona. Spain)] using a 25-gauge needle. Cell lysates were centrifuged at 13.500 rpm for 10 min at 4°C, and subsequently, 1 mg of protein extracts (measured by the Bradford technique) were incubated for 1 h at 4°C with the preloaded glutathione-sepharose beads previously washed with lysis buffer three times to remove the excess of GST-RBD-PAK1 protein. Proteins bound to beads were washed three times, resuspended in 2×Laemmli's sample buffer, and analyzed by Western blotting using the appropriate antibodies.

Analysis of Glucose uptake

Glucose uptake was performed on mouse primary astrocytes control vs *Epm2b*−/− following the technical procedure described in the Glucose Uptake-Glo™ Assay manual (Promega #J1341. Technical manual TM467). 30,000 cells/well were plated in 100 μL of culture medium in 96-well plates. Cells' maturation with dbcAMP was performed in the same support for 10 days. When indicated, cells were treated for 24 h with 2 μM 1.1-Dimethylbiguanide hydrochloride (Metformin) (D150959, Sigma-Aldrich, Madrid, Spain) before the assay. On the day of the assay, media was removed and cells were washed thoroughly with 1xPBS (BE17516Q, Lonza, Madrid, Spain) twice. 50 μL of 2-deoxyglucose (2-DG, final assay concentration of 1 mM) were added to each well for 10 min at room temperature. The assay was terminated by the addition of 25 μL of stop buffer, briefly mixed on an orbital shaker, and neutralized with 25 μL of neutralization buffer. Finally, 100 μL of 2-deoxyglucose 6-phosphate

(2DG6P) detection reagent was added to each well, briefly mixed on an orbital shaker, and incubated for 1 h at room temperature. Luminescence values were measured with a Tecan Spark microplate reader.

When indicated, glucose uptake was performed on cells in which the expression of P-Rex1 was silenced using an ON-TARGETplus Mouse P-Rex1 siRNA (Dharmacon/Horizon Discovery Ltd. Madrid, Spain). Mouse primary astrocytes were transfected with 20 nM SMARTpool P-Rex1 siRNAs, or with Non-Target siRNA, using Lipofectamine RNAiMAX (Thermo Fisher Scientific; Madrid, Spain), for 48 h before the glucose uptake assay. SMARTpool siRNAs of P-Rex1 include:

siRNA J-053658-09 Target sequence: GGUCAUUAUUUCCGUGUUA
siRNA J-053658-10 Target sequence: GCACCAGCGUGGCGAAUGA
siRNA J-053658-11 Target sequence: GCUUCAAGGUGUCGGAGGA
siRNA J-053658-12 Target sequence: GUGAGAUCCAGGACGCAUA

Analysis of cell surface proteins by biotinylation

Cell surface biotinylation in mouse primary astrocytes was performed with the Pierce Cell Surface Protein Isolation kit (89881. Thermo Fisher Scientific, Madrid, Spain), according to the manufacturer's protocol. Briefly, $4x10^6$ cells were grown on T75 Flasks. Cells' maturation with dbcAMP was performed in the same support for 10 days following 48 h in culture media without dbcAMP. On the day of the assay, cells were washed with PBS and incubated with EZ-LINK Sulfo-NHS-SS-biotin for 1 h at 4°C followed by the addition of a quenching solution. Cells were lysed with the lysis buffer (500 µL) provided by the kit. An aliquot (100 µL) of the lysate was saved for Western blotting (total fraction). The biotinylated fraction was isolated with NeutrAvidin beads, eluted by the sample buffer (400 µL) containing DTT, and subjected to Western blot analysis. Appropriate antibodies were used to detect the proteins biotinylated at the level of the plasma membrane.

Preparation of hippocampus and cortex samples from LD mouse models

Hippocampus and cortex samples were coming from mice brain were lysed separately in RIPA buffer [50 mM Tris-HCl, pH 8; 150 mM NaCl; 0.5% sodium deoxycholate; 0.1% SDS; 1% Nonidet P40; 1 mM PMSF; and complete protease inhibitor cocktail (Roche, Barcelona, Spain)] for 30 min at 4 C with occasional vortexing. The lysates were passed ten times through a 25 gauge needle in a 1 ml syringe and centrifuged at 13,000 x*g* for 15 min at 4 C. Supernatants were collected and total of 30 µg of protein, measured by Micro BCA Protein Assay Kit (Thermo Scientific™ 23235), according to the manufacturer's instructions, were resuspended in 2×Laemmli's sample buffer, and analyzed by Western blotting using the appropriate antibodies.

Statistical analysis

Results are shown as means +/- standard error of the mean (SEM) of at least three independent experiments. Differences between samples were analyzed by unpaired two-tailed Student's t-tests using Graph Pad Prism version 5.0 statistical software (La Jolla. CA. USA). *P*-values have been considered significant as *$p<0.05$, **$p<0.01$.

RESULTS

Results

1.- Search and discovery of possible new candidate-substrates of Malin E3-ubiquitin ligase through a technique that exploits its ubiquitination activity.

Identification of novel substrates

We transfected HEK293 cells with plasmids expressing either FLAG-Malin-WT or FLAG-Malin-P69A to look for potential new substrates of Malin. The *EPM2B* gene's most frequent mutation, P69A, results in an inactive version of Malin (Couarch, Vernia et al. 2011, Riva, Orsini et al. 2021). We used the bioUb method published in earlier studies (Lectez, Migotti et al. 2014, Ramirez, Martinez et al. 2015, Martinez, Lectez et al. 2017, Pirone, Xolalpa et al. 2017, Ramirez, Lectez et al. 2018, Elu, Osinalde et al. 2019, Ramirez, Morales et al. 2021), and analyzed differently ubiquitinated Malin substrates. Briefly, cells were transfected with ^{bio}Ub construct (Franco, Seyfried et al. 2011, Elu, Lectez et al. 2020), a plasmid expressing a precursor polypeptide composed of six biotinylatable versions of ubiquitin, conjugated to BirA, the *E. coli* biotin ligase enzyme. In the cells, endogenous deubiquitinating enzymes (DUBs) breakdown the bioUb complex (bioUb-BirA), resulting in the release of BirA and bio-Ub. BirA then detects each modified ubiquitin's short unique N-terminal region and biotinylates it, resulting in biotin-tagged-ubiquitins. This process is carried out quite effectively, with just minor off-targets. The biotin-tagged ubiquitins are subsequently integrated into the ubiquitination cascade, where they modify the corresponding proteins (Fig. 10A).

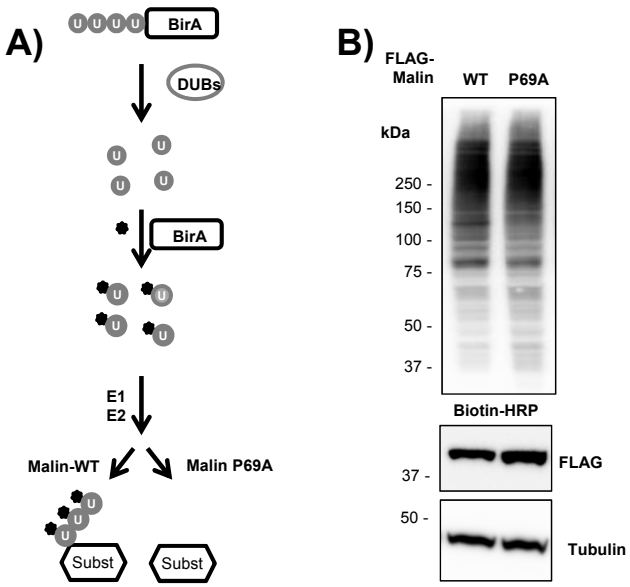

Fig. 10: Strategy for the analysis of Malin-dependent differentially ubiquitinated substrates. A) Diagram of the experimental reaction. See text for details. DUBs: endogenous deubiquitinating enzymes; U: ubiquitin; BirA: *E.coli* biotin ligase; biotin is depicted in black. B) Ubiquitinated status of cell extracts. HEK293 cells were transfected with plasmids expressing bioUb-BirA and FLAG-Malin WT or the inactive form FLAG-Malin P69A. 30 µg of cell extracts were analyzed by western blot using anti-biotin-HRP-conjugated, anti-FLAG, and anti-tubulin antibodies. Molecular weight markers are indicated on the left.

Then, ubiquitinated proteins are purified with streptavidin beads and quantitative proteomic experiments were carried out, following a previously described workflow (Martinez, Lectez et al. 2017, Ramirez, Lectez et al. 2018), to identify the ubiquitinated proteome of cells expressing Malin-WT vs. Malin-P69A. Experiments were performed in three independent samples and subjected to liquid chromatography with tandem mass spectrometry (LC-MS/MS) analysis. By comparing their ubiquitomes, we identified the differentially ubiquitinated proteins present in cells expressing Malin-WT vs Malin-P69A. Protein abundance in each sample was determined using label-free

quantification (LFQ) intensities (Cox, Hein et al. 2014). As a control of the protocol, we found similar amounts of FLAG-Malin-WT and FLAG-Malin-P69A in the cells, and the total amount of ubiquitinated proteins was also similar in all the cases, indicating that the expression of the Malin-P69A construct did not affect the overall ubiquitination process performed by endogenous E3-ligases (Fig. 10B).

Proteomic Analysis

Proteomic quantification can best be displayed on a volcano plot where abundance changes are provided on the X-axis, and the significance of these changes is displayed on the Y-axis (Figure 11A). Endogenous carboxylases (ACACA and PC) appeared unchanged between both datasets, indicating that the amount of biological material was equivalent in both samples; ubiquitin itself also appeared unchanged between both datasets, as well as the avidin that is used for the pulldown, all these control proteins indicating that the experiment has worked correctly. Malin itself (*NHLRC1*) also appeared mostly unchanged between the two datasets (Figure 11A). Out of the 4465 proteins quantified, 88 proteins (listed in Annex1) were found significantly enriched ($p<0.05$) by at least two-fold in cells expressing Malin-WT vs Malin-P69A. A DAVID analysis (https://david.ncifcrf.gov/) of these proteins indicated that the biological processes where they were involved were mostly protein folding, response to heat shock, and regulation of mitochondrial function (Fig. 11B, top panel) and their molecular functions were heat shock proteins and ubiquitin ligases (Fig. 11B, bottom panel). A STRING analysis (https://string-db.org/) of the selected proteins indicated that most of them clustered in two groups, the heat shock protein (HSPs) group and the OXPHOS group (Fig. 11C). Both in Figure 11A and Table 2, we show the list of differentially ubiquitinated proteins with a fold change higher than 4. In Table 2, only the first 24 most ubiquitinated proteins are listed. The complete list of ubiquitinated proteins can be found in Annex 1.

Gene names	MW (kDa)	Fold Change (WT/P69A	p-value	Peptides (unique)	Protein names
PREX1	175,9	18,48	0.00181	3	Phosphatidylinositol 3,4,5-trisphosphate-dependent Rac exchanger 1 protein (P-Rex1)
SEH1L	39,6	9,70	0,00027	3	Nucleoporin SEH1
HSPA4	94,3	8,59	0,00008	43	Heat shock 70 kDa protein 4
SCLT1	80,9	8,23	0,00004	6	Sodium channel and clathrin linker 1
YTHDF2	62,3	8,19	0,01791	7	YTH domain-containing family protein 2
FKBP5	51,2	7,80	0,03059	10	Peptidyl-prolyl cis-trans isomerase FKBP5
HSPA1L	70,4	7,11	0,04710	23	Heat shock 70 kDa protein 1-like
GLMN	68,2	6,89	0,00446	16	Glomulin
KLC2	68,9	6,14	0,01467	7	Kinesin light chain 2
LIN7C	21,8	5,93	0,01001	2	Protein lin-7 homolog C
ANKRD16	39,3	5,40	0,01252	5	Ankyrin repeat domain-containing protein 16
HSP90AB4P	58,3	5,35	0,00031	9	Putative heat shock protein HSP 90-beta 4
HSPH1	92,1	5,11	0,00011	40	Heat shock protein 105 kDa
HSPA4L	94,5	4,66	0,00007	27	Heat shock 70 kDa protein 4L
RCL1	40,8	4,65	0,04792	4	RNA 3-terminal phosphate cyclase-like protein
DLST	48,8	4,63	0,00064	2	Dihydrolipoyllysine-residue succinyltransferase component of 2-oxoglutarate dehydrogenase complex, mitochondrial
STIP1	62,6	4,42	0,00016	25	Stress-induced-phosphoprotein 1
DUSP1	39,3	4,14	0,00033	9	Dual specificity protein phosphatase 1
MKS1	63,3	4,02	0,00443	2	Meckel syndrome type 1 protein
TGFBRAP1	97,2	4,00	0,00582	5	Transforming growth factor-beta receptor-associated protein 1
ARFGAP2	56,7	3,72	0,04711	6	ADP-ribosylation factor GTPase-activating protein 2
HSP90AA1	84,7	3,69	0,00007	55	Heat shock protein HSP 90-alpha
CRYAB	20,2	3,66	0,00926	4	Alpha-crystallin B chain
UQCRC2	48,4	3,60	0,00026	7	Cytochrome b-c1 complex subunit 2, mitochondrial

Table 2: List of the first 24 ubiquitinated proteins. Differentially ubiquitinated proteins in cells expressing Malin-WT vs Malin-P69A with a fold change >4 and a p-value<0.05. The gene names, the molecular weight, the fold change, the p-value, the number of identified peptides supporting the ubiquitination, and the protein names are indicated.

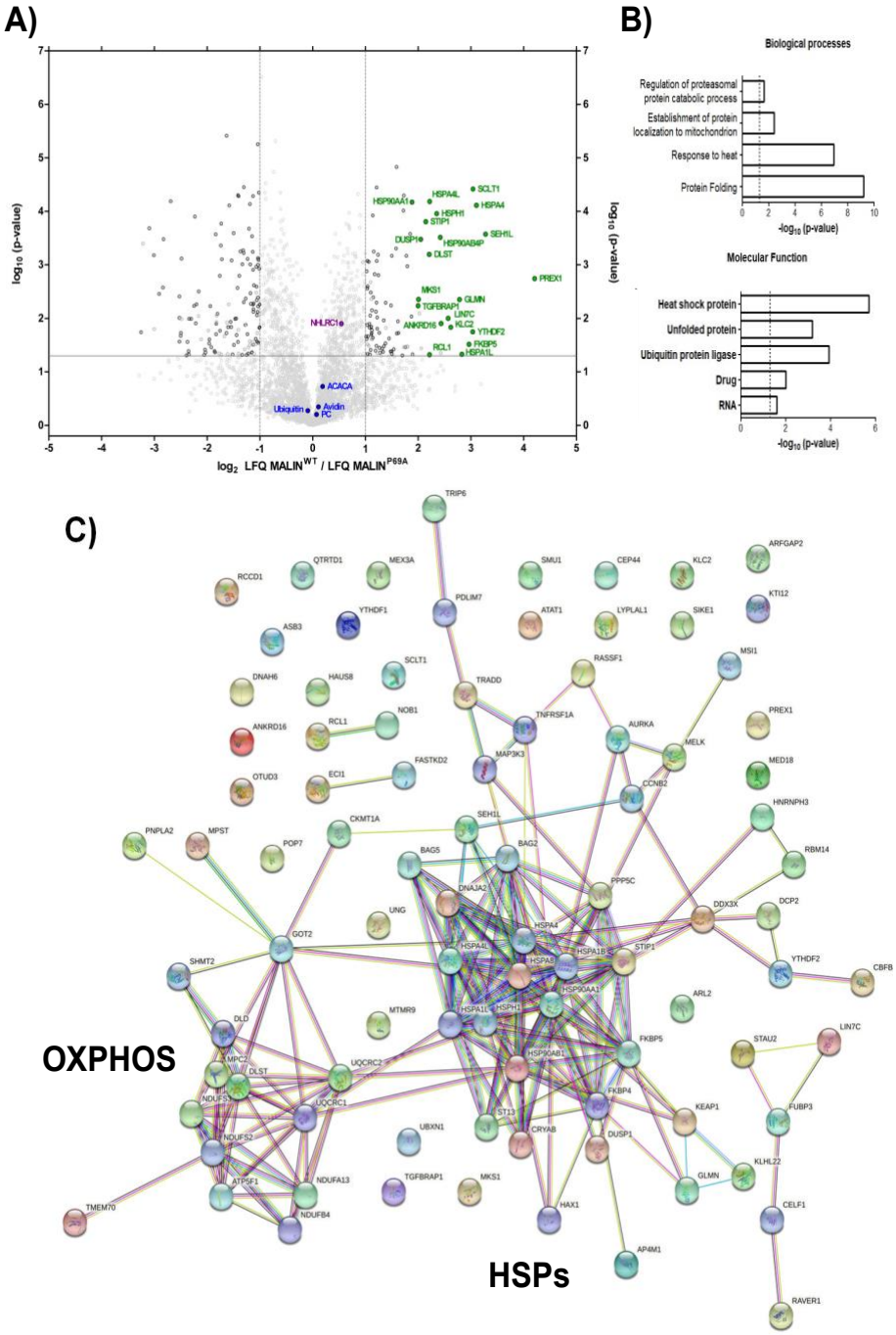
A)
log10 (p-value)
log2 LFQ MALIN^WT / LFQ MALIN^P69A
HSP90AA1
HSPA4L
SCLT1
HSPA4
HSPH1
STIP1
DUSP14
HSP90AB4P
SEH1L
DLST
PREX1
MKS1
GLMN
TGFBRAP1
LIN7C
NHLRC1
KLC2
ANKRD16
YTHDF2
RCL1
FKBP5
HSPA1L
ACACA
Ubiquitin
Avidin
PC
B)
Biological processes
Regulation of proteasomal protein catabolic process
Establishment of protein localization to mitochondrion
Response to heat
Protein Folding
-log10 (p-value)
Molecular Function
Heat shock protein
Unfolded protein
Ubiquitin protein ligase
Drug
RNA
-log10 (p-value)
C)
OXPHOS
HSPs

Fig. 11: In silico analysis of the Malin-ndent ubiquitinated proteins. A) Identification of candidate Malin substrates. Comparison of the abundance of the ubiquitinated proteins identified by MS upon Malin WT overexpression relative to cells overexpressing the Malin P69A mutant. Three independent samples from each case were analyzed. The volcano plot displays the LFQ Malin-WT/Malin-P69A ratios on $\log_2$ scale (*X*-axis) and the t-test P-values on $-\log_{10}$ scale (*Y*-axis). Malin candidate substrates with a significant (P-value < 0.05) LFQ Malin-WT/Malin-P69A ratio bigger than 4 are labelled in green. The ACACA and PC carboxylases, which use biotin as a cofactor, Ubiquitin, and the Avidin used for the pulldowns are labelled in blue. The Malin protein (NHLRC1) is labelled in magenta. A horizontal grey lane determines the statistical significance, while the vertical dashed lines determine a two-fold enrichment. B) David's analysis of the identified proteins. The grouped biological processes and molecular functions of the proteins are indicated. C) STRING analysis of the same set of proteins. Two major groups were identified, the heat shock protein (HSPs) group and the mitochondrial oxidative phosphorylation (OXPHOS) group.

Among the proteins on the list, we decided to characterize more deeply the consequences of the differential ubiquitination of P-Rex1 and Hsp90α for different reasons.

P-Rex1 was the protein whose ubiquitination was most elevated in cells expressing Malin-WT versus Malin-P69A (approximately 18-fold greater) and it is the first time that the activity of a Rac1 or Rac2 GEF has been modulated by ubiquitination, as opposed to the most common regulation of GEF activity by phosphorylation (Crespo, Schuebel et al. 1997, Llavero, Urzelai et al. 2015).

Regarding Hsp90α, a member of the HSP family, it is interesting to note that despite having a lower fold change in comparison with other heat shock proteins such as HspA4, HspA1L and others, it has a higher number of unique peptides. HspA1B has a greater number of peptide repeats than Hsp90AA1, but it also exhibits a smaller fold change in ubiquitination in cells expressing Malin-WT vs Malin-P69A. Furthermore, a previous study identified Hsp90α as one of the proteins that accumulate in polyglucosan bodies in RBCK1, a condition linked with polyglucosan accumulation in muscle, which also occurs in Lafora disease (Thomsen, Malfatti et al. 2022). Therefore, we thought it was important to investigate the biological implications of Hsp90α ubiquitination by Malin.

2.- Validate P-Rex1 as a substrate of Malin and delineate its ubiquitination effect.

Validation of P-Rex1 as a substrate of Malin

According to Uniprot (https://www.uniprot.org/uniprot/Q8TCU6), P-Rex1 is a phosphatidylinositol-3,4,5-triphosphate dependent Rac exchanger factor (Rac-GEF). To consider P-Rex1 as a bona fide substrate of Malin, we validated its Malin-dependent ubiquitination by an alternative method, based on the expression in HEK293 cells of a modified form of ubiquitin tagged with 6xHis residues and the purification of ubiquitinated proteins by cobalt affinity chromatography (Kaiser and Tagwerker 2005). Using specific antibodies, the presence of P-Rex1 in the pool of purified ubiquitinated proteins was determined. We expressed a myc-tagged version of P-Rex1 together with plasmids expressing Laforin and different forms of Malin since the expression of endogenous P-Rex1 in HEK293 cells was very low. In cells co-transfected with the functional complex Laforin-Malin and myc-P-Rex1 (Fig 12A, lane 4), we observed higher ubiquitination of P-Rex1 in comparison to cells expressing only P-Rex1 (Fig. 12A, lane 1). In cells in which we co-transfected Laforin together with the inactive form of Malin (P69A), the rate of ubiquitination of the substrate was lower in comparison to cells expressing the wild type form of Malin (Fig. 12A, lane 5). On the other hand, the ubiquitination of P-Rex1 was also present in cells that had simply been transfected with the Malin-WT plasmid, possibly because the endogenous levels of Laforin were adequate for Malin's activity (Fig 12A, lane 3). On the contrary, the expression of Laforin alone was not enough to enhance P-Rex1 ubiquitination (Fig. 12A, lane 2). These results enable P-Rex1 to go from being a candidate to a bona fide substrate of Malin.

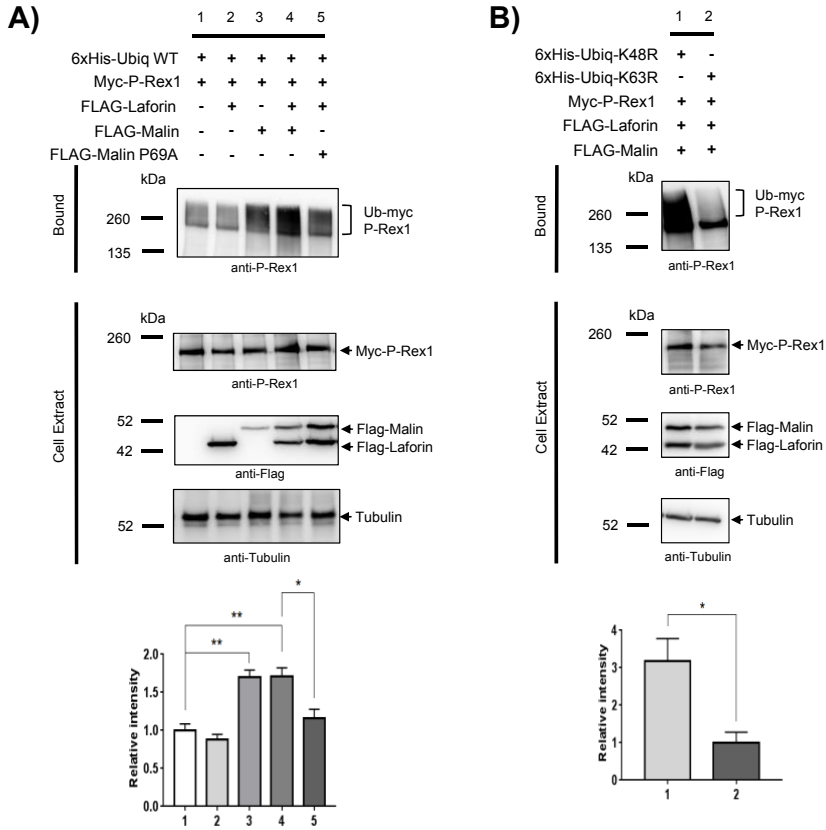

Fig. 12: Validation of P-Rex1 as a substrate of Malin. A) A functional Laforin/Malin complex ubiquitinates P-Rex1. HEK293 cells were transfected with the indicated plasmids and the ubiquitination analysis of P-Rex1 was performed as described in Materials and Methods. The analyses were carried out with wild type and inactive (P69A) forms of Malin. Proteins present in the bound fraction (Bound: proteins retained in the metal affinity resin) or in the crude cell extract (50 µg) were analyzed by Western blotting using the indicated antibodies. The lower panel shows the quantification of the ubiquitination signal. B) Topology of the ubiquitination reaction. Ubiquitination reactions were performed as in A) using modified forms of ubiquitin that carried K48R or K63R mutations, which prevent the formation of K48- or K63-linked chains, respectively. The lower panel shows the quantification of the ubiquitination signal. A) and B) are representative blots of three independent experiments. Values are the mean +/- SEM of three independent experiments (*$p<0.05$; **$p<0.01$).

Furthermore, we wanted to know what kind of polyubiquitin chains were formed on the substrate. Substrate ubiquitination can indicate a variety of cellular fates depending on the chain topology, the most well-known of which being degradation by the proteasome, which is common for substrates with K48 linked chains. (Komander and Rape 2012). For this purpose, we used ubiquitin forms that carried K48R or K63R mutations. The use of these ubiquitin mutants would prevent the formation of K48-linked chains, in the case of the mutated form K48R, or of K63-linked chains, in the case of the K63R mutant. Figure 12B shows that the Laforin-Malin complex promotes the attachment of K63-linked ubiquitin chains. We can observe in the second lane of Fig. 12B an impairment of the ubiquitination of P-Rex1 in cells expressing the mutated ubiquitin form K63R, contrary to lane 1 where cells expressed K48R-ubiquitins. This result confirms that Malin favors the attachment of K63-linked polyubiquitin chains as already described for other substrates in previous reports (Solaz-Fuster, Gimeno-Alcaniz et al. 2008, Moreno, Towler et al. 2010, Sharma, Mulherkar et al. 2012, Rubio-Villena, Garcia-Gimeno et al. 2013, Sanchez-Martin, Romá-Mateo et al. 2015, Viana, Lujan et al. 2015, Perez-Jimenez, Viana et al. 2020, Sanchez-Martin, Lahuerta et al. 2020).

The Laforin-Malin complex interacts physically with P-Rex1

Malin is classified as a TRIM-like protein in terms of structure. It is composed of an N-terminal RING domain which confers catalytic activity and a C-terminal domain composed of 6 NHL repeats (found in NCL1, HT2A, and LIN-41 proteins) (Gentry, Worby et al. 2005). Malin, opposed to the other TRIM proteins, lacks the B-box and coiled-coil domains. In general, TRIM-E3 ligases are known to interact with the target substrate via the RING domain to confer specificity in the transfer of ubiquitin during the last phase of the process (Budhidarmo, Nakatani et al. 2012). For this reason, we decided to look into the possibility of a physical interaction between the target substrate P-Rex1 and the Laforin-Malin complex. This analysis was carried out in HEK293 cells using

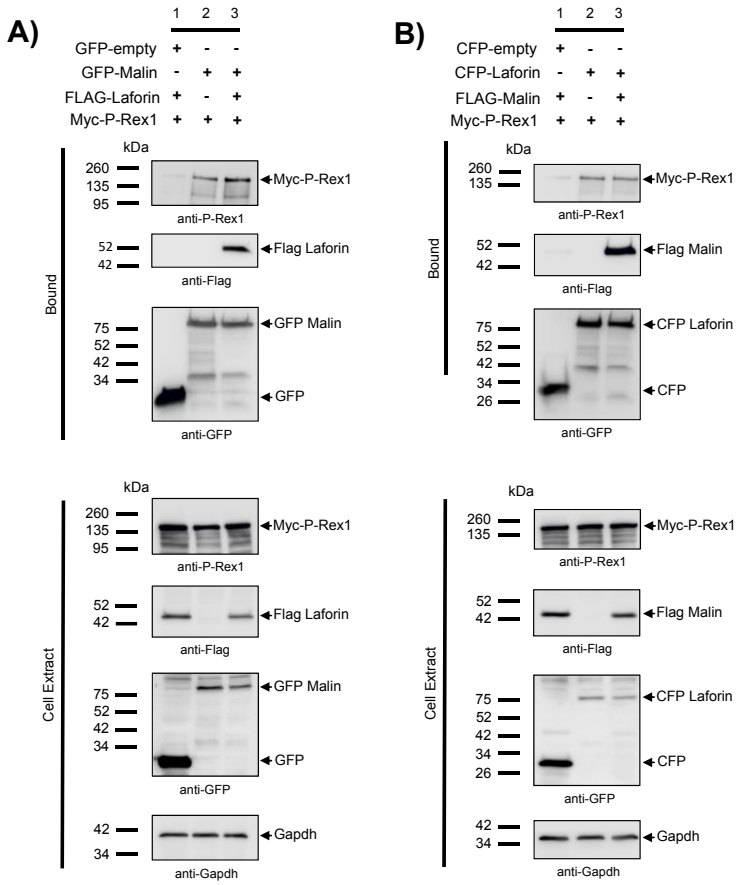

Fig. 13: The Laforin-Malin complex interacts physically with P-Rex1. A) GFP-Malin pull-downs P-Rex1. HEK293 cells were co-transfected with the indicated combination of plasmids expressing Myc-P-Rex1, FLAG-Laforin, GFP (empty), and GFP-Malin. Cells were lysed and 1.5 mg of proteins were incubated with GFP-trap beads, which bind the various GFP forms with high affinity. After washing, beads were boiled in loading buffer and the purified proteins were analyzed by SDS-PAGE and Western blot using anti-GFP. Anti-FLAG and anti-P-Rex1 antibodies, as indicated below the different panels. Bound: proteins retained in the beads; cell Extract: 30 µg of protein were loaded for the total fraction. B) CFP-Laforin pull-downs P-Rex1. HEK293 cells were co-transfected with the indicated combination of plasmids expressing Myc-P-Rex1, FLAG-Malin, CFP (empty), and CFP-Laforin. Extracts were analyzed as in A). A) and B) are representative blots of three independent experiments.

GFP-trap as described in Materials and Methods. In Figure 13A (lane 2), GFP-Malin was able to pull down P-Rex1 and this interaction was kept in the presence of Flag-Laforin (lane 3). P-Rex1 can interact with both Malin and Laforin, according to these studies. Similarly, we can see in Figure 13B the physical contact between Laforin and P-Rex1 (lane 2), which was maintained in the presence of Malin (lane 3) when the pulldown was carried using CFP-Laforin. These findings demonstrated that P-Rex1 may physically interact with Laforin and Malin both individually and as part of a complex.

Malin regulates P-Rex1 GEF activity on Rac1 GTPase

P-Rex1 is a member of the Rho guanine-nucleotide exchange factor (GEFs) family. They are characterized structurally by two types of catalytic domains (Dbl or DOCK) (Whitehead, Campbell et al. 1997, Machin, Tsonou et al. 2021), and are involved in the activation of Rac family small GTPase protein components (Rac1, Rac2, Rac3, and RhoG), which can control several cellular responses (Hall 1998, Wennerberg, Rossman et al. 2005). P-Rex1 contains the Dbl catalytic domain and, as a Rac-GEF, it promotes the release of GDP from Rac, which then binds to free GTP and assumes an active conformation. The active form of Rac, Rac-GTP, will promote its binding to downstream targets generating cellular responses (Rossman, Der et al. 2005, Cook, Rossman et al. 2014). Previous studies reported that P-Rex1 can activate the different members of the Rac family of small GTpases both *in vitro* and *in vivo*, with the exception that, *in vivo*, the isoform of Rac that gets activated depends mostly on the cell type and the upstream signal that initiates the cascade of activation. Indeed, Rac-GEFs, like P-Rex1, have a very low basal activity and, to activate small GTPases like Rac, they need an upstream stimulus (Welch, Coadwell et al. 2002, Welch 2015). Supported by these notions and by the work of other groups in demonstrating that P-Rex1 is an activator of Rac1 GTPase (Balamatsias, Kong et al. 2011, Thamilselvan, Gamage et al. 2020), one of our

goals was to understand whether the ubiquitination of P-Rex1 by Malin could affect its activity as a Rac1-GEF.

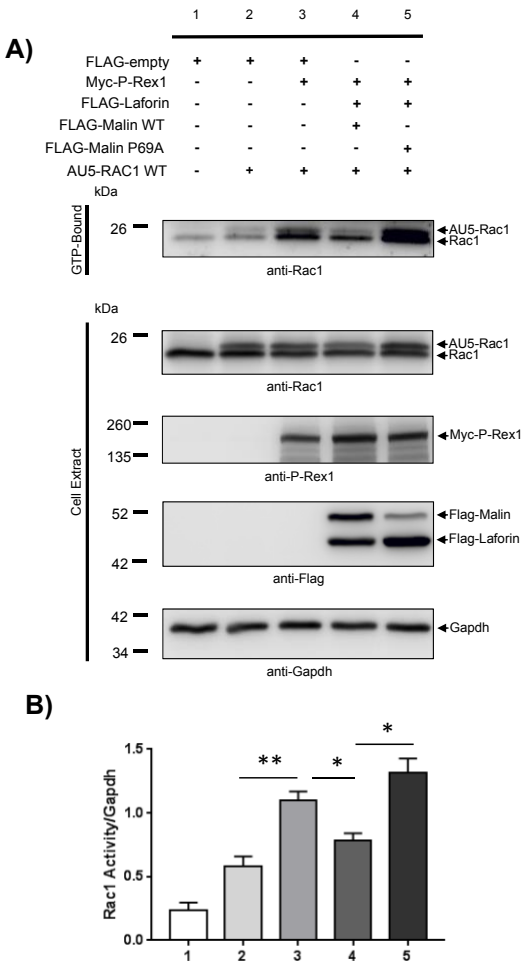

Fig. 14: Malin regulates Rac1 GTPase activity via P-Rex1. A) Rac1 pulldown assay was performed using a GST fusion protein containing the Rac1 binding domain of PAK1 (GST-RBD-PAK1). HEK293 cells were co-transfected with the plasmids expressing Myc-P-Rex1, FLAG-Laforin, FLAG-Malin, FLAG-Malin P69A, and AU5-Rac1 WT. Cells were lysed and 1.5 mg of protein were incubated with preloaded GST-RBD-PAK1-GSH-beads. The purified bound fraction and 30 µg of the crude extracts were analyzed by Western blot using the indicated antibodies. A representative blot of three independent experiments is shown. B) Quantification of the activated Rac1 signal related to the levels of Gapdh. Values are the mean +/- SEM of three independent experiments (*$p<0.05$, **$p<0.01$).

The first step was to confirm that P-Rex1 activates Rac1 GTPase in our cellular model. To measure Rac1 activation, a pulldown assay was performed, which involves the use of a Glutathione-S-Transferase (GST) fusion protein containing the Rac1 binding domain (RBD) of PAK1 (GST-RBD-PAK1) known to interact with Rac1 only when the GTPase is in its active form (Arrizabalaga, Lacerda et al. 2012). To have a better readout for the activated forms of Rac1, we expressed exogenously an AU5-tagged Rac1 construct. In lane 3 of Fig. 14A, we can observe that the expression of P-Rex1 in HEK293 cells was necessary to produce activated forms of Rac1 GTPase, both endogenous and in the form of AU5-Rac1 (compare the intensity of the Rac1 bands in lane 3 with those present in the absence of P-Rex1; lanes 1 and 2) (see Fig. 14B for quantification). However, the expression of a functional laforin-Malin complex produced a decrease in the amount of activated Rac1 GTPase forms (Fig. 14, lane 4; Fig. 14B). On the contrary, the expression of a non-functional Laforin-Malin complex, due to the presence of the Malin mutant form P69A, did not modify the level of activated forms of Rac1 present in lane 3 (Fig. 14, lane 14; Fig. 5B). Taken together, all these results lead us to hypothesize that the ubiquitination of P-Rex1 by Malin, through the introduction of polyubiquitin K63 chains, might result in a reduction in the activity of P-Rex1 as a Rac1-GEF. Next, we studied whether this effect could be due to an alteration in the stability of the protein due to its ubiquitination.

Malin-dependent ubiquitination of P-Rex1 reduces its protein stability

To establish whether the Malin-dependent ubiquitination of P-Rex1 could affect its protein stability we used primary astrocytes from the control and *Epm2b*-/- LD mouse model. Our group has already demonstrated that this LD mouse model recapitulates the hallmark of the disease (Rubio-Villena, Viana et al. 2018, Moreno-Estellés, Campos-Rodríguez et al. 2023). We have used this model since P-Rex1 has been proven to be expressed at the level of the brain

(Welch, Coadwell et al. 2002, Yoshizawa, Kawauchi et al. 2005), and primary astrocytes express enough levels of endogenous P-Rex1 to be detected by western blot using appropriate antibodies. So, we decided to measure its protein stability by subjecting primary astrocytes from control and *Epm2b-/-* mice to cycloheximide (CHX) treatment. The function of CHX is to block *de novo* protein synthesis and this allows us to evaluate the degradation rate of existing proteins following the initiation of the treatment. In this way, we can assess whether there is a difference in the degradation rate of the P-Rex1 substrate in control vs *Epm2b*-/- astrocytes.

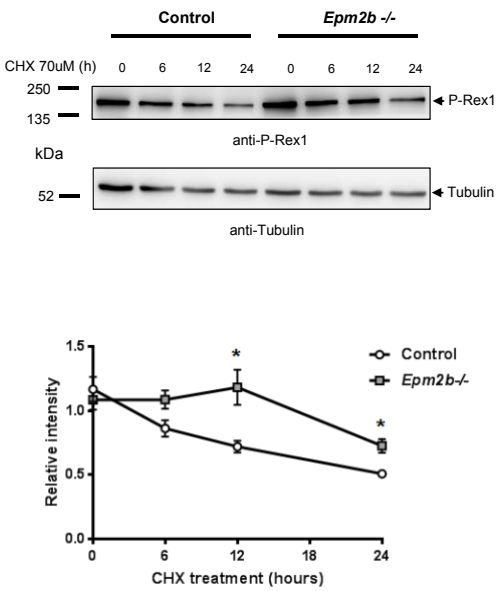

Fig. 15: Analysis of the Degradation Rate of P-Rex1. Primary astrocytes from *Epm2b-/-* and control mice were treated with 70 µM cycloheximide for different time points (from 0 to 24 h). Cells were lysed and 30 µg of the crude extracts were analyzed by Western blot. At the time points of 12 and 24 h, in *Epm2b*-/- astrocytes the amount of P-Rex1 was higher compared to the control, suggesting impairment in the rate of the degradation process due to the absence of Malin. A representative blot of five independent experiments is shown. In the lower panel, we show the quantification of the relative levels of P-Rex1 at each time point. Values are the mean +/- SEM of five independent experiments (*$p<0.05$).

As we can see in Figure 15, in the control astrocytes we could appreciate the rate of degradation of the substrate starting from 12 h of treatment with CHX. In comparison, at the same time point, in *Epm2b*-/- astrocytes the amount of P-Rex1 was higher, suggesting impairment in the rate of the degradation process due to the absence of Malin. After 24 h of CHX treatment, this difference in the degradation rate was still evident between control and *Epm2b*-/- samples. This result highlights the possibility that the Malin-dependent ubiquitination of endogenous P-Rex1 was responsible to direct P-Rex1 toward a degradative fate.

Increased glucose uptake in *Epm2b*-/- primary astrocytes

Then, we decided to focus on the physiological outcome of the longer half-life of P-Rex1 in *Epm2b*-/- astrocytes. In addition to the recognized role that P-Rex1 has in cancer (Qiu, Chang et al. 2020, Srijakotre, Liu et al. 2020, Beltran-Navarro, Reyes-Cruz et al. 2022), it also plays a role in glucose homeostasis (Moller, Klip et al. 2019, Machin, Tsonou et al. 2021). In this sense, it has been demonstrated that P-Rex1 promotes the translocation of the glucose transporter GLUT4 to the plasma membrane on 3T3-L1 adipocytes cells (Balamatsias, Kong et al. 2011). Supported by these data, we compared the rate of glucose uptake in primary astrocytes from control and *Epm2b*-/- mice, as described in Materials and Methods. As a control, we treated astrocytes with metformin, a compound known to increase glucose uptake (Polianskyte-Prause, Tolvanen et al. 2019). As can be observed in Fig. 16A, we found higher glucose uptake in astrocytes from *Epm2b*-/- than in controls. Treatment with metformin increased glucose uptake in control, and *Epm2b*-/- astrocytes.

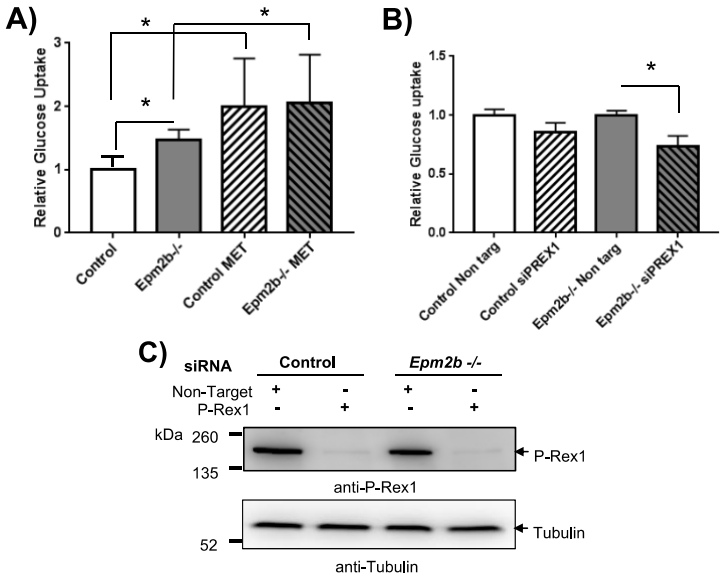

Fig. 16: Glucose uptake A) Primary astrocytes (Control and *Epm2b-/-*) were used to measure the rate of glucose uptake as indicated in Materials and Methods. To minimize differences between different samples, we performed the experiment by platting control and *Epm2b-/-* cells at the same time. Then we analyze the glucose uptake and plotted the relative values of glucose transport related to those found in the control sample, which was adjusted to 1. Astrocytes were also treated with 2 mM Metformin for 24 hours, as a control for an increase in glucose uptake. Values are the mean of four independent experiments +/- SEM (*$p<0.05$). B) The expression of P-Rex1 was silenced in primary astrocytes (Control and *Epm2b-/-*) by using 20 nM of SmartPool P-Rex1 siRNA or Non-Target siRNA (see Materials and Methods). Then, glucose uptake was measured as above. Values are referred to the corresponding cells treated with Non-Target siRNA, which was adjusted to 1. Values are the mean of three independent experiments +/- SEM (*$p<0.05$). C) An aliquot of the treated siRNA cells was analyzed by western blot using anti-P-Rex1 and anti-tubulin (loading control) antibodies. Molecular size markers are indicated on the left.

In order to assess for the possible connection between P-Rex1 and glucose uptake in *Epm2b-/-* astrocytes we decided to silence the expression of P-Rex1 in these cells. As it is indicated in Fig. 16B, the silencing of P-Rex1 in *Epm2b-/-* astrocytes resulted in a statistically significant decrease in glucose uptake. Silencing of control astrocytes also showed a tendency to decrease

glucose uptake (Fig. 16C confirms the reduction in P-Rex1 expression upon silencing). These results suggest a close relationship between the levels of P-Rex1 and the capacity to uptake glucose.

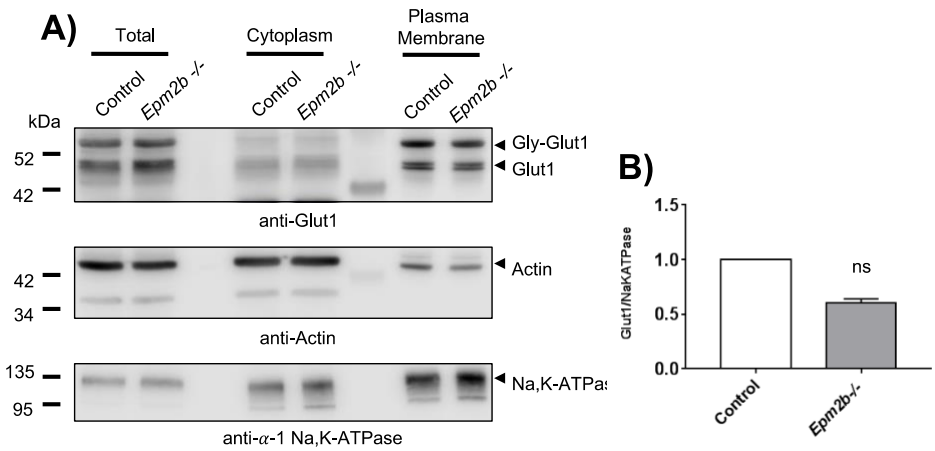

Fig. 17: Analysis of cell surface proteins by biotinylation. A) Analysis of the cell surface biotinylation assay performed as indicated in Materials and Methods. An aliquot of the lysate was saved for Western blotting (Total fraction). The biotinylated fraction was isolated with NeutrAvidin beads, eluted by the sample buffer containing DTT, and subjected to Western blot analysis (Plasma membrane fraction). The unbound fraction (Cytoplasm) was analyzed too. No differences were observed in the levels of the glycosylated (55 kDa; Gly-GLUT1) or the non-glycosylated (45 kDa; GLUT1) forms of GLUT1 either in the total fraction or in the plasma membrane fraction. Actin and Na+/K+-ATPase were used as controls of cytoplasm and plasma membrane fractions, respectively. Blots are representative images of three independent experiments. B) Quantification of the levels of GLUT1 related to the levels of Na+,K+-ATPase at the plasma membrane fraction. Values are the mean +/- SEM of three independent experiments; ns: no statistically significant differences.

Next, we wanted to check if the increase in glucose uptake in *Epm2b-/-* astrocytes was due to higher levels of glucose transporters at the plasma membrane. With this aim, we used the Pierce Cell Surface Protein Isolation Kit, which consists in treating the cells with EZ-LINK Sulfo-NHS-SS-biotin that will bind to the proteins of the plasma membrane. The biotinylated protein

fraction, corresponding only to plasma membrane proteins, is then isolated with NeutrAvidin beads. We analyzed the presence of GLUT1, the main glucose transporter present in astrocytes, in the purified fraction by using GLUT1-specific antibodies. As shown in Fig. 17A, the purified biotinylated fraction of plasma membrane proteins was enriched in the Na+/K+-ATPase (lower panel), a regular plasma membrane protein, and decreased In the levels of actin, a cytosolic marker (middle panel). However, we did not observe any difference in the levels of the glycosylated (55 kDa) or the non-glycosylated (45 kDa) forms of GLUT1 between control and *Epm2b-/-* astrocytes (Fig. 17A upper panel, and 17B). Taken together, these results indicate that the differences in glucose uptake that we appreciate in *Epm2b*-/- compared to control must depend probably on the increased activity of the glucose transporter rather than on changes in its protein levels at the cell surface.

3.- Validate Hsp90 as a substrate of Malin and outline its ubiquitination effect

Validation of Hsp90α as a substrate of Malin

To date, it is known that Hsp90α is ubiquitinated by three E3 ubiquitin ligases: HECTD1 (Sarkar and Zohn 2012), CHIP (Kundrat and Regan 2010) and FBXL6 (Shi, Feng et al. 2020). In order to add Malin among the known E3 ubiquitin ligases for Hsp90α we transfected HEK293 cells with the combination of plasmids reported in Figure 18.

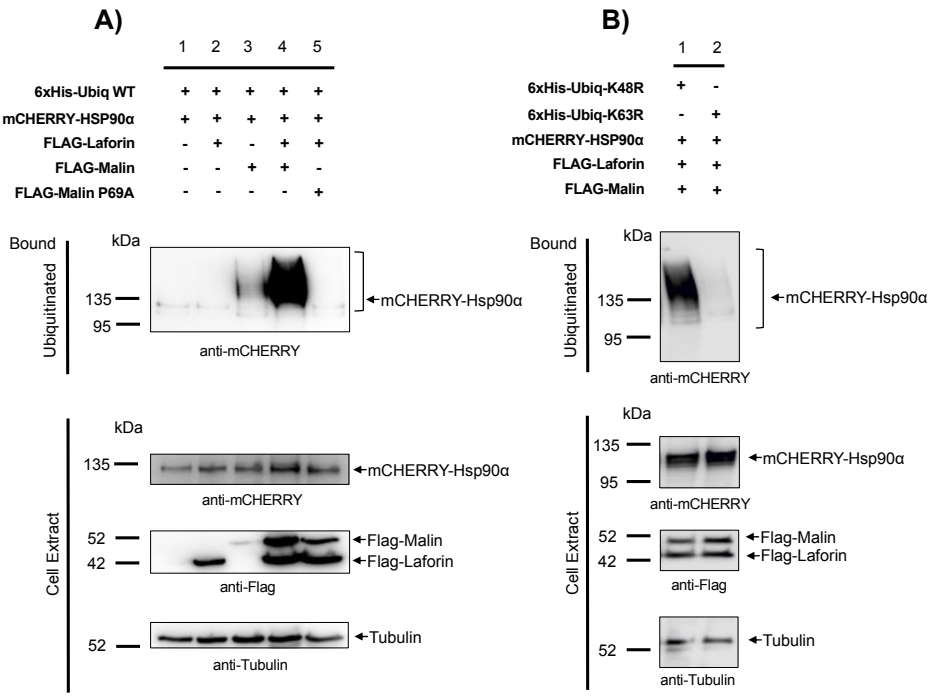

Fig. 18: Validation of Hsp90α as a substrate of Malin. A) A functional Laforin/Malin complex ubiquitinates over expressed Hsp90α. HEK293 cells were transfected with the indicated plasmids and the ubiquitination analysis was performed as described in Materials and Methods. The analyses were carried out with wild type and inactive (P69A) forms of Malin. Proteins present in the bound fraction (Bound: proteins retained in the metal affinity resin) or in the crude cell extract (50 µg) were analyzed by Western blotting using the indicated antibodies. B) Topology of the ubiquitination reaction. Ubiquitination reactions were performed as in A) using modified forms of ubiquitin that carried K48R or K63R mutations, which prevent the formation of K48- or K63-linked chains, respectively.

To be sure to detect a ubiquitination signal, we overexpressed Hsp90α and subsequently, we also performed the ubiquitination assay without overexpressing Hsp90α (Fig 19). The reason why we also tried to seek for endogenous levels of ubiquitinated Hsp90α, resides in the fact that this protein is abundant in many types of cells and, as described in the Human Protein Atlas

(https://www.proteinatlas.org/ENSG00000080824-HSP90AA1/cell+line), it has a sufficient level of expression in HEK293 to be detected endogenously.

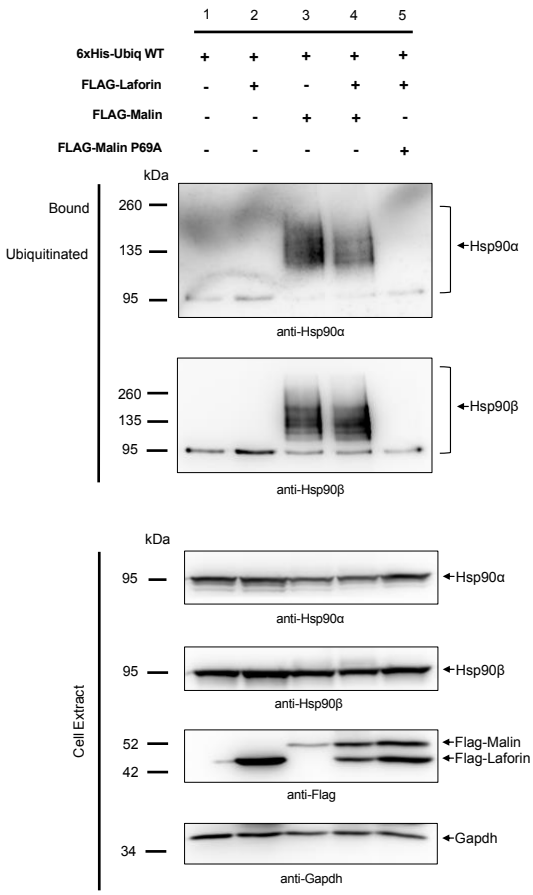

Fig. 19: Validation of endogenous Hsp90α as a substrate of Malin. Laforin/Malin complex ubiquitinates Hsp90α at its endogenous levels. HEK293 cells were transfected with the indicated plasmids and the ubiquitination analysis was performed as described in Materials and Methods. The analyses were carried out with wild type and inactive (P69A) forms of Malin. Proteins present in the bound fraction (Bound: proteins retained in the metal affinity resin) or in the crude cell extract (50 µg) were analyzed by Western blotting using the indicated antibodies.

From the experiments performed, we can see that both in lane 4 of Fig. 18A and in Fig. 19, overexpressed and endogenous Hsp90α were ubiquitinated in cells co-transfected with the functional complex of Laforin-Malin compared

to cells expressing only pCMV-6xHisUbiq (Fig. 18A and Fig. 19, lanes 1). Also, ubiquitination of overexpressed and endogenous Hsp90α was absent in cells co-transfected with Laforin and the inactive form of Malin (P69A) compared to cells expressing the wild type version of Malin (Fig 18A and Fig. 19, lanes 5). In addition, similarly to the co-transfection of cells with the functional complex in lane 4, overexpressed and endogenous Hsp90α were ubiquitinated in cells that have been transfected only with Malin-WT plasmid (Fig 18A and Fig 19, lanes 3), probably indicating that the endogenous levels of Laforin present inside the cells were enough for Malin to perform its ubiquitin E3 ligase activity. However, this was not the case of the transfection of cells with only Laforin (Fig 18A and Fig 19, lanes 2) suggesting that Malin had to be overexpressed to manifest its function. These findings identify Hsp90α to be a proven substrate of Malin that can be consequently added to the list of known E3 ubiquitin ligases for Hsp90α. In addition, we also checked the β isoform of the chaperone due to the fact that it is among the list of 88 candidates of the proteomic analysis.

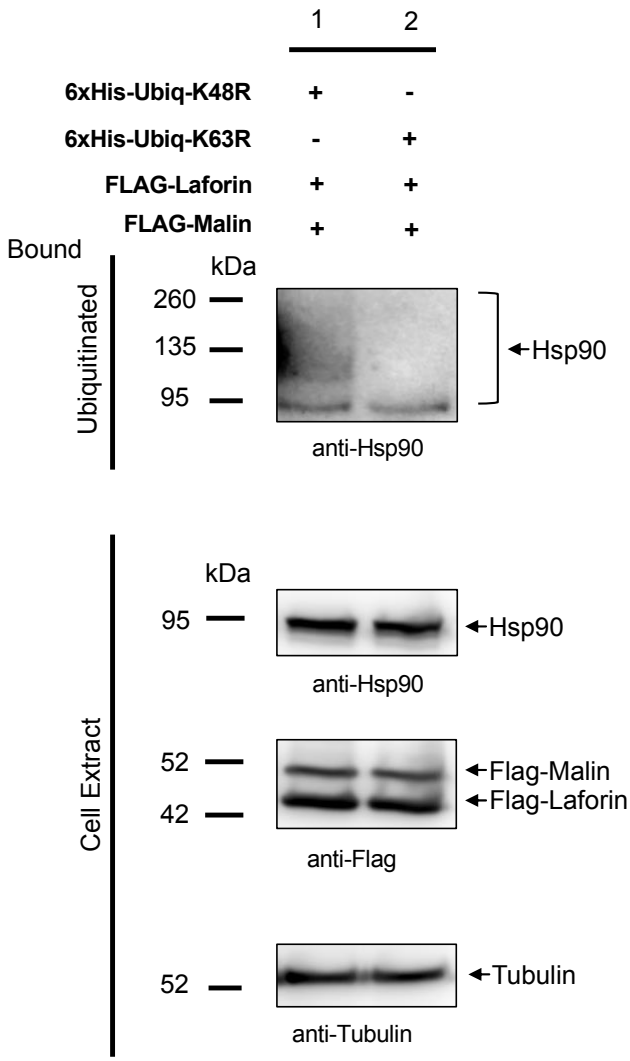

Fig. 20: Topology of the ubiquitination reaction. Ubiquitination reactions were performed by using modified forms of ubiquitin that carried K48R or K63R mutations, which prevent the formation of K48- or K63-linked chains, respectively. Proteins present in the bound fraction (Bound: proteins retained in the metal affinity resin) or in the crude cell extract (50 μg) were analyzed by Western blotting using the indicated antibodies.

Similarly, to the other novel substrate described in this thesis, also for Hsp90α we wanted to check the topology of the polyubiquitin chains that get attached to the substrate. As it occurs for P-Rex1 also for Hsp90α, the Laforin-Malin complex increases the attachment of K63-linked ubiquitin chains both to overexpressed Hsp90α and endogenous Hsp90 (Fig 18B and Fig 20). The mutated form of K63, given by overexpression of K63R ubiquitin in lane 2 of figure 18B and lane 3 of Fig 20, prevented the ubiquitination of Hsp90α and total endogenous Hsp90, respectively. On the contrary, the mutated form of K48, given by overexpression of K48R ubiquitin in lane 1 of figure 18B and lane 2 of Fig 20, did not prevent the ubiquitination of overexpressed Hsp90α and total endogenous Hsp90. In this regard, in Figure 20, to check endogenous ubiquitination of the chaperone, it seems convenient to use an antibody that recognizes both the α and β form since we know that also the latter isoform is a substrate of Malin. This outcome, again, confirms the observations that Malin prefers the attachment of K63-linked polyubiquitin chains on its substrates.

Hsp90α physically interacts with Malin but not with Laforin

As a chaperone, Hsp90 may interact with a wide range of client proteins (Karagoz and Rudiger 2015, Shi, Feng et al. 2020) including Malin (as reported in https://www.picard.ch/downloads/Hsp90interactors.pdf). With the fact that we are focusing on a particular isoform of Hsp90, we wanted to verify if the alpha isoform can physically interact with Malin or Laforin. Also, in this case, the interaction between the proteins of the complex and the chaperone were analyzed in over-expressed and endogenous conditions of the latter. For this, we performed a GFP-trap experiment in which HEK293 cells were transfected with the combination of plasmids shown in Figures 21, 22 and 23.

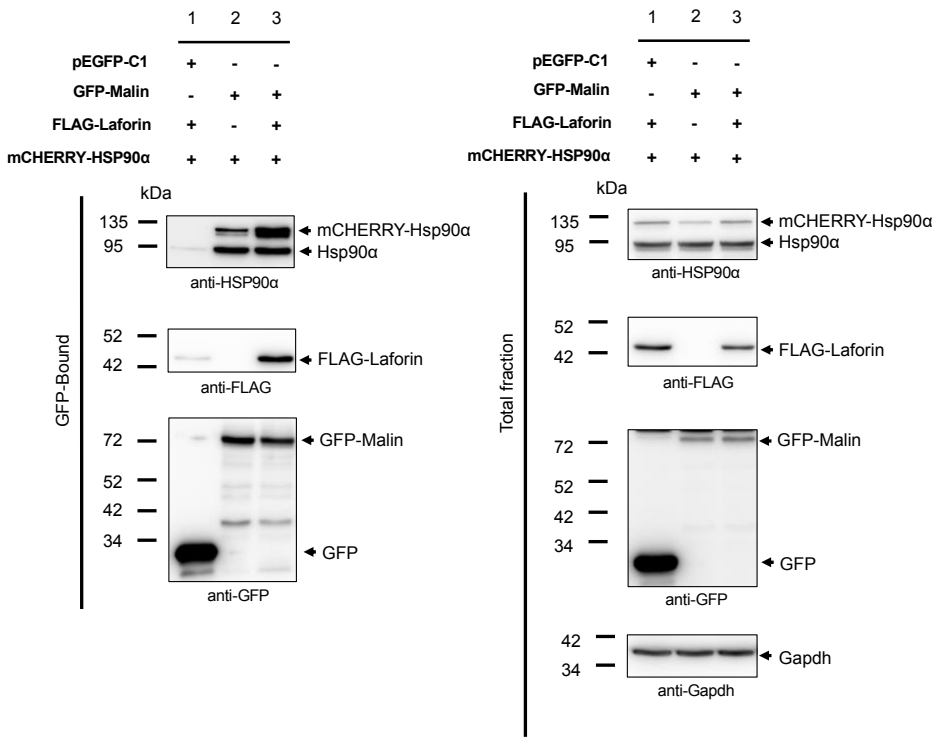

Fig. 21: Malin interacts physically with over expressed Hsp90α. HEK293 cells were co-transfected with the indicated combination of plasmids expressing mCHERRY-Hsp90α, FLAG-Laforin, pEGFP-C1 (empty), and GFP-Malin. Cells were lysed and 1.5 mg of proteins were incubated with GFP-trap beads which bind the various GFP forms with high affinity. After washing, beads were boiled in loading buffer and the purified proteins were analyzed by SDS-PAGE and Western blot using anti-GFP, anti-FLAG and anti- Hsp90α antibodies, as indicated below the different panels. Bound: proteins retained in the beads; Cell Extract: 30 μg of protein were loaded for the total fraction.

By analyzing the interaction between over-expressed Hsp90α and Malin, in Figure 21 (lane 2) we can see that GFP-Malin is able to pull down over-expressed Hsp90α and with the introduction of Flag-Laforin WT, in lane 3, the interaction is maintained. Since, during these experiments we noticed that GFP-Malin was also able to pulldown endogenous Hsp90α, we decided to perform the GFP-trap experiment in endogenous conditions. In addition, knowing that the mutated form of Malin P69A is not able to ubiquitinate

Hsp90α, we wanted to understand, if in terms of interaction, such site was essential or not. For this purpose, we performed the GFP-trap experiments also by adding additional conditions in which GFP-Malin P69A was over-expressed during GFP-Malin pulldown.

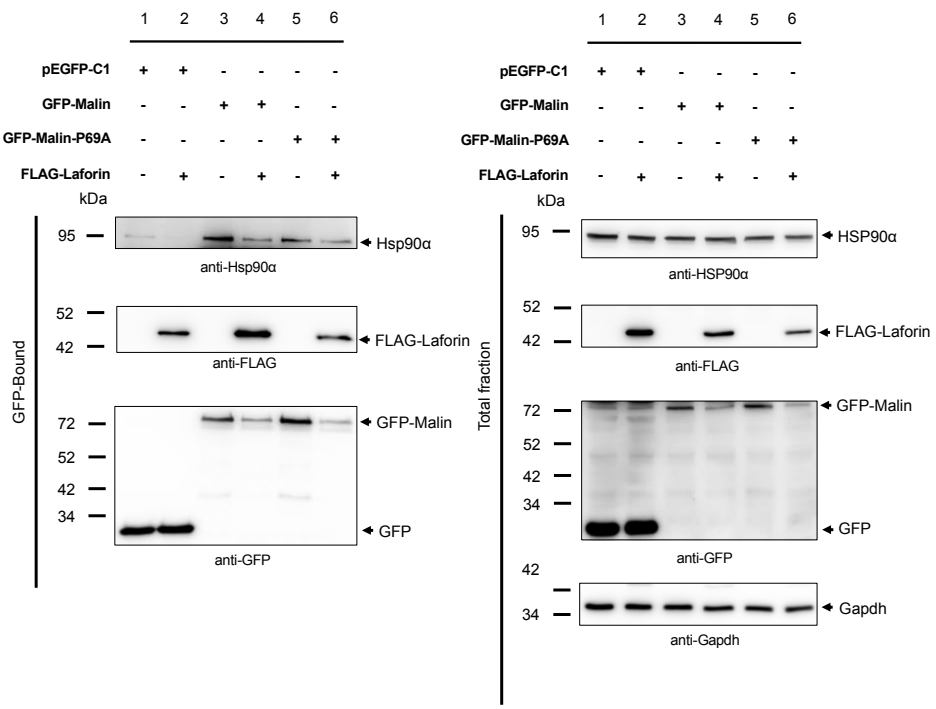

Fig. 22: Malin interacts physically with endogenous Hsp90α. HEK293 cells were co-transfected with the indicated combination of plasmids expressing FLAG-Laforin, pEGFP-C1 (empty), GFP-Malin and GFP-Malin P69A. Cells were lysed and 1.5 mg of proteins were incubated with GFP-trap beads which bind the various GFP forms with high affinity. After washing, beads were boiled in loading buffer and the purified proteins were analyzed by SDS-PAGE and Western blot using anti-GFP, anti-FLAG and anti- Hsp90α antibodies, as indicated below the different panels. Bound: proteins retained in the beads; Cell Extract: 30 µg of protein were loaded for the total fraction.

In lane 3 of Figure 22 we can see that GFP-Malin can pulldown endogenous Hsp90α and that interaction is kept also when Flag-Laforin is over-expressed. Similar results were achieved and reported in Figure 21. Also, GFP-Malin-P69A (Fig. 22, lane 5) can pulldown endogenous Hsp90α and in the presence of Flag-Laforin, interaction is present but to a lesser extent (Fig. 22, lane 6).

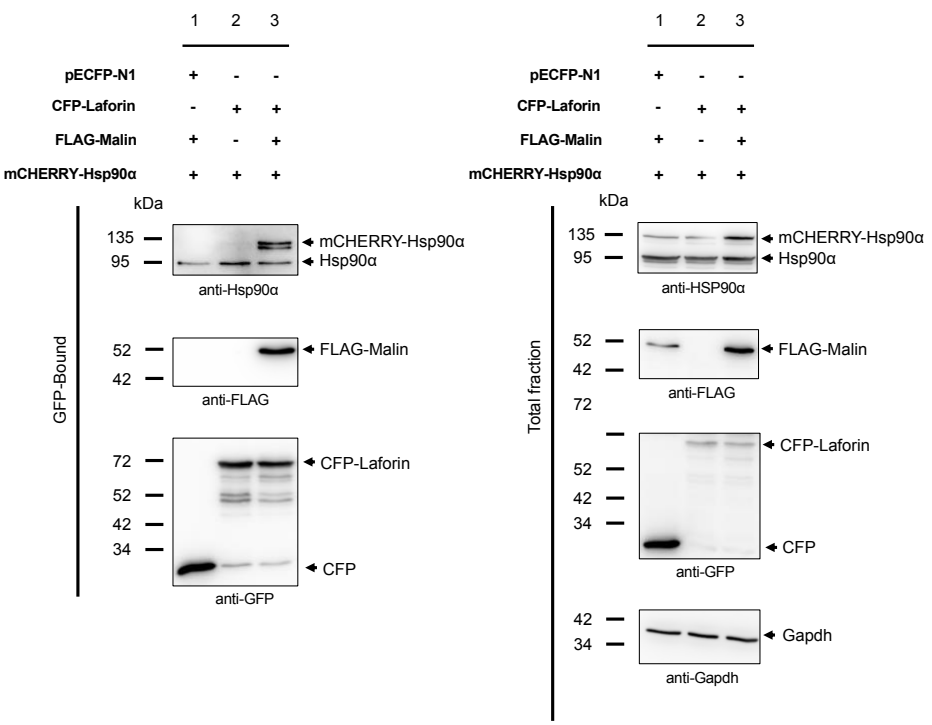

Fig. 23: Laforin cannot interact physically with over expressed Hsp90α. HEK293 cells were co-transfected with the indicated combination of plasmids expressing mCHERRY-Hsp90α, FLAG-Malin, pECFP-N1 (empty), and CFP-Laforin. Cells were lysed and 1.5 mg of proteins were incubated with GFP-trap beads which bind the various GFP forms with high affinity. After washing, beads were boiled in loading buffer and the purified proteins were analyzed by SDS-PAGE and Western blot using anti-GFP, anti-FLAG and anti- Hsp90α antibodies, as indicated below the different panels. Bound: proteins retained in the beads; Cell Extract: 30 μg of protein were loaded for the total fraction.

Then, we analyzed the ability of CFP-Laforin to pull-down Hsp90α. In Figure 23, CFP-Laforin, in lane 2, is not able to pulldown the over-expressed form of Hsp90α. However, CFP-Laforin can pulldown the over-expressed substrate when Flag-Malin WT is introduced.

In summary, these data suggest that the Hsp90α isoform can physically interact with Malin, both in its WT form and in its mutated form but, it is not able to interact with Laforin. It is important to underline that for this type of study we can only corroborate whether there is interaction between Hsp90α and either Laforin or Malin, but we are not able to define or measure the amount of interaction. Moreover, pulldown of the endogenous substrate by GFP-Malin-P69A seems to suggest that the inactive form conserves the interaction with Hsp90α even if the ubiquitination of this substrate is lost.

Malin-dependent ubiquitination of Hsp90α does not alter its protein stability

After analyzing interaction status between the molecular chaperone and the protein of the complex, we wondered whether a lack of ubiquitination of Hsp90α by Malin could lead to degradation. In the first place, we wanted to investigate whether the stability of Hsp90α is affected in somehow in the primary astrocytes from the control and *Epm2b*-/- LD mouse model (Rubio-Villena, Viana et al. 2018, Moreno-Estellés, Campos-Rodríguez et al. 2023) through CHX treatment.

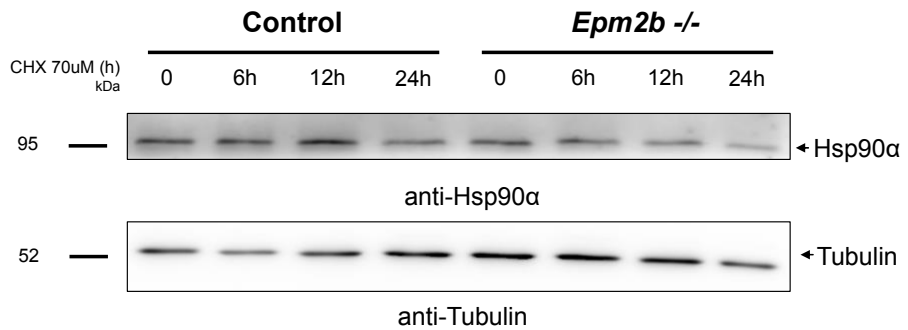

Fig. 24: Analysis of the Degradation Rate of Hsp90α. Primary astrocytes from *Epm2b-/-* and control mice were treated with 70 μM cycloheximide for different time points (from 0 to 24 h). Cells were lysed and 30 μg of the crude extracts were analyzed by Western blot.

By performing the experiment several times, following the conditions reported in Figure 24, we could only conclude that the stability of Hsp90α seems not to be affected in our disease cell model.

Hsp90 isoforms in the cortex and hippocampus of LD mouse model

To sustain the previous result of the CHX experiment, we also analyzed the levels of the molecular chaperones in the cortex and hippocampus (Fig. 25 A, B and C) coming from control and *Epm2b*-/- LD mouse model. These regions were analyzed since studies show that, together with the cerebellum, cortex and hippocampus are characterized by the presence of high amounts of LBs in *Epm2b*-/- mice (Criado, Aguado et al. 2012). As we can see in Figure 25A, in cortex, there is no difference in the levels of Hsp90 isoforms in *Epm2b*-/- compared to control. The same happens at the level of hippocampus: there is no difference of either of the Hsp90 isoforms (Fig. 25 B and C). From these results, we can only conclude that the stability of the isoforms of the molecular chaperone Hsp90 are not affected in these brain regions in of *Epm2b*-/- mice.

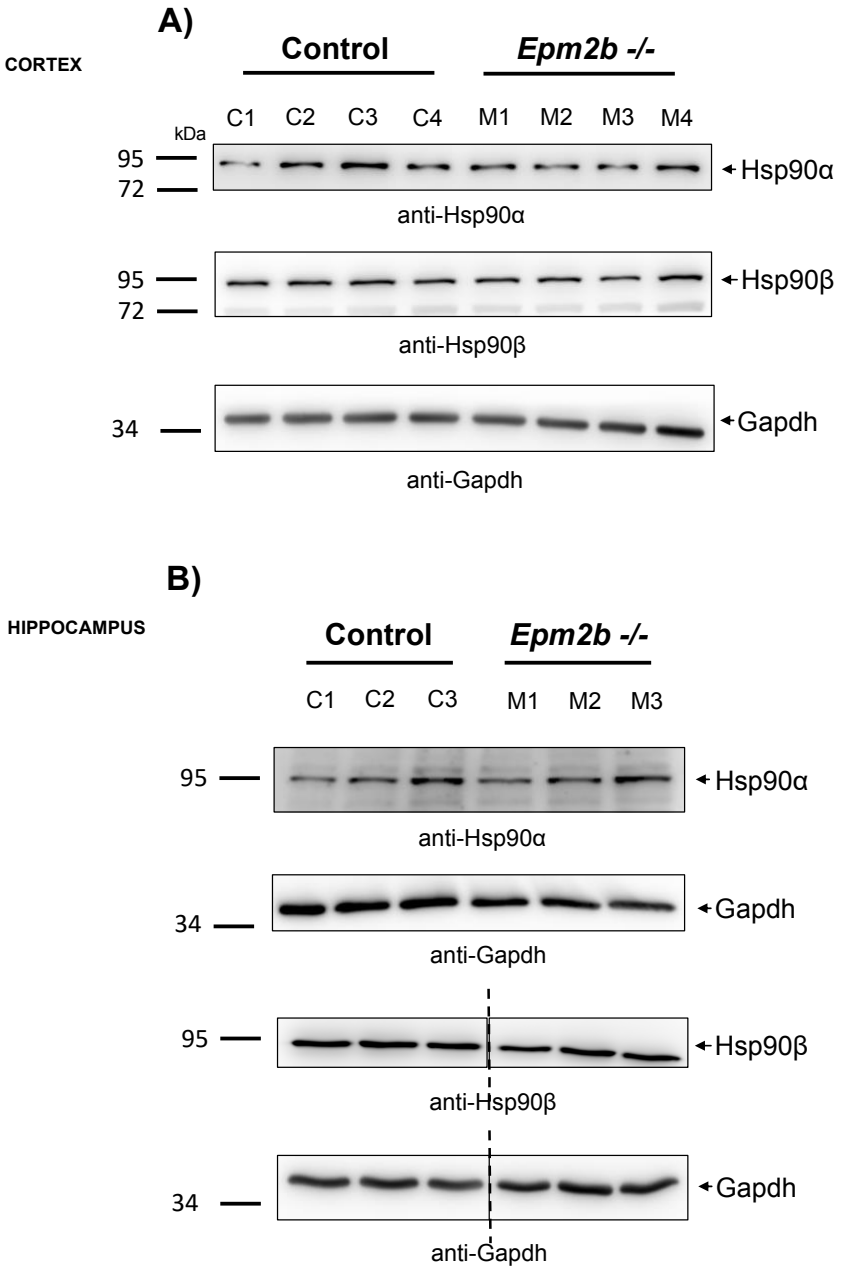

Fig. 25: Hsp90 isoforms in cortex and hippocampus mice sample. Cortex and hippocampus tissue samples were obtained from *Epm2b-/-* and control mice of 16 month. Cortex and hippocampus were lysed separately. 30 µg of the crude extracts were analyzed by Western blot. The dashed line indicates the elimination of some unrelated lanes in the same filter.

DISCUSSION

Discussion

Lafora disease is characterized by different physiological dysfunctions (Garcia-Gimeno, Knecht et al. 2018). Many of these still need more elucidations on different molecular aspects. In this thesis, I have particularly focused on the function of Malin, which is known to have an E3 ubiquitin ligase activity. Malin places ubiquitin moieties on certain proteins which in turn are directed towards different destinies. In the absence of a functional Malin, it follows that these substrates, not undergoing the post-translational modification of ubiquitin, can lead to pathological and dysfunctional consequences. For this reason, it is necessary to focus enough attention on finding new substrates of Malin. This can help better delineate the dysfunctions already described by us and by other groups present in LD, and, eventually, also find out other possible defects that are still unknown and that could better define this rare disease.

To date, several substrates have been discovered and described for Lafora disease and these were identified thanks to studies focusing on the physical interaction between Malin and the substrates (Solaz-Fuster, Gimeno-Alcañiz et al. 2008, Moreno, Towler et al. 2010, Sharma, Mulherkar et al. 2012, Rubio-Villena, Garcia-Gimeno et al. 2013, Sanchez-Martin, Romá-Mateo et al. 2015, Viana, Lujan et al. 2015, Perez-Jimenez, Viana et al. 2020, Sanchez-Martin, Lahuerta et al. 2020). Therefore, techniques such as Co-Immunoprecipitation, yeast two-hybrid, etc. have been adopted (Table 1). However, it should be taken into consideration that the interaction between an E3 ligase and a protein does not always presuppose the ubiquitination of the second by the first. Thus, there might be other reasons why a given protein may interact with a particular E3 ligase, such as the need to structurally stabilize itself or simply the need to form a certain complex with other proteins. Therefore, in the search for new possible candidate substrates, we decided to adopt an alternative strategy that instead exploited the ubiquitination activity of Malin. For this reason, upon collaboration with the group of Dr Ugo Mayor

(Department of Biochemistry and Molecular Biology. Faculty of Science and Technology. UPV/EHU. Leioa. Bizkaia), the first step of this work was to identify novel candidate substrates of Malin through an unbiased approach based on the activity of Malin as an E3-ubiquitin ligase using the bioUb strategy (Franco, Seyfried et al. 2011, Martinez, Lectez et al. 2017, Ramirez, Lectez et al. 2018). This procedure enabled the enrichment and isolation of ubiquitin conjugates present in cells expressing Malin-WT or an inactive form of Malin (P69A).

Throughout a proteomic analysis ran over the data obtained thanks to the bioUb strategy, 88 differentially ubiquitinated potential candidates were discovered (listed in Annex 1). Further analysis of these proteins indicated that the biological processes they were involved in were mainly protein folding, heat shock response, and regulation of mitochondrial function (Fig. 11B, upper panel), and that their molecular functions were heat shock proteins and ubiquitin ligases (Fig. 11B, lower panel). Most of the potential candidates clustered into two groups, the heat shock protein (HSP) group and the OXPHOS group (Fig. 11C) (Table 2). Among the list of proteins, we thought we would see some of the known substrates of Malin related to glycogen biosynthesis/regulation, but eventually, none of them made it through the stringent filters employed to identify candidates with the bioUb strategy. This could have been determined by the fact that maybe glycogen-related proteins had lower ubiquitination rates than the rest of the identified proteins, and/or that the levels of these proteins were lower than the more abundant modified proteins present in cells. Nevertheless, the results obtained correlate with previous studies that report that Malin can interact with several heat shock proteins by yeast two-hybrid or co-immunoprecipitation (Garyali, Siwach et al. 2009, Rao, Sharma et al. 2010, Sun, Dukhande et al. 2019).

Among the 88 candidates obtained, we decided to focus on two of them. The first is P-Rex1, which prevailed among all other candidates in terms of ubiquitination rate (>18 fold). The second is Hsp90α, a heat shock protein

(HSP). Besides Hsp90α, we identified other HSPs belonging to this group. However, the choice to study this heat shock protein was due to the fact that, among the chaperones, Hsp90α was the one that had a major number of unique peptides in the proteomic analysis. In addition, Hsp90α expression can be studied endogenously and is enhanced by stress conditions, unlike the isoform Hsp90β which is constitutively expressed (Csermely, Schnaider et al. 1998). We thought it appropriate to take this aspect into account as the stress conditions could be exploited further to explain the existence of a relationship between Hsp90α and Malin and how the ubiquitination by the latter could affect the former. In addition to Hsp90α, we thought it appropriate to also analyze the isoform β as a possible substrate of Malin since the two isoforms share ~85% sequence identity (Johnson 2012, Hoter, El-Sabban et al. 2018).

P-Rex1

To establish whether P-Rex1, the candidate with the highest ubiquitination rate of all, was indeed a substrate of Malin, we proceeded to verify if it was ubiquitinated by this E3 ubiquitin ligase. The direct ubiquitination assay performed for this purpose showed how P-Rex1 was ubiquitinated in the presence of the Laforin-Malin complex and how this ubiquitination decreased in the presence of an inactive form of Malin (Fig. 12A). Through the same method, we also confirmed for this substrate, the tendency of Malin to introduce K63-type polyubiquitin chains (Fig. 12B), as in the case of other substrates described in previous reports by us and other groups [see (Garcia-Gimeno et al., 2018) for review]. This Malin-dependent ubiquitination of P-Rex1 was promoted by a physical protein-protein interaction between the Laforin/Malin complex and P-Rex1 (Fig. 13A and 13B).

P-Rex1 is a Rac-GEF whose function is to activate GTPases that are in their inactive state (Welch, Coadwell et al. 2002, Hill and Welch 2006). Rac1 is one of the GTPases that is activated by P-Rex1 (Balamatsias, Kong et al. 2011,

Thamilselvan, Gamage et al. 2020). According to this, our goal was to determine whether the Laforin-Malin complex could alter P-Rex1 action on Rac1. We verified that P-Rex1 could activate Rac1 and, more significantly, we showed that the Laforin/Malin complex blocked Rac1 activation in HEK293 cells. However, expression of a non-functional Laforin/Malin complex (characterized by the Malin P69A form) had no impact on the amounts of Rac1's activated forms (Fig. 14). We want to draw attention to the fact that, in contrast to the more well-known regulation of GEF activity by phosphorylation (Crespo, Schuebel et al. 1997, Llavero, Urzelai et al. 2015), our work defines for the first time that the activity of a Rac1 GEF can be altered by ubiquitination.

These findings prompted us to hypothesize that P-Rex1 ubiquitination by Malin has an impact on the protein's stability and that may have caused the substrate to degrade. Since HEK293 cells only produce very low amounts of this protein, we had to change our experimental strategy to a cellular system where endogenous P-Rex1 levels could be measured to confirm this theory. For this reason, we used cell cultures of astrocytes from *Epm2b*-/- and WT mice. We concluded that the rate of substrate breakdown in primary *Epm2b*-/- astrocytes was slower than in WT astrocytes by subjecting these cells to cycloheximide (CHX), a *de novo* protein synthesis inhibitor (Fig. 15). This enabled us to hypothesize that P- Rex1's degradation rate is decreased in the absence Malin, potentially due to an improper substrate ubiquitination.

Next, we wanted to check if this increase in the levels of P-Rex1 was modulating any physiological process. Given that P-Rex1 promotes the translocation of the glucose transporter GLUT4 to the plasma membrane on 3T3-L1 (Balamatsias, Kong et al. 2011), which has been linked to glucose homeostasis (Moller, Klip et al. 2019, Machin, Tsonou et al. 2021), we examined glucose uptake in astrocytes from control and *Epm2b*-/- mice. We observed increased glucose uptake in *Epm2b*-/- astrocytes, which suggests that Malin's absence promotes the transport of more glucose into the cell (Fig 16A).

We hypothesize that this increase might be caused by P-Rex1 whose activity is regulated by Malin through ubiquitination. This idea is supported by the results obtained when silencing P-Rex1 (Fig. 16C). In fact, when we reduced P-Rex1 expression, by siRNA, we saw a significant reduction in glucose uptake in *Epm2b*-/- (Fig. 16B).

We were interested in investigating whether P-Rex1 could regulate the translocation of GLUT1 as it does for GLUT4 because GLUT1 is the primary glucose transporter present in astrocytes (Koepsell 2020). Recent reports indicate that GLUT1 is also present in intracellular depots that act as reservoirs in addition to being localized to the plasma membrane (Wu, Zheng et al. 2013, Muraleedharan, Gawali et al. 2020). The plasma membrane level of the glucose transporter GLUT1 was not altered in our cellular system (astrocytes) (Fig 17A). We also verified the presence of GLUT3 and GLUT4 in the purified plasma membrane fraction but, since astrocytes produce very little of these isoforms (Koepsell 2020), we were unable to find any signals (data not shown). As a result, we concluded that Malin deficiency in astrocytes could influence glucose transporters' activity rather than their concentration on the plasma membrane. It is worth emphasizing that GLUT1 activity changes depending on its location in specific areas of the plasma membrane (lipid rafts) (Koepsell 2020). Inferring from this, we can speculate that a lack of ubiquitination of P-Rex1 by Malin, could lead to the increase in glucose uptake seen in the Malin-deficient condition. In addition to this, we also think that this can contribute to the characteristic glycogen accumulation described in LD models (Rubio-Villena, Viana et al. 2018, Moreno-Estellés, Campos-Rodríguez et al. 2023). A discovery of such kind adds new insight in understanding Lafora disease and, at the same time, lays the foundations for a new line of research aimed in investigating this route in more deep molecular levels for the development of innovative therapy.

Hsp90α

As for P-Rex1, we also validated Hsp90α as a substrate of Malin through a direct ubiquitination assay. We performed the assay first under over expressing conditions of the substrate (Fig. 18) and subsequently we evaluated the ubiquitination of endogenous Hsp90α (Fig. 19). The rationale lies in the fact that, until now, ubiquitination assays performed for most of Malin's known substrates needed to be overexpressed to study its ubiquitination. This is due on the one hand to the technical complications and limitations that reside in the assay itself; in fact, we must always consider that the yield of ubiquitination of a particular substrate is poor and therefore, large amounts of the substrate are needed to be analyzed in order to study this post-translational modification. Therefore, it will be challenging to identify the substrate we are investigating endogenously if its expression is minimal, as we have observed for P-Rex1. On the contrary, Hsp90α, together with the other isoforms of the Hsp90 family (Hoter, El-Sabban et al. 2018) is highly expressed at the cellular level. In fact, it constitutes about 2% of the total protein content of a cell (Scheibel, Weikl et al. 1998). For this reason, we were successful in detecting the ubiquitination of endogenous Hsp90α, being to date, the only substrate whose ubiquitination by Malin has been detected at its endogenous levels.

Under both conditions (overexpression and endogenous levels) we were able to validate Hsp90α as a substrate of Malin (Fig 18 and 19). In addition, the analysis of the type of chain that is introduced by Malin on Hsp90α indicated that it received mainly ubiquitins linked by K63 linkages (Fig. 20).

Although we majorly focused our attention on Hsp90α, we also validated Hsp90β, the isoform of Hsp90 which is constitutively expressed, as a substrate of Malin. It is worth mentioning that Hsp90β is also among Malin's 88 possible candidate substrates. However, further experimental analysis present in this thesis, were performed only for Hsp90α. We thought on focusing majorly on this substrate since is the one that it is stress-sensitive and this aspect could

be useful for the future when seeking for the biological relevance that the ubiquitination of Hsp90α could lead to in LD.

Through the analysis of GFP-trap (Fig. 21-23), we were able to confirm that Hsp90α is able to interact with Malin both in its active and inactive (P69A) forms. On the contrary, we were not able to detect any physical interaction between Hsp90α and Laforin. In agreement with this notion, only Malin but not Laforin is in the list of putative clients of Hsp90 defined by Dr. Didier Picard and that can be found at the following website: http://www.picard.ch/downloads/Hsp90interactors.pdf.

As a first analysis, to study the consequence of a lack of ubiquitination by Malin of the Hsp90α substrate, we wanted to analyze its stability as we did for P-Rex1 in *Epm2b-/-* mice. We performed the experiment on primary cultures of astrocytes from control and *Epm2b-/-* mice treated with CHX, as in the case of P-Rex1. However, we did not observe any effect on the protein stability of Hsp90α (Fig. 24). In addition, we also compared the protein levels of the molecular chaperones Hsp90α and Hsp90β in the cortex and hippocampus of 16-month-old WT vs *Epm2b-/-* mice (Fig 25 A and B). However, we did not see any difference in the protein levels of the two Hsp90 isoforms in these regions of the brain, known to mostly accumulate polyglucosans (Criado, Aguado et al. 2012).

Hsp90 is a chaperone whose general function in the cell is to help proteins fold correctly or even to correct any existing misfolded proteins. Hsp90 and Hsp70 are the two large and main families of chaperones responsible for carrying out this function (Walter and Buchner 2002, Cox and Johnson 2018).

In relation to LD, studies support the hypothesis that the functional synergy that exists between Malin and Laforin may participate in protein clearance. In fact, Laforin and Malin together with Hsp70 form a complex able to control cytotoxic conditions produced by the accumulation of misfolded proteins. In detail, it appears that Laforin acts as a bridge between Hsp70 and

misfolded proteins in order to recruit Malin which, in turn, favors the ubiquitination of these proteins by directing them towards degradation. To date, other E3 ligases already exist which play a role in protein clearance and the Laforin-Malin complex could become part of this group (Garyali, Siwach et al. 2009).

In the case of our study, we could only validate that Hsp90α (and Hsp90β) are substrates of Malin and that it can interact with the E3-ligase but not with Laforin. As a future perspective, it would be interesting to understand the role that the lack of ubiquitination of Hsp90α may play in Lafora disease. In particular, if this could have any impact on how the Hsp90-mediated protein folding mechanism works at a physiological level and, or especially, what could happen when the cell comes to be in a condition of stress or in a pathological state, such as accumulation of misfolded proteins. The reason why it would be interesting to follow this line of investigation resides in the studies that demonstrate that the two major chaperones, Hsp70 and Hsp90, are involved not only in protein folding, that is mediated during the so called "chaperone cycle", but also in a process of degradation that is mediated by another interesting player that is CHIP. CHIP is an E3 ubiquitin ligase that comes into play when, under certain cellular conditions, protein homeostasis is shifted towards the route of degradation rather than folding (Kundrat and Regan 2010, Muller, Ruckova et al. 2013, Bhattacharya, Weidenauer et al. 2020). In this regard, for structural reasons, Hsp90 binds to Hsp70 through HOP/Stip1 protein, that mediates the passage of client proteins from Hsp70 to Hsp90, in order to be correctly folded. However, when degradation of a certain misfolded protein or client protein is necessary, Hsp90 favors its binding to CHIP in order for it to carry proper ubiquitination and direct misfolded or client proteins towards degradation (Kundrat and Regan 2010, Muller, Ruckova et al. 2013, Bhattacharya, Weidenauer et al. 2020). The fact that Hsp90 cannot bind at the same time to HOP and CHIP, indicate that protein folding and degradation,

mediated by this chaperone, are two conditions that cannot co-exist. Therefore, it would be of certain interest, investigate whether interactions between Hsp90α and HOP/Stip1 or CHIP occur and if they are altered when Malin is inactive. This would recognize Malin to be an important co-chaperone able to regulate the chaperone-cycle mediated by Hsp90 through its ubiquitination.

CONCLUSIONS

Conclusions:

1. Upon the use of the bioUb strategy, we identified 88 Malin-differentially ubiquitinated candidate-substrates.
2. One of these candidates was P-Rex1, which was validated as a substrate of Malin.
3. Through the ubiquitination of P-Rex1, the Laforin-Malin complex negatively regulates its activity as a GEF of Rac1.
4. *Epm2b-/-* astrocytes show a decrease in the degradation rate of P-Rex1 compared to WT astrocytes, suggesting a negative role of Malin on the stability of P-Rex1.
5. *Epm2b-/-* astrocytes show an increase in glucose uptake compared to WT astrocytes. This effect is related to the action of P-Rex1.
6. The increase in glucose uptake is caused by an increase in the activity of GLUT1 rather than in an increase in the amount of transporters at the plasma membrane.
7. Other candidates of the bioUb strategy such as Hsp90α and Hsp90β have been validated as substrates of Malin.
8. Hsp90α interacts physically with Malin but not with Laforin.
9. In the absence of Malin, there is not a change in the stability of Hsp90α.

BIBLIOGRAPHY

Bibliography

Aguado, C., S. Sarkar, V. I. Korolchuk, O. Criado, S. Vernia, P. Boya, P. Sanz, S. R. de Cordoba, E. Knecht and D. C. Rubinsztein (2010). "Laforin, the most common protein mutated in Lafora disease, regulates autophagy." Hum Mol Genet **19**(14): 2867-2876.

Ahonen, S., S. Nitschke, T. R. Grossman, H. Kordasiewicz, P. Wang, X. Zhao, D. R. Guisso, S. Kasiri, F. Nitschke and B. A. Minassian (2021). "Gys1 antisense therapy rescues neuropathological bases of murine Lafora disease." Brain **144**(10): 2985-2993.

Akimov, V., I. Barrio-Hernandez, S. V. F. Hansen, P. Hallenborg, A. K. Pedersen, D. B. Bekker-Jensen, M. Puglia, S. D. K. Christensen, J. T. Vanselow, M. M. Nielsen, I. Kratchmarova, C. D. Kelstrup, J. V. Olsen and B. Blagoev (2018). "UbiSite approach for comprehensive mapping of lysine and N-terminal ubiquitination sites." Nat Struct Mol Biol **25**(7): 631-640.

Ali, M. M., S. M. Roe, C. K. Vaughan, P. Meyer, B. Panaretou, P. W. Piper, C. Prodromou and L. H. Pearl (2006). "Crystal structure of an Hsp90-nucleotide-p23/Sba1 closed chaperone complex." Nature **440**(7087): 1013-1017.

Arrizabalaga, O., H. M. Lacerda, A. M. Zubiaga and J. L. Zugaza (2012). "Rac1 protein regulates glycogen phosphorylase activation and controls interleukin (IL)-2-dependent T cell proliferation." J Biol Chem **287**(15): 11878-11890.

Aslan, J. E., A. M. Spencer, C. P. Loren, J. Pang, H. C. Welch, D. L. Greenberg and O. J. McCarty (2011). "Characterization of the Rac guanine nucleotide exchange factor P-Rex1 in platelets." J Mol Signal **6**: 11.

Backe, S. J., R. A. Sager, M. R. Woodford, A. M. Makedon and M. Mollapour (2020). "Post-translational modifications of Hsp90 and translating the chaperone code." J Biol Chem **295**(32): 11099-11117.

Baindur-Hudson, S., A. L. Edkins and G. L. Blatch (2015). "Hsp70/Hsp90 organising protein (hop): beyond interactions with chaperones and prion proteins." Subcell Biochem **78**: 69-90.

Balamatsias, D., A. M. Kong, J. E. Waters, A. Sriratana, R. Gurung, C. G. Bailey, J. E. Rasko, T. Tiganis, S. L. Macaulay and C. A. Mitchell (2011). "Identification of P-Rex1 as a novel Rac1-guanine nucleotide exchange factor (GEF) that promotes actin remodeling and GLUT4 protein trafficking in adipocytes." J Biol Chem **286**(50): 43229-43240.

Barber, M. A., A. Hendrickx, M. Beullens, H. Ceulemans, D. Oxley, S. Thelen, M. Thelen, M. Bollen and H. C. Welch (2012). "The guanine-nucleotide-exchange factor P-Rex1 is activated by protein phosphatase 1alpha." Biochem J **443**(1): 173-183.
Beckett, D., E. Kovaleva and P. J. Schatz (1999). "A minimal peptide substrate in biotin holoenzyme synthetase-catalyzed biotinylation." Protein Sci **8**(4): 921-929.
Beltran-Navarro, Y. M., G. Reyes-Cruz and J. Vazquez-Prado (2022). "P-Rex1 Signaling Hub in Lower Grade Glioma Patients, Found by In Silico Data Mining, Correlates With Reduced Survival and Augmented Immune Tumor Microenvironment." Front Oncol **12**: 922025.
Bhattacharya, K., L. Weidenauer, T. M. Luengo, E. C. Pieters, P. C. Echeverria, L. Bernasconi, D. Wider, Y. Sadian, M. B. Koopman, M. Villemin, C. Bauer, S. G. D. Rudiger, M. Quadroni and D. Picard (2020). "The Hsp70-Hsp90 co-chaperone Hop/Stip1 shifts the proteostatic balance from folding towards degradation." Nat Commun **11**(1): 5975.
Brewer, M. K. and M. S. Gentry (2019). "Brain Glycogen Structure and Its Associated Proteins: Past, Present and Future." Adv Neurobiol **23**: 17-81.
Budhidarmo, R., Y. Nakatani and C. L. Day (2012). "RINGs hold the key to ubiquitin transfer." Trends Biochem Sci **37**(2): 58-65.
Carretero-Ortega, J., C. T. Walsh, R. Hernandez-Garcia, G. Reyes-Cruz, J. H. Brown and J. Vazquez-Prado (2010). "Phosphatidylinositol 3,4,5-triphosphate-dependent Rac exchanger 1 (P-Rex-1), a guanine nucleotide exchange factor for Rac, mediates angiogenic responses to stromal cell-derived factor-1/chemokine stromal cell derived factor-1 (SDF-1/CXCL-12) linked to Rac activation, endothelial cell migration, and in vitro angiogenesis." Mol Pharmacol **77**(3): 435-442.
Chan, E. M., E. J. Young, L. Ianzano, I. Munteanu, X. Zhao, C. C. Christopoulos, G. Avanzini, M. Elia, C. A. Ackerley, N. J. Jovic, S. Bohlega, E. Andermann, G. A. Rouleau, A. V. Delgado-Escueta, B. A. Minassian and S. W. Scherer (2003). "Mutations in NHLRC1 cause progressive myoclonus epilepsy." Nat Genet **35**(2): 125-127.
Chaudhury, S., T. R. Welch and B. S. Blagg (2006). "Hsp90 as a target for drug development." ChemMedChem **1**(12): 1331-1340.
Cheng, A., M. Zhang, M. S. Gentry, C. A. Worby, J. E. Dixon and A. R. Saltiel (2007). "A role for AGL ubiquitination in the glycogen storage disorders of Lafora and Cori's disease." Genes Dev **21**(19): 2399-2409.
Chiti, F. and C. M. Dobson (2006). "Protein misfolding, functional amyloid, and human disease." Annu Rev Biochem **75**: 333-366.

Cloutier, P. and B. Coulombe (2013). "Regulation of molecular chaperones through post-translational modifications: decrypting the chaperone code." Biochim Biophys Acta **1829**(5): 443-454.
Connell, P., C. A. Ballinger, J. Jiang, Y. Wu, L. J. Thompson, J. Hohfeld and C. Patterson (2001). "The co-chaperone CHIP regulates protein triage decisions mediated by heat-shock proteins." Nat Cell Biol **3**(1): 93-96.
Cook, D. R., K. L. Rossman and C. J. Der (2014). "Rho guanine nucleotide exchange factors: regulators of Rho GTPase activity in development and disease." Oncogene **33**(31): 4021-4035.
Couarch, P., S. Vernia, I. Gourfinkel-An, G. Lesca, S. Gataullina, E. Fedirko, O. Trouillard, C. Depienne, O. Dulac, D. Steschenko, E. Leguern, P. Sanz and S. Baulac (2011). "Lafora progressive myoclonus epilepsy: NHLRC1 mutations affect glycogen metabolism." J Mol Med (Berl) **89**(9): 915-925.
Cox, J., M. Y. Hein, C. A. Luber, I. Paron, N. Nagaraj and M. Mann (2014). "Accurate proteome-wide label-free quantification by delayed normalization and maximal peptide ratio extraction, termed MaxLFQ." Mol Cell Proteomics **13**(9): 2513-2526.
Cox, J. and M. Mann (2008). "MaxQuant enables high peptide identification rates, individualized p.p.b.-range mass accuracies and proteome-wide protein quantification." Nat Biotechnol **26**(12): 1367-1372.
Cox, M. B. and J. L. Johnson (2018). "Evidence for Hsp90 Co-chaperones in Regulating Hsp90 Function and Promoting Client Protein Folding." Methods Mol Biol **1709**: 397-422.
Crespo, P., K. E. Schuebel, A. A. Ostrom, J. S. Gutkind and X. R. Bustelo (1997). "Phosphotyrosine-dependent activation of Rac-1 GDP/GTP exchange by the vav proto-oncogene product." Nature **385**(6612): 169-172.
Criado, O., C. Aguado, J. Gayarre, L. Duran-Trio, A. M. Garcia-Cabrero, S. Vernia, B. San Millan, M. Heredia, C. Romá-Mateo, S. Mouron, L. Juana-Lopez, M. Dominguez, C. Navarro, J. M. Serratosa, M. Sanchez, P. Sanz, P. Bovolenta, E. Knecht and S. Rodriguez de Cordoba (2012). "Lafora bodies and neurological defects in malin-deficient mice correlate with impaired autophagy." Hum Mol Genet **21**(7): 1521-1533.
Csermely, P., T. Schnaider, C. Soti, Z. Prohaszka and G. Nardai (1998). "The 90-kDa molecular chaperone family: structure, function, and clinical applications. A comprehensive review." Pharmacol Ther **79**(2): 129-168.

de Boer, E., P. Rodriguez, E. Bonte, J. Krijgsveld, E. Katsantoni, A. Heck, F. Grosveld and J. Strouboulis (2003). "Efficient biotinylation and single-step purification of tagged transcription factors in mammalian cells and transgenic mice." Proc Natl Acad Sci U S A **100**(13): 7480-7485.
de Curtis, I. (2008). "Functions of Rac GTPases during neuronal development." Dev Neurosci **30**(1-3): 47-58.
Dickey, C. A., P. Ash, N. Klosak, W. C. Lee, L. Petrucelli, M. Hutton and C. B. Eckman (2006). "Pharmacologic reductions of total tau levels; implications for the role of microtubule dynamics in regulating tau expression." Mol Neurodegener **1**: 6.
Dickey, C. A., J. Dunmore, B. Lu, J. W. Wang, W. C. Lee, A. Kamal, F. Burrows, C. Eckman, M. Hutton and L. Petrucelli (2006). "HSP induction mediates selective clearance of tau phosphorylated at proline-directed Ser/Thr sites but not KXGS (MARK) sites." FASEB J **20**(6): 753-755.
Dickey, C. A., A. Kamal, K. Lundgren, N. Klosak, R. M. Bailey, J. Dunmore, P. Ash, S. Shoraka, J. Zlatkovic, C. B. Eckman, C. Patterson, D. W. Dickson, N. S. Nahman, Jr., M. Hutton, F. Burrows and L. Petrucelli (2007). "The high-affinity HSP90-CHIP complex recognizes and selectively degrades phosphorylated tau client proteins." J Clin Invest **117**(3): 648-658.
Dimidschstein, J., L. Passante, A. Dufour, J. van den Ameele, L. Tiberi, T. Hrechdakian, R. Adams, R. Klein, D. C. Lie, Y. Jossin and P. Vanderhaeghen (2013). "Ephrin-B1 controls the columnar distribution of cortical pyramidal neurons by restricting their tangential migration." Neuron **79**(6): 1123-1135.
Donald, S., K. Hill, C. Lecureuil, R. Barnouin, S. Krugmann, W. John Coadwell, S. R. Andrews, S. A. Walker, P. T. Hawkins, L. R. Stephens and H. C. Welch (2004). "P-Rex2, a new guanine-nucleotide exchange factor for Rac." FEBS Lett **572**(1-3): 172-176.
Dong, X., Z. Mo, G. Bokoch, C. Guo, Z. Li and D. Wu (2005). "P-Rex1 is a primary Rac2 guanine nucleotide exchange factor in mouse neutrophils." Curr Biol **15**(20): 1874-1879.
Dou, F., W. J. Netzer, K. Tanemura, F. Li, F. U. Hartl, A. Takashima, G. K. Gouras, P. Greengard and H. Xu (2003). "Chaperones increase association of tau protein with microtubules." Proc Natl Acad Sci U S A **100**(2): 721-726.
Dubey, D. and S. Ganesh (2008). "Modulation of functional properties of laforin phosphatase by alternative splicing reveals a novel mechanism for

the EPM2A gene in Lafora progressive myoclonus epilepsy." Hum Mol Genet **17**(19): 3010-3020.
Elu, N., B. Lectez, J. Ramirez, N. Osinalde and U. Mayor (2020). "Mass Spectrometry-Based Characterization of Ub- and UbL-Modified Proteins." Methods Mol Biol **2051**: 265-276.
Elu, N., N. Osinalde, J. Beaskoetxea, J. Ramirez, B. Lectez, K. Aloria, J. A. Rodriguez, J. M. Arizmendi and U. Mayor (2019). "Detailed Dissection of UBE3A-Mediated DDI1 Ubiquitination." Front Physiol **10**: 534.
Fang, S., L. Li, B. Cui, S. Men, Y. Shen and X. Yang (2013). "Structural insight into plant programmed cell death mediated by BAG proteins in Arabidopsis thaliana." Acta Crystallogr D Biol Crystallogr **69**(Pt 6): 934-945.
Felts, S. J. and D. O. Toft (2003). "p23, a simple protein with complex activities." Cell Stress Chaperones **8**(2): 108-113.
Franco, M., N. T. Seyfried, A. H. Brand, J. Peng and U. Mayor (2011). "A novel strategy to isolate ubiquitin conjugates reveals wide role for ubiquitination during neural development." Mol Cell Proteomics **10**(5): M110 002188.
Galigniana, M. D., P. C. Echeverria, A. G. Erlejman and G. Piwien-Pilipuk (2010). "Role of molecular chaperones and TPR-domain proteins in the cytoplasmic transport of steroid receptors and their passage through the nuclear pore." Nucleus **1**(4): 299-308.
Ganesh, S., K. L. Agarwala, K. Amano, T. Suzuki, A. V. Delgado-Escueta and K. Yamakawa (2001). "Regional and developmental expression of Epm2a gene and its evolutionary conservation." Biochem Biophys Res Commun **283**(5): 1046-1053.
Garcia-Gimeno, M. A., E. Knecht and P. Sanz (2018). "Lafora Disease: A Ubiquitination-Related Pathology." Cells **7**(8).
Garyali, P., P. Siwach, P. K. Singh, R. Puri, S. Mittal, S. Sengupta, R. Parihar and S. Ganesh (2009). "The malin-laforin complex suppresses the cellular toxicity of misfolded proteins by promoting their degradation through the ubiquitin-proteasome system." Hum Mol Genet **18**(4): 688-700.
Genton, P. (2007). "[Lafora's disease (EPM2)]." Rev Neurol (Paris) **163**(1): 47-53.
Gentry, M. S., C. Romá-Mateo and P. Sanz (2013). "Laforin, a protein with many faces: glucan phosphatase, adapter protein, et alii." FEBS J **280**(2): 525-537.

Gentry, M. S., C. A. Worby and J. E. Dixon (2005). "Insights into Lafora disease: malin is an E3 ubiquitin ligase that ubiquitinates and promotes the degradation of laforin." Proc Natl Acad Sci U S A **102**(24): 8501-8506.
Goedert, M., A. Klug and R. A. Crowther (2006). "Tau protein, the paired helical filament and Alzheimer's disease." J Alzheimers Dis **9**(3 Suppl): 195-207.
Goedert, M. and M. G. Spillantini (2006). "A century of Alzheimer's disease." Science **314**(5800): 777-781.
Grammatikakis, N., A. Vultur, C. V. Ramana, A. Siganou, C. W. Schweinfest, D. K. Watson and L. Raptis (2002). "The role of Hsp90N, a new member of the Hsp90 family, in signal transduction and neoplastic transformation." J Biol Chem **277**(10): 8312-8320.
Guilherme, A., N. A. Soriano, S. Bose, J. Holik, A. Bose, D. P. Pomerleau, P. Furcinitti, J. Leszyk, S. Corvera and M. P. Czech (2004). "EHD2 and the novel EH domain binding protein EHBP1 couple endocytosis to the actin cytoskeleton." J Biol Chem **279**(11): 10593-10605.
Gupta, R. S. (1995). "Phylogenetic analysis of the 90 kD heat shock family of protein sequences and an examination of the relationship among animals, plants, and fungi species." Mol Biol Evol **12**(6): 1063-1073.
Hall, A. (1998). "Rho GTPases and the actin cytoskeleton." Science **279**(5350): 509-514.
Han, T. W., M. Kato, S. Xie, L. C. Wu, H. Mirzaei, J. Pei, M. Chen, Y. Xie, J. Allen, G. Xiao and S. L. McKnight (2012). "Cell-free formation of RNA granules: bound RNAs identify features and components of cellular assemblies." Cell **149**(4): 768-779.
Hershko, A. and A. Ciechanover (1998). "The ubiquitin system." Annu Rev Biochem **67**: 425-479.
Herter, J. M., J. Rossaint, H. Block, H. Welch and A. Zarbock (2013). "Integrin activation by P-Rex1 is required for selectin-mediated slow leukocyte rolling and intravascular crawling." Blood **121**(12): 2301-2310.
Hertz, L., L. Peng and J. C. Lai (1998). "Functional studies in cultured astrocytes." Methods **16**(3): 293-310.
Hill, K. and H. C. Welch (2006). "Purification of P-Rex1 from neutrophils and nucleotide exchange assay." Methods Enzymol **406**: 26-41.

Hoter, A., M. El-Sabban and H. Naim (2018). "The HSP90 Family: Structure, Regulation, Function, and Implications in Health and Disease." International Journal of Molecular Sciences **19**(9): 2560.
Jackson, S. E. (2013). "Hsp90: structure and function." Top Curr Chem **328**: 155-240.
Jaiswal, M., R. Dvorsky and M. R. Ahmadian (2013). "Deciphering the molecular and functional basis of Dbl family proteins: a novel systematic approach toward classification of selective activation of the Rho family proteins." J Biol Chem **288**(6): 4486-4500.
Johnson, J. L. (2012). "Evolution and function of diverse Hsp90 homologs and cochaperone proteins." Biochim Biophys Acta **1823**(3): 607-613.
Kaiser, P. and C. Tagwerker (2005). Is This Protein Ubiquitinated?, Elsevier**:** 243-248.
Kalviainen, R. (2015). "Progressive Myoclonus Epilepsies." Semin Neurol **35**(3): 293-299.
Karagoz, G. E. and S. G. Rudiger (2015). "Hsp90 interaction with clients." Trends Biochem Sci **40**(2): 117-125.
Knowles, T. P., M. Vendruscolo and C. M. Dobson (2014). "The amyloid state and its association with protein misfolding diseases." Nat Rev Mol Cell Biol **15**(6): 384-396.
Koepsell, H. (2020). "Glucose transporters in brain in health and disease." Pflügers Archiv - European Journal of Physiology **472**(9): 1299-1343.
Komander, D. and M. Rape (2012). "The ubiquitin code." Annu Rev Biochem **81**: 203-229.
Kumarasinghe, L., L. Xiong, M. A. Garcia-Gimeno, E. Lazzari, P. Sanz and G. Meroni (2021). "TRIM32 and Malin in Neurological and Neuromuscular Rare Diseases." Cells **10**(4).
Kundrat, L. and L. Regan (2010). "Balance between folding and degradation for Hsp90-dependent client proteins: a key role for CHIP." Biochemistry **49**(35): 7428-7438.
Kundrat, L. and L. Regan (2010). "Identification of residues on Hsp70 and Hsp90 ubiquitinated by the cochaperone CHIP." J Mol Biol **395**(3): 587-594.
Lackie, R. E., A. Maciejewski, V. G. Ostapchenko, J. Marques-Lopes, W. Y. Choy, M. L. Duennwald, V. F. Prado and M. A. M. Prado (2017). "The Hsp70/Hsp90 Chaperone Machinery in Neurodegenerative Diseases." Front Neurosci **11**: 254.

Lafora, G. R. and B. Glueck (1911). "Beitrag zur Histopathologie der myoklonischen Epilepsie." Zeitschrift für die gesamte Neurologie und Psychiatrie **6**(1): 1-14.
Lahuerta, M., C. Aguado, P. Sanchez-Martin, P. Sanz and E. Knecht (2018). "Degradation of altered mitochondria by autophagy is impaired in Lafora disease." FEBS J **285**(11): 2071-2090.
Lahuerta, M., D. Gonzalez, C. Aguado, A. Fathinajafabadi, J. L. Garcia-Gimenez, M. Moreno-Estelles, C. Romá-Mateo, E. Knecht, F. V. Pallardo and P. Sanz (2020). "Reactive Glia-Derived Neuroinflammation: a Novel Hallmark in Lafora Progressive Myoclonus Epilepsy That Progresses with Age." Mol Neurobiol **57**(3): 1607-1621.
Lectez, B., R. Migotti, S. Y. Lee, J. Ramirez, N. Beraza, B. Mansfield, J. D. Sutherland, M. L. Martinez-Chantar, G. Dittmar and U. Mayor (2014). "Ubiquitin profiling in liver using a transgenic mouse with biotinylated ubiquitin." J Proteome Res **13**(6): 3016-3026.
Lewis, J. P., N. D. Palmer, J. B. Ellington, J. Divers, M. C. Ng, L. Lu, C. D. Langefeld, B. I. Freedman and D. W. Bowden (2010). "Analysis of candidate genes on chromosome 20q12-13.1 reveals evidence for BMI mediated association of PREX1 with type 2 diabetes in European Americans." Genomics **96**(4): 211-219.
Li, J., J. Soroka and J. Buchner (2012). "The Hsp90 chaperone machinery: conformational dynamics and regulation by co-chaperones." Biochim Biophys Acta **1823**(3): 624-635.
Llavero, F., B. Urzelai, N. Osinalde, P. Galvez, H. M. Lacerda, L. A. Parada and J. L. Zugaza (2015). "Guanine nucleotide exchange factor alphaPIX leads to activation of the Rac 1 GTPase/glycogen phosphorylase pathway in interleukin (IL)-2-stimulated T cells." J Biol Chem **290**(14): 9171-9182.
Lopez-Gonzalez, I., R. Viana, P. Sanz and I. Ferrer (2017). "Inflammation in Lafora Disease: Evolution with Disease Progression in Laforin and Malin Knock-out Mouse Models." Mol Neurobiol **54**(5): 3119-3130.
Luo, W., F. Dou, A. Rodina, S. Chip, J. Kim, Q. Zhao, K. Moulick, J. Aguirre, N. Wu, P. Greengard and G. Chiosis (2007). "Roles of heat-shock protein 90 in maintaining and facilitating the neurodegenerative phenotype in tauopathies." Proc Natl Acad Sci U S A **104**(22): 9511-9516.
Machin, P. A., E. Tsonou, D. C. Hornigold and H. C. E. Welch (2021). "Rho Family GTPases and Rho GEFs in Glucose Homeostasis." Cells **10**(4).

Magistretti, P. J., M. Manthorpe, F. E. Bloom and S. Varon (1983). "Functional receptors for vasoactive intestinal polypeptide in cultured astroglia from neonatal rat brain." Regul Pept **6**(1): 71-80.
Mallette, F. A. and S. Richard (2012). "K48-linked ubiquitination and protein degradation regulate 53BP1 recruitment at DNA damage sites." Cell Res **22**(8): 1221-1223.
Martinez, A., B. Lectez, J. Ramirez, O. Popp, J. D. Sutherland, S. Urbe, G. Dittmar, M. J. Clague and U. Mayor (2017). "Quantitative proteomic analysis of Parkin substrates in Drosophila neurons." Mol Neurodegener **12**(1): 29.
Mayeenuddin, L. H. and J. C. Garrison (2006). "Phosphorylation of P-Rex1 by the cyclic AMP-dependent protein kinase inhibits the phosphatidylinositiol (3,4,5)-trisphosphate and Gbetagamma-mediated regulation of its activity." J Biol Chem **281**(4): 1921-1928.
Mayer, M. P. and B. Bukau (2005). "Hsp70 chaperones: cellular functions and molecular mechanism." Cell Mol Life Sci **62**(6): 670-684.
Minassian, B. A., J. R. Lee, J. A. Herbrick, J. Huizenga, S. Soder, A. J. Mungall, I. Dunham, R. Gardner, C. Y. Fong, S. Carpenter, L. Jardim, P. Satishchandra, E. Andermann, O. C. Snead, 3rd, I. Lopes-Cendes, L. C. Tsui, A. V. Delgado-Escueta, G. A. Rouleau and S. W. Scherer (1998). "Mutations in a gene encoding a novel protein tyrosine phosphatase cause progressive myoclonus epilepsy." Nat Genet **20**(2): 171-174.
Mittal, S., M. Upadhyay, P. K. Singh, R. Parihar and S. Ganesh (2015). "Interdependence of laforin and malin proteins for their stability and functions could underlie the molecular basis of locus heterogeneity in Lafora disease." J Biosci **40**(5): 863-871.
Mollapour, M. and L. Neckers (2012). "Post-translational modifications of Hsp90 and their contributions to chaperone regulation." Biochim Biophys Acta **1823**(3): 648-655.
Moller, L. L. V., A. Klip and L. Sylow (2019). "Rho GTPases-Emerging Regulators of Glucose Homeostasis and Metabolic Health." Cells **8**(5).
Monaghan, T. S. and N. Delanty (2010). "Lafora Disease." **24**(7): 549-561.
Montero, J. C., S. Seoane and A. Pandiella (2013). "Phosphorylation of P-Rex1 at serine 1169 participates in IGF-1R signaling in breast cancer cells." Cell Signal **25**(11): 2281-2289.
Moreno, D., M. C. Towler, D. G. Hardie, E. Knecht and P. Sanz (2010). "The laforin-malin complex, involved in Lafora disease, promotes the incorporation of K63-linked ubiquitin chains into AMP-activated protein kinase beta subunits." Mol Biol Cell **21**(15): 2578-2588.

Moreno-Estellés, M., Á. Campos-Rodríguez, C. Rubio-Villena, L. Kumarasinghe, M. A. Garcia-Gimeno and P. Sanz (2023). "Deciphering the Polyglucosan Accumulation Present in Lafora Disease Using an Astrocytic Cellular Model." International Journal of Molecular Sciences **24**(7): 6020.

Muller, M. S., R. Fox, A. Schousboe, H. S. Waagepetersen and L. K. Bak (2014). "Astrocyte glycogenolysis is triggered by store-operated calcium entry and provides metabolic energy for cellular calcium homeostasis." Glia **62**(4): 526-534.

Muller, P., E. Ruckova, P. Halada, P. J. Coates, R. Hrstka, D. P. Lane and B. Vojtesek (2013). "C-terminal phosphorylation of Hsp70 and Hsp90 regulates alternate binding to co-chaperones CHIP and HOP to determine cellular protein folding/degradation balances." Oncogene **32**(25): 3101-3110.

Munoz-Ballester, C., A. Berthier, R. Viana and P. Sanz (2016). "Homeostasis of the astrocytic glutamate transporter GLT-1 is altered in mouse models of Lafora disease." Biochim Biophys Acta **1862**(6): 1074-1083.

Muraleedharan, R., M. V. Gawali, D. Tiwari, A. Sukumaran, N. Oatman, J. Anderson, D. Nardini, M. A. N. Bhuiyan, I. Tkac, A. L. Ward, M. Kundu, R. Waclaw, L. M. Chow, C. Gross, R. Rao, S. Schirmeier and B. Dasgupta (2020). "AMPK-Regulated Astrocytic Lactate Shuttle Plays a Non-Cell-Autonomous Role in Neuronal Survival." Cell Rep **32**(9): 108092.

Murphy, P. J., K. C. Kanelakis, M. D. Galigniana, Y. Morishima and W. B. Pratt (2001). "Stoichiometry, abundance, and functional significance of the hsp90/hsp70-based multiprotein chaperone machinery in reticulocyte lysate." J Biol Chem **276**(32): 30092-30098.

Orsini, A., A. Valetto, V. Bertini, M. Esposito, N. Carli, B. A. Minassian, A. Bonuccelli, D. Peroni, R. Michelucci and P. Striano (2019). "The best evidence for progressive myoclonic epilepsy: A pathway to precision therapy." Seizure **71**: 247-257.

Osinalde, N., V. Sanchez-Quiles, V. Akimov, B. Blagoev and I. Kratchmarova (2015). "SILAC-based quantification of changes in protein tyrosine phosphorylation induced by Interleukin-2 (IL-2) and IL-15 in T-lymphocytes." Data Brief **5**: 53-58.

Pederson, B. A., J. Turnbull, J. R. Epp, S. A. Weaver, X. Zhao, N. Pencea, P. J. Roach, P. W. Frankland, C. A. Ackerley and B. A. Minassian (2013). "Inhibiting glycogen synthesis prevents Lafora disease in a mouse model." Ann Neurol **74**(2): 297-300.

Perez-Jimenez, E., R. Viana, C. Muñoz-Ballester, C. Vendrell-Tornero, R. Moll-Diaz, M. A. Garcia-Gimeno and P. Sanz (2020). "Endocytosis of the glutamate transporter 1 is regulated by laforin and malin: Implications in Lafora disease." Glia.

Petrucelli, L., D. Dickson, K. Kehoe, J. Taylor, H. Snyder, A. Grover, M. De Lucia, E. McGowan, J. Lewis, G. Prihar, J. Kim, W. H. Dillmann, S. E. Browne, A. Hall, R. Voellmy, Y. Tsuboi, T. M. Dawson, B. Wolozin, J. Hardy and M. Hutton (2004). "CHIP and Hsp70 regulate tau ubiquitination, degradation and aggregation." Hum Mol Genet **13**(7): 703-714.

Pirone, L., W. Xolalpa, J. O. Sigurethsson, J. Ramirez, C. Perez, M. Gonzalez, A. R. de Sabando, F. Elortza, M. S. Rodriguez, U. Mayor, J. V. Olsen, R. Barrio and J. D. Sutherland (2017). "A comprehensive platform for the analysis of ubiquitin-like protein modifications using in vivo biotinylation." Sci Rep **7**: 40756.

Polianskyte-Prause, Z., T. A. Tolvanen, S. Lindfors, V. Dumont, M. Van, H. Wang, S. N. Dash, M. Berg, J. B. Naams, L. C. Hautala, H. Nisen, T. Mirtti, P. H. Groop, K. Wahala, J. Tienari and S. Lehtonen (2019). "Metformin increases glucose uptake and acts renoprotectively by reducing SHIP2 activity." FASEB J **33**(2): 2858-2869.

Pondrelli, F., L. Muccioli, L. Licchetta, B. Mostacci, C. Zenesini, P. Tinuper, L. Vignatelli and F. Bisulli (2021). "Natural history of Lafora disease: a prognostic systematic review and individual participant data meta-analysis." Orphanet J Rare Dis **16**(1): 362.

Prodromou, C. (2016). "Mechanisms of Hsp90 regulation." Biochem J **473**(16): 2439-2452.

Prodromou, C., B. Panaretou, S. Chohan, G. Siligardi, R. O'Brien, J. E. Ladbury, S. M. Roe, P. W. Piper and L. H. Pearl (2000). "The ATPase cycle of Hsp90 drives a molecular 'clamp' via transient dimerization of the N-terminal domains." EMBO J **19**(16): 4383-4392.

Puri, R. and S. Ganesh (2012). "Autophagy defects in Lafora disease: cause or consequence?" Autophagy **8**(2): 289-290.

Qian, F., G. C. Le Breton, J. Chen, J. Deng, J. W. Christman, D. Wu and R. D. Ye (2012). "Role for the guanine nucleotide exchange factor phosphatidylinositol-3,4,5-trisphosphate-dependent rac exchanger 1 in platelet secretion and aggregation." Arterioscler Thromb Vasc Biol **32**(3): 768-777.

Qiu, W., Y. Chang, J. Liu, X. Yang, Y. Yu, J. Li, Q. Liang and G. Sun (2020). "Identification of P-Rex1 in the Regulation of Liver Cancer Cell

Proliferation and Migration via HGF/c-Met/Akt Pathway." Onco Targets Ther **13**: 9481-9495.
Quintana-Gallardo, L., J. Martin-Benito, M. Marcilla, G. Espadas, E. Sabido and J. M. Valpuesta (2019). "The cochaperone CHIP marks Hsp70- and Hsp90-bound substrates for degradation through a very flexible mechanism." Sci Rep **9**(1): 5102.
Ramirez, J., B. Lectez, N. Osinalde, M. Siva, N. Elu, K. Aloria, M. Prochazkova, C. Perez, J. Martinez-Hernandez, R. Barrio, K. G. Saskova, J. M. Arizmendi and U. Mayor (2018). "Quantitative proteomics reveals neuronal ubiquitination of Rngo/Ddi1 and several proteasomal subunits by Ube3a, accounting for the complexity of Angelman syndrome." Hum Mol Genet **27**(11): 1955-1971.
Ramirez, J., A. Martinez, B. Lectez, S. Y. Lee, M. Franco, R. Barrio, G. Dittmar and U. Mayor (2015). "Proteomic Analysis of the Ubiquitin Landscape in the Drosophila Embryonic Nervous System and the Adult Photoreceptor Cells." PLoS One **10**(10): e0139083.
Ramirez, J., M. Morales, N. Osinalde, I. Martinez-Padron, U. Mayor and A. Ferrus (2021). "The ubiquitin ligase Ariadne-1 regulates neurotransmitter release via ubiquitination of NSF." J Biol Chem **296**: 100408.
Ramirez, J., G. Prieto, A. Olazabal-Herrero, E. Borras, E. Fernandez-Vigo, U. Alduntzin, N. Osinalde, J. Beaskoetxea, B. Lectez, K. Aloria, J. A. Rodriguez, A. Paradela, E. Sabido, J. Munoz, F. Corrales, J. M. Arizmendi and U. Mayor (2021). "A Proteomic Approach for Systematic Mapping of Substrates of Human Deubiquitinating Enzymes." Int J Mol Sci **22**(9).
Ramirez, J., G. Prieto, A. Olazabal-Herrero, E. Borras, E. Fernandez-Vigo, U. Alduntzin, N. Osinalde, J. Beaskoetxea, B. Lectez, K. Aloria, J. A. Rodriguez, A. Paradela, E. Sabido, J. Munoz, F. Corrales, J. M. Arizmendi and U. Mayor (2021). "A Proteomic Approach for Systematic Mapping of Substrates of Human Deubiquitinating Enzymes." Int J Mol Sci **22**(9): 4851.
Rao, S. N., J. Sharma, R. Maity and N. R. Jana (2010). "Co-chaperone CHIP stabilizes aggregate-prone malin, a ubiquitin ligase mutated in Lafora disease." J Biol Chem **285**(2): 1404-1413.
Raththagala, M., M. K. Brewer, M. W. Parker, A. R. Sherwood, B. K. Wong, S. Hsu, T. M. Bridges, B. C. Paasch, L. M. Hellman, S. Husodo, D. A. Meekins, A. O. Taylor, B. D. Turner, K. D. Auger, V. V. Dukhande, S. Chakravarthy, P. Sanz, V. L. Woods, Jr., S. Li, C. W. Vander Kooi and M. S. Gentry (2015). "Structural mechanism of laforin

function in glycogen dephosphorylation and lafora disease." Mol Cell **57**(2): 261-272.
Riva, A., A. Orsini, M. Scala, V. Taramasso, L. Canafoglia, G. d'Orsi, M. T. Di Claudio, C. Avolio, A. D'Aniello, M. Elia, S. Franceschetti, G. Di Gennaro, F. Bisulli, P. Tinuper, M. Tappata, A. Romeo, E. Freri, C. Marini, C. Costa, V. Sofia, E. Ferlazzo, A. Magaudda, P. Veggiotti, E. Gennaro, A. Pistorio, C. Minetti, A. Bianchi, S. Striano, R. Michelucci, F. Zara, B. A. Minassian, P. Striano and C. Italian League Against Epilepsy Genetic (2021). "Italian cohort of Lafora disease: Clinical features, disease evolution, and genotype-phenotype correlations." J Neurol Sci **424**: 117409.
Rohl, A., J. Rohrberg and J. Buchner (2013). "The chaperone Hsp90: changing partners for demanding clients." Trends Biochem Sci **38**(5): 253-262.
Romá-Mateo, C., C. Aguado, J. L. Garcia-Gimenez, J. S. Ibanez-Cabellos, M. Seco-Cervera, F. V. Pallardo, E. Knecht and P. Sanz (2015). "Increased oxidative stress and impaired antioxidant response in Lafora disease." Mol Neurobiol **51**(3): 932-946.
Romá-Mateo, C., D. Moreno, S. Vernia, T. Rubio, T. M. Bridges, M. S. Gentry and P. Sanz (2011). "Lafora disease E3-ubiquitin ligase malin is related to TRIM32 at both the phylogenetic and functional level." BMC Evol Biol **11**: 225.
Romá-Mateo, C., M. Raththagala, M. S. Gentry and P. Sanz (2016). "Assessing the Biological Activity of the Glucan Phosphatase Laforin." Methods Mol Biol **1447**: 107-119.
Romá-Mateo, C., P. Sanz and M. S. Gentry (2012). "Deciphering the role of malin in the lafora progressive myoclonus epilepsy." IUBMB Life **64**(10): 801-808.
Rossman, K. L., C. J. Der and J. Sondek (2005). "GEF means go: turning on RHO GTPases with guanine nucleotide-exchange factors." Nat Rev Mol Cell Biol **6**(2): 167-180.
Rowlands, M., C. McAndrew, C. Prodromou, L. Pearl, A. Kalusa, K. Jones, P. Workman and W. Aherne (2010). "Detection of the ATPase activity of the molecular chaperones Hsp90 and Hsp72 using the TranscreenerTM ADP assay kit." J Biomol Screen **15**(3): 279-286.
Rubio, T., R. Viana, M. Moreno-Estelles, A. Campos-Rodriguez and P. Sanz (2023). "TNF and IL6/Jak2 signaling pathways are the main contributors of the glia-derived neuroinflammation present in Lafora disease, a fatal form of progressive myoclonus epilepsy." Neurobiol Dis **176**: 105964.

Rubio-Villena, C., M. A. Garcia-Gimeno and P. Sanz (2013). "Glycogenic activity of R6, a protein phosphatase 1 regulatory subunit, is modulated by the laforin-malin complex." Int J Biochem Cell Biol **45**(7): 1479-1488.
Rubio-Villena, C., R. Viana, J. Bonet, M. A. Garcia-Gimeno, M. Casado, M. Heredia and P. Sanz (2018). "Astrocytes: new players in progressive myoclonus epilepsy of Lafora type." Hum Mol Genet **27**(7): 1290-1300.
Rynkiewicz, N. K., H. J. Liu, D. Balamatsias and C. A. Mitchell (2012). "INPP4A/INPP4B and P-Rex proteins: related but different?" Adv Biol Regul **52**(1): 265-279.
Sakai, M., J. Austin, F. Witmer and L. Trueb (1970). "Studies in myoclonus epilepsy (Lafora body form). II. Polyglucosans in the systemic deposits of myoclonus epilepsy and in corpora amylacea." Neurology **20**(2): 160-176.
Sanchez-Martin, P., M. Lahuerta, R. Viana, E. Knecht and P. Sanz (2020). "Regulation of the autophagic PI3KC3 complex by laforin/malin E3-ubiquitin ligase, two proteins involved in Lafora disease." Biochim Biophys Acta Mol Cell Res **1867**(2): 118613.
Sanchez-Martin, P., C. Romá-Mateo, R. Viana and P. Sanz (2015). "Ubiquitin conjugating enzyme E2-N and sequestosome-1 (p62) are components of the ubiquitination process mediated by the malin-laforin E3-ubiquitin ligase complex." Int J Biochem Cell Biol **69**: 204-214.
Sarkar, A. A. and I. E. Zohn (2012). "Hectd1 regulates intracellular localization and secretion of Hsp90 to control cellular behavior of the cranial mesenchyme." J Cell Biol **196**(6): 789-800.
Scheibel, T., T. Weikl and J. Buchner (1998). "Two chaperone sites in Hsp90 differing in substrate specificity and ATP dependence." Proceedings of the National Academy of Sciences **95**(4): 1495-1499.
Schopf, F. H., M. M. Biebl and J. Buchner (2017). "The HSP90 chaperone machinery." Nat Rev Mol Cell Biol **18**(6): 345-360.
Sengupta, S., I. Badhwar, M. Upadhyay, S. Singh and S. Ganesh (2011). "Malin and laforin are essential components of a protein complex that protects cells from thermal stress." J Cell Sci **124**(Pt 13): 2277-2286.
Serratosa, J. M., P. Gomez-Garre, M. E. Gallardo, B. Anta, D. B. de Bernabe, D. Lindhout, P. B. Augustijn, C. A. Tassinari, R. M. Malafosse, M. Topcu, D. Grid, C. Dravet, S. F. Berkovic and S. R. de Cordoba (1999). "A novel protein tyrosine phosphatase gene is mutated in progressive myoclonus epilepsy of the Lafora type (EPM2)." Hum Mol Genet **8**(2): 345-352.

Sharma, J., S. Mulherkar, D. Mukherjee and N. R. Jana (2012). "Malin regulates Wnt signaling pathway through degradation of dishevelled2." J Biol Chem **287**(9): 6830-6839.
Shi, W., L. Feng, S. Dong, Z. Ning, Y. Hua, L. Liu, Z. Chen and Z. Meng (2020). "FBXL6 governs c-MYC to promote hepatocellular carcinoma through ubiquitination and stabilization of HSP90AA1." Cell Commun Signal **18**(1): 100.
Shiber, A. and T. Ravid (2014). "Chaperoning proteins for destruction: diverse roles of Hsp70 chaperones and their co-chaperones in targeting misfolded proteins to the proteasome." Biomolecules **4**(3): 704-724.
Shimura, H., Y. Miura-Shimura and K. S. Kosik (2004). "Binding of tau to heat shock protein 27 leads to decreased concentration of hyperphosphorylated tau and enhanced cell survival." J Biol Chem **279**(17): 17957-17962.
Singh, P. K., S. Singh and S. Ganesh (2012). "The laforin-malin complex negatively regulates glycogen synthesis by modulating cellular glucose uptake via glucose transporters." Mol Cell Biol **32**(3): 652-663.
Singh, S. and S. Ganesh (2009). "Lafora progressive myoclonus epilepsy: a meta-analysis of reported mutations in the first decade following the discovery of the EPM2A and NHLRC1 genes." Hum Mutat **30**(5): 715-723.
Slack, F. J. and G. Ruvkun (1998). "A novel repeat domain that is often associated with RING finger and B-box motifs." Trends Biochem Sci **23**(12): 474-475.
Solaz-Fuster, M. C., J. V. Gimeno-Alcaniz, S. Ros, M. E. Fernandez-Sanchez, B. Garcia-Fojeda, O. Criado Garcia, D. Vilchez, J. Dominguez, M. Garcia-Rocha, M. Sanchez-Piris, C. Aguado, E. Knecht, J. Serratosa, J. J. Guinovart, P. Sanz and S. Rodriguez de Cordoba (2008). "Regulation of glycogen synthesis by the laforin-malin complex is modulated by the AMP-activated protein kinase pathway." Hum Mol Genet **17**(5): 667-678.
Solaz-Fuster, M. C., J. V. Gimeno-Alcañiz, S. Ros, M. E. Fernandez-Sanchez, B. Garcia-Fojeda, O. C. Garcia, D. Vilchez, J. Dominguez, M. Garcia-Rocha, M. Sanchez-Piris, C. Aguado, E. Knecht, J. Serratosa, J. J. Guinovart, P. Sanz and S. R. De Córdoba (2008). "Regulation of glycogen synthesis by the laforin–malin complex is modulated by the AMP-activated protein kinase pathway." Human Molecular Genetics **17**(5): 667-678.

Sreedhar, A. S., E. Kalmar, P. Csermely and Y. F. Shen (2004). "Hsp90 isoforms: functions, expression and clinical importance." FEBS Lett **562**(1-3): 11-15.
Srijakotre, N., H. J. Liu, M. Nobis, J. Man, H. Y. K. Yip, A. Papa, H. E. Abud, K. I. Anderson, H. C. E. Welch, T. Tiganis, P. Timpson, C. A. McLean, L. M. Ooms and C. A. Mitchell (2020). "PtdIns(3,4,5)P(3)-dependent Rac exchanger 1 (P-Rex1) promotes mammary tumor initiation and metastasis." Proc Natl Acad Sci U S A **117**(45): 28056-28067.
Sun, R. C., V. V. Dukhande, Z. Zhou, L. E. A. Young, S. Emanuelle, C. F. Brainson and M. S. Gentry (2019). "Nuclear Glycogenolysis Modulates Histone Acetylation in Human Non-Small Cell Lung Cancers." Cell Metab **30**(5): 903-916 e907.
Tagliabracci, V. S., J. Turnbull, W. Wang, J. M. Girard, X. Zhao, A. V. Skurat, A. V. Delgado-Escueta, B. A. Minassian, A. A. Depaoli-Roach and P. J. Roach (2007). "Laforin is a glycogen phosphatase, deficiency of which leads to elevated phosphorylation of glycogen in vivo." Proc Natl Acad Sci U S A **104**(49): 19262-19266.
Thamilselvan, V., S. Gamage, A. Harajli, S. A. Chundru and A. Kowluru (2020). "P-Rex1 Mediates Glucose-Stimulated Rac1 Activation and Insulin Secretion in Pancreatic beta-Cells." Cell Physiol Biochem **54**(6): 1218-1230.
Thomsen, C., E. Malfatti, A. Jovanovic, M. Roberts, O. Kalev, C. Lindberg and A. Oldfors (2022). "Proteomic characterisation of polyglucosan bodies in skeletal muscle in RBCK1 deficiency." Neuropathol Appl Neurobiol **48**(1): e12761.
Tsutsumi, S., M. Mollapour, C. Prodromou, C. T. Lee, B. Panaretou, S. Yoshida, M. P. Mayer and L. M. Neckers (2012). "Charged linker sequence modulates eukaryotic heat shock protein 90 (Hsp90) chaperone activity." Proc Natl Acad Sci U S A **109**(8): 2937-2942.
Turnbull, J., A. A. DePaoli-Roach, X. Zhao, M. A. Cortez, N. Pencea, E. Tiberia, M. Piliguian, P. J. Roach, P. Wang, C. A. Ackerley and B. A. Minassian (2011). "PTG depletion removes Lafora bodies and rescues the fatal epilepsy of Lafora disease." PLoS Genet **7**(4): e1002037.
Turnbull, J., J. R. Epp, D. Goldsmith, X. Zhao, N. Pencea, P. Wang, P. W. Frankland, C. A. Ackerley and B. A. Minassian (2014). "PTG protein depletion rescues malin-deficient Lafora disease in mouse." Ann Neurol **75**(3): 442-446.
Turnbull, J., J.-M. Girard, H. Lohi, E. M. Chan, P. Wang, E. Tiberia, S. Omer, M. Ahmed, C. Bennett, A. Chakrabarty, A. Tyagi, Y. Liu, N.

Pencea, X. Zhao, S. W. Scherer, C. A. Ackerley and B. A. Minassian (2012). "Early-onset Lafora body disease." Brain **135**(9): 2684-2698.
Turnbull, J., J. M. Girard, H. Lohi, E. M. Chan, P. Wang, E. Tiberia, S. Omer, M. Ahmed, C. Bennett, A. Chakrabarty, A. Tyagi, Y. Liu, N. Pencea, X. Zhao, S. W. Scherer, C. A. Ackerley and B. A. Minassian (2012). "Early-onset Lafora body disease." Brain **135**(Pt 9): 2684-2698.
Turnbull, J., E. Tiberia, P. Striano, P. Genton, S. Carpenter, C. A. Ackerley and B. A. Minassian (2016). "Lafora disease." Epileptic Disorders **18**(S2): 38-62.
Tyanova, S., T. Temu, P. Sinitcyn, A. Carlson, M. Y. Hein, T. Geiger, M. Mann and J. Cox (2016). "The Perseus computational platform for comprehensive analysis of (prote)omics data." Nat Methods **13**(9): 731-740.
Urano, D., A. Nakata, N. Mizuno, K. Tago and H. Itoh (2008). "Domain-domain interaction of P-Rex1 is essential for the activation and inhibition by G protein betagamma subunits and PKA." Cell Signal **20**(8): 1545-1554.
Uryu, K., C. Richter-Landsberg, W. Welch, E. Sun, O. Goldbaum, E. H. Norris, C. T. Pham, I. Yazawa, K. Hilburger, M. Micsenyi, B. I. Giasson, N. M. Bonini, V. M. Lee and J. Q. Trojanowski (2006). "Convergence of heat shock protein 90 with ubiquitin in filamentous alpha-synuclein inclusions of alpha-synucleinopathies." Am J Pathol **168**(3): 947-961.
Viana, R., P. Lujan and P. Sanz (2015). "The laforin/malin E3-ubiquitin ligase complex ubiquitinates pyruvate kinase M1/M2." BMC Biochem **16**: 24.
Vigil, D., J. Cherfils, K. L. Rossman and C. J. Der (2010). "Ras superfamily GEFs and GAPs: validated and tractable targets for cancer therapy?" Nat Rev Cancer **10**(12): 842-857.
Voellmy, R. and F. Boellmann (2007). "Chaperone regulation of the heat shock protein response." Adv Exp Med Biol **594**: 89-99.
Walter, S. and J. Buchner (2002). "Molecular chaperones--cellular machines for protein folding." Angew Chem Int Ed Engl **41**(7): 1098-1113.
Wandinger, S. K., K. Richter and J. Buchner (2008). "The Hsp90 chaperone machinery." J Biol Chem **283**(27): 18473-18477.
Wang, Z., X. Dong, Z. Li, J. D. Smith and D. Wu (2008). "Lack of a significant role of P-Rex1, a major regulator of macrophage Rac1 activation and chemotaxis, in atherogenesis." Prostaglandins Other Lipid Mediat **87**(1-4): 9-13.

Waters, J. E., M. V. Astle, L. M. Ooms, D. Balamatsias, R. Gurung and C. A. Mitchell (2008). "P-Rex1 - a multidomain protein that regulates neurite differentiation." J Cell Sci **121**(Pt 17): 2892-2903.
Wayne, N., P. Mishra and D. N. Bolon (2011). "Hsp90 and client protein maturation." Methods Mol Biol **787**: 33-44.
Welch, H. C. (2015). "Regulation and function of P-Rex family Rac-GEFs." Small GTPases **6**(2): 49-70.
Welch, H. C., W. J. Coadwell, C. D. Ellson, G. J. Ferguson, S. R. Andrews, H. Erdjument-Bromage, P. Tempst, P. T. Hawkins and L. R. Stephens (2002). "P-Rex1, a PtdIns(3,4,5)P3- and Gbetagamma-regulated guanine-nucleotide exchange factor for Rac." Cell **108**(6): 809-821.
Welch, H. C., A. M. Condliffe, L. J. Milne, G. J. Ferguson, K. Hill, L. M. Webb, K. Okkenhaug, W. J. Coadwell, S. R. Andrews, M. Thelen, G. E. Jones, P. T. Hawkins and L. R. Stephens (2005). "P-Rex1 regulates neutrophil function." Curr Biol **15**(20): 1867-1873.
Wennerberg, K., K. L. Rossman and C. J. Der (2005). "The Ras superfamily at a glance." J Cell Sci **118**(Pt 5): 843-846.
Whitehead, I. P., S. Campbell, K. L. Rossman and C. J. Der (1997). "Dbl family proteins." Biochim Biophys Acta **1332**(1): F1-23.
Wolmarans, A., B. Lee, L. Spyracopoulos and P. LaPointe (2016). "The Mechanism of Hsp90 ATPase Stimulation by Aha1." Sci Rep **6**: 33179.
Wu, N., B. Zheng, A. Shaywitz, Y. Dagon, C. Tower, G. Bellinger, C. H. Shen, J. Wen, J. Asara, T. E. McGraw, B. B. Kahn and L. C. Cantley (2013). "AMPK-dependent degradation of TXNIP upon energy stress leads to enhanced glucose uptake via GLUT1." Mol Cell **49**(6): 1167-1175.
Yoshizawa, M., T. Kawauchi, M. Sone, Y. V. Nishimura, M. Terao, K. Chihama, Y. Nabeshima and M. Hoshino (2005). "Involvement of a Rac activator,P-Rex1, in neurotrophin-derived signaling and neuronal migration." J Neurosci **25**(17): 4406-4419.
Zheng, N. and N. Shabek (2017). "Ubiquitin Ligases: Structure, Function, and Regulation." Annu Rev Biochem **86**: 129-157.
Zierer, B. K., M. Rubbelke, F. Tippel, T. Madl, F. H. Schopf, D. A. Rutz, K. Richter, M. Sattler and J. Buchner (2016). "Importance of cycle timing for the function of the molecular chaperone Hsp90." Nat Struct Mol Biol **23**(11): 1020-1028.
Zuehlke, A. D., K. Beebe, L. Neckers and T. Prince (2015). "Regulation and function of the human HSP90AA1 gene." Gene **570**(1): 8-16.

ANNEX 1

Annex 1: Complete list of ubiquitinated proteins. Complete set of differentially ubiquitinated proteins in cells expressing Malin-WT vs Malin-P69A (Fold change >2). The gene names, the molecular weight the fold change, the p-value, the number of identified peptides supporting the ubiquitination, and the protein names are indicated.

Gene names	MW (kDa)	Fold Change (WT/P69A)	p-value	Peptides (unique)	Protein names
PREX1	175,9	18,48	0,00181	3	Phosphatidylinositol 3,4,5-trisphosphate-dependent Rac exchanger 1 protein (P-Rex1)
SEH1L	39,6	9,70	0,00027	3	Nucleoporin SEH1
HSPA4	94,3	8,59	0,00008	43	Heat shock 70 kDa protein 4
SCLT1	80,9	8,23	0,00004	6	Sodium channel and clathrin linker 1
YTHDF2	62,3	8,19	0,01791	7	YTH domain-containing family protein 2
FKBP5	51,2	7,80	0,03059	10	Peptidyl-prolyl cis-trans isomerase FKBP5
HSPA1L	70,4	7,11	0,04710	23	Heat shock 70 kDa protein 1-like
GLMN	68,2	6,89	0,00446	16	Glomulin
KLC2	68,9	6,14	0,01467	7	Kinesin light chain 2
LIN7C	21,8	5,93	0,01001	2	Protein lin-7 homolog C
ANKRD16	39,3	5,40	0,01252	5	Ankyrin repeat domain-containing protein 16
HSP90AB4P	58,3	5,35	0,00031	9	Putative heat shock protein HSP 90-beta 4
HSPH1	92,1	5,11	0,00011	40	Heat shock protein 105 kDa
HSPA4L	94,5	4,66	0,00007	27	Heat shock 70 kDa protein 4L
RCL1	40,8	4,65	0,04792	4	RNA 3-terminal phosphate cyclase-like protein
DLST	48,8	4,63	0,00064	2	Dihydrolipoyllysine-residue succinyltransferase component of 2-oxoglutarate dehydrogenase complex, mitochondrial

STIP1	62,6	4,42	0,00016	25	Stress-induced-phosphoprotein 1
DUSP1	39,3	4,14	0,00033	9	Dual specificity protein phosphatase 1
MKS1	63,3	4,02	0,00443	2	Meckel syndrome type 1 protein
TGFBRAP1	97,2	4,00	0,00582	5	Transforming growth factor-beta receptor-associated protein 1
ARFGAP2	56,7	3,72	0,04711	6	ADP-ribosylation factor GTPase-activating protein 2
HSP90AA1	84,7	3,69	0,00007	55	Heat shock protein HSP 90-alpha
CRYAB	20,2	3,66	0,00926	4	Alpha-crystallin B chain
UQCRC2	48,4	3,60	0,00026	7	Cytochrome b-c1 complex subunit 2, mitochondrial
RCCD1	40,1	3,47	0,00106	6	RCC1 domain-containing protein 1
DNAH6	289,6	3,42	0,00068	2	Dynein heavy chain 6, axonemal
RASSF1	21,9	3,39	0,03454	2	Ras association domain-containing protein 1
HSPA8	70,9	3,32	0,00005	47	Heat shock cognate 71 kDa protein
HSP90AB1	83,3	3,29	0,00010	53	Heat shock protein HSP 90-beta
PNPLA2	55,3	3,25	0,04933	2	Patatin-like phospholipase domain-containing protein 2
ATAT1	36,3	3,09	0,01871	3	Alpha-tubulin N-acetyltransferase 1
TRIP6	50,3	3,07	0,01140	2	Thyroid receptor-interacting protein 6
OTUD3	45,1	3,02	0,01918	2	OTU domain-containing protein 3
HSPA1B	70,1	3,01	0,00001	60	Heat shock 70 kDa protein 1B
TMEM70	29,0	2,99	0,00050	3	Transmembrane protein 70, mitochondrial
ECI1	30,9	2,90	0,03783	3	Enoyl-CoA delta isomerase 1, mitochondrial
RAVER1	77,9	2,83	0,04602	7	Ribonucleoprotein PTB-binding 1
ST13	41,3	2,83	0,00068	10	Hsc70-interacting protein
CEP44	44,1	2,82	0,04127	2	Centrosomal protein of 44 kDa

ATP5F1	28,9	2,80	0,00573	8	ATP synthase F(0) complex subunit B1, mitochondrial
MTMR9	63,5	2,79	0,04151	2	Myotubularin-related protein 9
HNRNPH3	35,2	2,73	0,02382	14	Heterogeneous nuclear ribonucleoprotein H3
UNG	34,6	2,61	0,00509	6	Uracil-DNA glycosylase
SIKE1	23,7	2,60	0,02927	3	Suppressor of IKBKE 1
KEAP1	69,7	2,55	0,03321	8	Kelch-like ECH-associated protein 1
TRADD	34,2	2,54	0,01093	3	Tumor necrosis factor receptor type 1-associated DEATH domain protein
AP4M1	50,0	2,53	0,04247	3	AP-4 complex subunit mu-1
MED18	23,7	2,50	0,03668	3	Mediator of RNA polymerase II transcription subunit 18
FASTKD2	74,5	2,43	0,04388	4	FAST kinase domain-containing protein 2
BAG5	51,2	2,41	0,03546	6	BAG family molecular chaperone regulator 5
ARL2	20,9	2,40	0,01863	3	ADP-ribosylation factor-like protein 2
FUBP3	61,6	2,37	0,00156	25	Far upstream element-binding protein 3
DDX3X	71,4	2,36	0,00065	33	ATP-dependent RNA helicase DDX3X
LYPLAL1	26,3	2,33	0,00958	5	Lysophospholipase-like protein 1
NDUFA13	16,7	2,33	0,01562	5	NADH dehydrogenase [ubiquinone] 1 alpha subcomplex subunit 13
CKMT1A	47,0	2,32	0,00085	4	Creatine kinase U-type, mitochondrial
BAG2	23,8	2,32	0,00004	8	BAG family molecular chaperone regulator 2
CCNB2	45,3	2,31	0,00507	11	G2/mitotic-specific cyclin-B2
MPC2	14,3	2,31	0,03262	2	Mitochondrial pyruvate carrier 2
DNAJA2	45,7	2,30	0,00749	5	DnaJ homolog subfamily A member 2
AURKA	45,8	2,29	0,04020	5	Aurora kinase A
CBFB	21,5	2,26	0,00149	4	Core-binding factor subunit beta
KTI12	38,6	2,23	0,00056	5	Protein KTI12 homolog

MSI1	39,1	2,22	0,00406	11	RNA-binding protein Musashi homolog 1
QTRTD1	46,7	2,21	0,02307	5	Queuine tRNA-ribosyltransferase subunit QTRTD1
PDLIM7	49,8	2,20	0,00012	7	PDZ and LIM domain protein 7
ASB3	49,6	2,18	0,01659	2	Ankyrin repeat and SOCS box protein 3
SMU1	57,5	2,18	0,00709	10	WD40 repeat-containing protein SMU1
MPST	33,2	2,18	0,02455	2	3-mercaptopyruvate sulfurtransferase
GOT2	47,5	2,17	0,01874	8	Aspartate aminotransferase, mitochondrial
DCP2	44,4	2,17	0,02005	4	m7GpppN-mRNA hydrolase
MEX3A	54,2	2,16	0,01441	4	RNA-binding protein MEX3A
SHMT2	53,5	2,15	0,00328	6	Serine hydroxymethyltransferase, mitochondrial
HAUS8	38,5	2,14	0,03892	4	HAUS augmin-like complex subunit 8
NDUFS2	51,9	2,13	0,00889	6	NADH dehydrogenase [ubiquinone] iron-sulfur protein 2, mitochondrial
STAU2	52,0	2,13	0,04749	12	Double-stranded RNA-binding protein Staufen homolog 2
CELF1	50,1	2,11	0,01488	7	CUGBP Elav-like family member 1
NDUFS3	30,2	2,11	0,01266	8	NADH dehydrogenase [ubiquinone] iron-sulfur protein 3, mitochondrial
MAP3K3	70,9	2,09	0,00088	4	Mitogen-activated protein kinase kinase kinase 3
PPP5C	56,9	2,07	0,02163	4	Serine/threonine-protein phosphatase 5
YTHDF1	60,9	2,06	0,00252	13	YTH domain-containing family protein 1
KLHL22	55,6	2,06	0,04627	9	Kelch-like protein 22
POP7	15,7	2,05	0,00085	2	Ribonuclease P protein subunit p20
RBM14	69,5	2,05	0,00276	23	RNA-binding protein 14
NOB1	46,7	2,05	0,01328	6	RNA-binding protein NOB1

HAX1	31,6	2,03	0,00132	6	HCLS1-associated protein X-1
MELK	71,2	2,03	0,02444	4	Maternal embryonic leucine zipper kinase
UBXN1	33,3	2,02	0,02197	8	UBX domain-containing protein 1

ANNEX 2

Annex 2: Resumen amplio de la tesis redactado en una lengua oficial de la Universitat de València.

Resumen

La enfermedad de Lafora es una rara enfermedad genética que afecta principalmente a los adolescentes y pertenece al grupo de enfermedades conocidas como Epilepsias Mioclónicas Progresivas (PME). Es una forma fatal de epilepsia mioclónica progresiva y tiene una incidencia de menos de 4 casos en un millón de personas en todo el mundo. La LD está causada por la acumulación de inclusiones aberrantes similares al glucógeno conocidas como cuerpos de Lafora (LBs), que están presentes en varios tejidos pero se encuentran predominantemente en el cerebro. Estos LB son insolubles y su agregación conduce a la toxicidad celular, generando varios síntomas neurológicos progresivos, que incluyen convulsiones de difícil control, mioclonías, ataxia, demencia y otros síntomas. Actualmente no existe una cura definitiva para la LD, y el tratamiento es principalmente sintomático y de apoyo, centrándose en controlar las convulsiones y manejar otros síntomas a medida que surgen. La enfermedad está causada por mutaciones localizadas en genes que codifican para dos proteínas diferentes: Laforina y Malina. Estas proteínas tienen diferentes funciones pero constituyen un complejo funcional.

Durante mi doctorado, los estudios se centraron especialmente en Malina, conocida por ser una ubiquitina ligasa E3 que desempeña un papel importante en un proceso llamado ubiquitinación. Por lo tanto, la actividad de Malina convierte la enfermedad de Lafora en una enfermedad relacionada con el sistema de ubiquitinación. Se han identificado varios sustratos de Malina hasta ahora, incluidos los implicados en la acumulación de poliglucosanos, deterioro en los procesos de degradación a nivel del proteasoma y autofagia, alteración de la transmisión glutamatérgica y disfunción mitocondrial. Sin embargo, muchos mecanismos moleculares que conducen a estas condiciones necesitan mayor aclaración. La búsqueda de nuevos sustratos podría ayudar a identificar

disfunciones de enfermedades no identificadas previamente y una mejor comprensión de las alteraciones fisiopatológicas anteriores. Un análisis proteómico utilizando la estrategia bioUb identificó 88 candidatos potenciales diferencialmente ubiquitinados involucrados en el plegamiento de proteínas, la respuesta al choque térmico y la regulación de la función mitocondrial. Se eligieron dos proteínas, P-Rex1 y Hsp90α, para su posterior estudio debido a su alta tasa de ubiquitinación y número de péptidos únicos en el análisis proteómico. En esta tesis, se han reportado evidencias que demuestran cómo el primer sustrato se relaciona con la enfermedad de Lafora. Se ha validado la ubiquitinación de P-Rex1 dependiente de Malina y hemos estudiado como esta modificación altera la actividad de P-Rex1 como factor intercambiador de nucleótidos de guanina (GEF) sobre la GTPasa Rac1 y en la toma de glucosa. El análisis realizado sobre este sustrato establece la génesis de una vía molecular que conduce a la alteración de la captación de glucosa, lo que podría ser uno de los orígenes de la acumulación de los poliglucosanos presentes en la enfermedad.

Los experimentos realizados para Hsp90α la han validado como sustrato de Malina y, asimismo, se ha hipotetizado cómo podría estar relacionada con la enfermedad.

Objetivos

Los objetivos de esta tesis se pueden resumir en los siguientes puntos.

1. Búsqueda y descubrimiento de posibles nuevos sustratos candidatos de Malina E3-ubiquitina ligasa mediante una técnica que explota su actividad de ubiquitinación.

2. Validar P-Rex1 como sustrato de Malina y delinear el efecto de su ubiquitinación.

3. Validar Hsp90 como sustrato de Malina y delinear el efecto de su ubiquitinación.

Metodología

Cultivos celulares de mamífero

Se utilizaron células de riñón embrionario humano (HEK293) (HPA Culture Collection #851820602) para experimentos de transfección. Las células se cultivaron en el medio Eagle modificado de Dulbecco (DMEM) (Lonza. Barcelona. España), suplementado con suero bovino fetal inactivado al 10% (FBS) (Invitrogen. Madrid. España), L-glutamina 1%, 100 unidades/ml de penicilina y 100 μg/ml de estreptomicina en atmósfera humidificada a 37°C y 5% (vol/vol) de CO_2.

Preparación de astrocitos primarios de ratón

Los ratones deficientes en Malina *(*Knockout *Epm2b*-/-) (Criado, Aguado et al. 2012) se obtuvieron sobre un fondo B6 puro cruzando más de 10 generaciones con los correspondientes ratones C57BL/6JRccHsd (WT) de los laboratorios Harlan. Los ratones se mantuvieron en las instalaciones del IBV-CSIC en un ciclo de 12 h luz/oscuridad con comida y agua *ad libitum*. Este estudio se ha realizado en estricta conformidad con las recomendaciones de la Guía para el cuidado y uso de animales de laboratorio del Consejo Superior de Investigaciones Científicas (CSIC) y aprobado por la Consellería de Agricultura, Medio Ambiente, Cambio Climático y Desarrollo Rural de la Generalitat Valenciana. Todos los procedimientos con ratones fueron aprobados por el comité de experimentación animal del Instituto de Biomedicina de Valencia-CSIC [Número de permiso: IBV-51, 2019/VSC/PEA/0271]. Se hicieron todos los esfuerzos para minimizar el sufrimiento de los animales. Se obtuvieron astrocitos primarios de ratón de ratones control y *Epm2b*-/- (Lahuerta, González et al. 2020) de ratones P0 a P1. Se diseccionaron la corteza cerebral y el hipocampo, se extirparon las meninges y se homogeneizaron los tejidos utilizando el kit de disociación de tejidos neurales y el disociador

GentleMACS de Mylteny Biotec (Madrid, España). La contaminación por microglía se eliminó utilizando microperlas CD11b en un campo magnético (Mylteny Biotec. Madrid, España). Las células se cultivaron en el medio Eagle modificado de Dulbecco (Lonza. barcelona. España) que contiene un 20% de FBS inactivado, suplementado con L-glutamina 1%, glucosa 7,5 mM, 100 unidades/ml de penicilina y 100 µg/ml de estreptomicina, en atmósfera humidificada a 37°C con un 5% de CO2. Después de 48 h, el FBS se redujo al 10%. Durante los siguientes 10 días, se añadieron dibutiril-cAMP 0,25 mM (dbcAMP) (D0627, Sigma-Aldrich) a los cultivos para favorecer la maduración de los astrocitos. Al final del proceso de maduración, los astrocitos primarios se cultivaron durante otras 48 h en ausencia de dbcAMP para evitar cualquier efecto no deseado derivado del compuesto (Magistretti, Manthorpe et al. 1983, Hertz, Peng et al. 1998, Muller, Fox et al. 2014).

Construcciones plásmidos

Los plasmidos pFLAG-Laforin, pECFP-Laforin, pEGFP-Malin y pFLAG-Malin se describen en la referencia (Sanchez-Martin, Romá-Mateo et al. 2015). El plásmido pFLAG-Malin P69A fue descrito en referencia (Couarch, Vernia et al. 2011). El Dr. Atanasio Pandiella (CIC-Salamanca) amablemente proporcionó el plásmido Myc-P-Rex1; el plásmido pCMV-6xHisUbiq fue generosamente proporcionado por el Dr. Manuel Rodríguez (Unidad de Proteómica. CIC-bioGUNE, Bizkaia, España) y los plásmidos pCMV-6xHis-Ubiq-K48R y pCMV-6xHis-Ubiq-K63R fueron un generoso regalo del Dr. Ch. Blattner (Instituto de Toxicología y Genética. Instituto de Tecnología de Karlsruhe, Karlsruhe, Alemania). El plásmido pCEFL-AU5-Rac1 fue proporcionado por el Dr. Jose Luis Zugaza (Achucarro Basque Center for Neuroscience. Leioa, Bizkaia, España). La proteína de fusión GST que contiene el dominio de unión Rac1 de PAK1 (GST-RBD-PAK1) se obtuvo como se describe en (Arrizabalaga, Lacerda et al. 2012). El plásmido pCAG-(bioUb)x6-BirA se describió en (Ramirez, Prieto et al. 2021). mCherry Hsp90α fue

comprado de Addgene (#108222). pEGFP-C1-Hsp90α fue clonado usando pEGFP-C1 y mCherry Hsp90α. pEGFP-C1-Hsp90α se clonó mediante la digestión de mCherry Hsp90α (*BamH1*) y se subclonó el fragmento que contenía la secuencia codificante de Hsp90α en el vector pEGFP-C1 (*BamH1*) comprado de Clontech (#6084-1).

Pulldown de biotina

Para el análisis de los sustratos de Malina diferencialmente ubiquitinados, aplicamos la estrategia bioUb descrita en trabajos anteriores (Lectez, Migotti et al. 2014, Ramirez, Martinez et al. 2015, Martinez, Lectez et al. 2017, Pirone, Xolalpa et al. 2017, Ramirez, Lectez et al. 2018, Elu, Osinalde et al. 2019, Ramirez, Morales et al. 2021). Brevemente, se sembraron 13,5 x 10^6 células en tres placas independientes de 150 mm para cada condición experimental (WT y Malin-P69A). Después de 48 h, las células se transfectaron con FLAG-Malin o FLAG-Malin P69A y el plásmido pCAG-(bioUb)x6-BirA (Franco, Seyfried et al. 2011, Elu, Lectez et al. 2020), una construcción que expresa un polipéptido precursor compuesto por seis secuencias biotinilables de ubiquitina, conjugadas con BirA, la enzima biotina ligasa de *E. coli*, utilizando el reactivo lipofectamina 3000 (Invitrogen. Madrid, España), siguiendo las instrucciones del fabricante, y complementado con una solución de biotina 50 µM. La construcción bioUb (bioUb-BirA) se digiere en las células por las enzimas deubiquitinasas endógenas (DUBs) que conducen a la liberación de BirA y bio-Ub. Luego, BirA reconoce la secuencia N-terminal específica de cada ubiquitina modificada y la biotinila, generando ubiquitinas marcadas con biotina. Las ubiquitinas marcadas con biotina se incorporan a la cascada del proceso de ubiquitinación para modificar las proteínas correspondientes (Fig. 10ª). Al día siguiente, se recolectaron las células y se lisaron con 2,5 ml de una solución que contenía urea 8 M, SDS 1 %, N-etilmaleimida 50 mM (Sigma-Aldrich) y un cóctel completo de inhibidores de la proteasa (Roche Diagnostics, Barcelona, España). Los lisados se pasaron a través de una aguja de 20G 10

veces y se aplicaron a una columna de desalinización PD10 (GE Healthcare. Barcelona, España), previamente equilibrado con 25 ml de urea 3 M, NaCl 1 M, SDS 0,25% y N-etilmaleimida 50 mM. Los eluidos recuperados se incubaron con 150 µl de suspensión de perlas de agarosa NeutrAvidin (Thermo Fisher Scientific, Waltham, MA. USA), y agitación suave durante 40 min a temperatura ambiente y 2 h a 4ºC. Posteriormente, las perlas se lavaron con las siguientes soluciones: dos veces con 8 M de urea y 0,25 % de SDS, tres veces con guanidina-HCl 6 M, una vez con urea 6,4 M, NaCl 1 M y SDS 0,2 %, tres veces con urea 4 M, NaCl 1 M, isopropanol 10 %, etanol 10 % y SDS 0,2 %, una vez más con urea 8 M y SDS 0,25 %, una vez con urea 8 M y SDS 1 %, y tres veces con SDS 2 %. Todas las soluciones fueron preparadas en PBS. El material ubiquitinado se eluyó con 80 µl de tampón de elución (Tris-HCl, pH 7,5 250 mM, glicerol 40%, SDS 4%, azul de bromofenol 0,2% y TDT 100 mM) hirviéndolas a 95ºC durante 5 min. Las muestras se sometieron a centrifugación final a 16.000 x g en una unidad de microcentrífuga PES Vivaclear Mini (Sartorius. Madrid, España) para descartar la resina NeutrAvidin utilizada. Se recuperó una cantidad similar de material ubiquitinado total en células transfectadas con FLAG-Malin o FLAG-Malin P69A (Fig. 10B).

Cromatografía líquida con espectrometría de masas en tándem (LC-MS/MS)

Las fracciones eluidas de los ensayos de pulldown de biotina se resolvieron mediante SDS-PAGE utilizando geles prefabricados Bolt Bis-Tris Plus al 4-12% (Invitrogen. Carlsbad. CA. USA) y se visualizaron con el reactivo GelCode Blue Stain siguiendo las instrucciones del fabricante (Thermo Fisher Scientific, Waltham, MA. Estados Unidos). Después de la exclusión de los monómeros y dímeros de avidina, cada carril se cortó en cuatro rodajas y se sometió a una digestión en gel como se describió anteriormente (Osinalde, Sanchez-Quiles et al. 2015, Ramirez, Prieto et al. 2021).

Los análisis espectrométricos de masas se realizaron en un sistema de cromatografía líquida EASY-nLC 1200 interconectado a través de una fuente de iones flex de nanospray con Q Exactive HF-X (Thermo Fisher Scientific. Waltham, Estados Unidos). Los péptidos se cargaron en una precolumna Acclaim PepMap100 (75 mm × 2 cm. Thermo Fisher Scientific. Waltham, USA) conectada a una columna analítica Acclaim PepMap RSLC (50 mm × 25 cm Thermo Fisher Scientific. Waltham, USA). Los péptidos se eluyeron de las columnas utilizando un gradiente de dos pasos de 2,4 a 24% (90 min) y 24 a 32% (2 min) de acetonitrilo en ácido fórmico 0,1% a una velocidad de flujo de 300 nL min−1 durante 92 min. Se adquirieron escaneos completos de MS de m/z 375 a 1850 con una resolución de 60.000 a m/z 200. Los 10 iones más intensos se fragmentaron por disociación de colisión de alta energía (HCD) con una energía de colisión normalizada de 28 y se registraron espectros MS/MS con una resolución de 15.000 a m/z 200. El tiempo máximo de inyección fue de 50 ms para el estudio y de 100 ms para las exploraciones MS/MS, mientras que los valores objetivo AGC de 3 × 106 y 1 × 105 se utilizaron para el estudio y las exploraciones MS/MS, respectivamente. Para evitar la secuenciación repetida de péptidos, se aplicó la exclusión dinámica durante 20 s. Los iones cargados individualmente o los iones con estados de carga no asignados también se excluyeron de MS/MS. Los datos se adquirieron utilizando el software Xcalibur (Thermo Fisher Scientific. Waltham, Estados Unidos).

Procesamiento de datos y análisis bioinformático

Los archivos de datos brutos adquiridos se procesaron con el software MaxQuant (Cox y Mann 2008) (versiones 1.5.3.17 y 1.6.0.16) utilizando el motor de búsqueda interno Andromeda y se buscaron en la base de datos UniProtKB restringida a *Homo sapiens* (20,187 entradas), como se describe en (Ramirez, Prieto et al. 2021). Se combinaron los espectros originados a partir de los diferentes cortes correspondientes a la misma muestra biológica. La carbamidometilación © se estableció como modificación fija, mientras que la

oxidación de Met, la acetilación de proteína N-terminal y Lys GlyGly (no C-term) se definieron como modificaciones variables. La tolerancia de masa se estableció en 8 y 20 ppm a nivel de MS y MS/MS, respectivamente; excepto en el análisis de los datos TOF para los cuales se utilizaron los valores de 0,006 Da y 40 ppm, respectivamente. La especificidad enzimática se estableció en base a tripsina, lo que permite la escisión N-terminal a Pro y entre Asp y Pro con un máximo de dos escisiones perdidas. La opción de coincidencia entre carreras se habilitó con una ventana de tiempo de coincidencia de 1,5 minutos y una ventana de alineación de 20 minutos para hacer coincidir la identificación entre las muestras. La longitud mínima del péptido se estableció en siete aminoácidos. La tasa de falsos descubrimientos de péptidos y proteínas se fijó en el 1%. Las intensidades normalizadas de cuantificación espectral sin marcado de proteínas (LFQ) se calcularon utilizando el algoritmo MaxLFQ. Para aclarar aún más, se utilizaron los siguientes parámetros predeterminados de MaxQuant: Modo señuelo, revertir; PSM FDR, 0,01; Proteína FDR, 0,01; Sitio FDR, 0.01. Los datos de salida de MaxQuant se analizaron con el software Perseus (versión 1.6.0.7) (Tyanova, Temu et al. 2016), y las diferencias estadísticamente significativas en la abundancia de proteínas se determinaron mediante una prueba t de Student de dos colas.

Análisis de ubiquitinación de proteínas

El método descrito en (Kaiser y Tagwerker 2005) se utilizó para estudiar la ubiquitinación de P-Rex1. Para ello, se transfectaron células HEK293 con los plásmidos indicados en cada experimento utilizando el reactivo de transfección X-treme GENE HP según el protocolo del fabricante (Roche Diagnostics, Barcelona, España). Después de 24-36 h de transfección, las células se lisaron utilizando una aguja de calibre 25G en tampón A (guanidinio-HCl 6 M, fosfato de sodio 0,1 M, Tris-HCl pH 8,0 0,1 M) para inhibir la acción de las deubiquitinasas endógenas. los extractos proteicos se clarificaron después de la centrifugación (12.000 × g 15 min) y la concentración de proteínas se

midió mediante la técnica de Bradford. Se incubaron 1,5 mg de proteína con 150 µl de resina de cobalto TALON (Clontech. Barcelona. España) equilibrado en tampón B que contiene imidazol 10 mM, guanidinio-HCl 6 M, fosfato de sodio 0,1 M, Tris-HCl pH 8,0 0,1 M. Para purificar las proteínas marcadas con His, la incubación se llevó a cabo durante 2 h a temperatura ambiente en una plataforma oscilante. Luego, la resina se lavó con 1 mL de tampón B y cuatro veces con tampón C (tampón B, pero con 8 M de urea en lugar de 6 M de guanidinio-HCl). Las proteínas unidas se hirvieron a 95 °C durante 5 min en 50 µl de tampón de muestra de 2×Laemmli y se analizaron mediante Western blot utilizando los anticuerpos apropiados. Para determinar la topología de las cadenas de ubiquitina, cuando se indicó, se utilizaron plásmidos pCMV-6xHis-Ubiq-K48R y pCMV-6xHis-Ubiq-K63R en el ensayo en lugar de pCMV-6xHis-Ubiq tipo WT.

Análisis GFP-trap de interacciones proteína-proteína

Las células HEK293 se transfectaron con las construcciones específicas de Laforin, Malin y la proteína de interés. Las células se lavaron dos veces con solución salina tamponada con fosfato frío (PBS) y se rasparon en hielo en tampón de lisis [10 mM Tris-HCl pH 7.5, 150 mM NaCl, 0.5 mM EDTA, 0.5% (v/v) Nonidet P-40, cóctel completo de inhibidores de proteasa (Roche Diagnostics. Barcelona. España), 1 mM PMSF, 2,5 mM NaF, 0,5 mM NaVO4 y 2,5 mM Na4P2O7]. Los lisados se recogieron en un tubo de Eppendorf y la lisis adicional se realizó con una aguja de calibre 25G. Los lisados celulares se centrifugaron a 13.000 × g durante 10 min a 4°C. Los sobrenadantes (1,5 mg de proteína total, medidos mediante la técnica de Bradford) se incubaron con perlas GFP-trap de Chromotek (Chromotek, Planegg-Martinsried, Alemania) durante 30 min en una plataforma oscilante a 4 °C. Las perlas se lavaron dos veces con 1 ml de tampón de lisis y una vez con el tampón de lisis que contenía 300 mM de NaCl. Las proteínas unidas se hirvieron a 95°C durante 5 min en 30 µl de tampón de muestra de 2×Laemmli. Las proteínas fusionadas con GFP y CFP se

analizaron mediante inmunotransferencia utilizando anticuerpos específicos. Como control negativo, se utilizó un constructo que expresa proteínas CFP o GFP (plásmido pECFP-N1 y pEGFP-N1, respectivamente), para confirmar la especificidad de la interacción.

Análisis de Western blot

30 µg de proteína total de la fracción soluble de lisados celulares fueron analizados por SDS-PAGE y las proteínas fueron transferidas a membranas de PVDF (Millipore. Madrid. España). Las membranas se bloquearon con leche descremada al 5% (p/v) en tampón Tween20 salino tamponado con Tris [TBS-T: 50 mM Tris-HCl pH 7.4, 150 mM NaCl, 0.1% (v/v) Tween20] durante 1 h a temperatura ambiente y se incubaron durante la noche a 4°C con los anticuerpos primarios correspondientes: conejo anti-P-Rex1 (13168. Cell Signaling Technology, Barcelona, España), ratón anti-P-Rex1 (ab264535. Abcam, Madrid, España), ratón anti-Flag (F3165. Sigma-Aldrich, Madrid, España), conejo anti-GFP (210-PS-1GFP. Inmunokontackt, Madrid, España), ratón anti-Rac1 (05-389. Merck; Madrid, España), conejo anti-Pygm (ab81901. Abcam. Madrid, España), conejo anti-Pygb (ab154969. Abcam. Madrid, España), conejo anti-GLUT1 (PA1-46152. Invitrogen. Madrid, España), anticuerpo anti-biotina-HRP-conjugado de cabra (#7075. Cell Signaling Technology, Barcelona, España), ratón anti-Na+/K+-ATPasa (ab7671. Abcam. Madrid, España), conejo anti-Hsp90 (4874. Cell Signaling Technology, Barcelona, España), ratón anti-Hsp90α (ab79849. Abcam, Madrid, España), y ratón anti-Hsp90β (ab53497. Abcam, Madrid, España). Los anticuerpos ratón anti-Gapdh (sc-32233. Santa Cruz Biotechnologies, Madrid, España), ratón anti-Tubulina (T6199. Sigma-Aldrich, Madrid, España), y conejo anti-Actina (A2066. Sigma-Aldrich, Madrid, España), se utilizaron como controles de carga. Después del lavado, las membranas se incubaron con los correspondientes anticuerpos secundarios conjugados con HRP a temperatura ambiente. Las señales se visualizaron utilizando Lumi-Light Western Blotting Substrate (Roche Applied Science.

Barcelona. España) o ECL Prime Western Blotting Detection Reagent (GE Healthcare. Barcelona. España) y se analizaron por quimioluminiscencia utilizando el lector de imágenes FujiLAS400 (GE Healthcare, Barcelona, España). La cuantificación de las bandas de proteínas se llevó a cabo utilizando el software image Studio versión 5.2 (LI-COR Biosciences, Alemania).

Análisis de la tasa de degradación de P-Rex1

Los astrocitos primarios de ratón de *Epm2b-/-* y ratones control fueron tratados con cicloheximida 70 μM (CHX; Sigma-Aldrich, Madrid, España) para los tiempos indicados (de 0 a 24 h). Las células se lisaron en tampón de lisis [10 mM Tris pH 7.6, 150 mM NaCl, 1% Nonidet P-40, 10 mM $MgCl_2$, 1mM PMSF, cóctel completo de inhibidores de proteasa (Roche Diagnostics. Barcelona. España)], utilizando una aguja de calibre 25G. Los lisados celulares se centrifugaron a 13.500 rpm durante 10 min a 4°C. 25 μg de extractos celulares (medidos por la técnica de Bradford) se analizaron mediante Western blot utilizando anticuerpos anti-P-Rex1. Los mismos extractos se analizaron utilizando anticuerpos anti-Tubulina como control de carga.

Ensayo de activación Rac1

El ensayo pulldown Rac1 se realizó utilizando la proteína de fusión GST-RBD-PAK1 descrita anteriormente. 50 μg de esta proteína de fusión se acoplaron a perlas de glutatión-sefarosa durante 1 h a 4°C. Las células HEK293 se transfectaron el día anterior con los plásmidos indicados en el experimento. Las células HEK293 se lisaron en tampón de lisis [10 mM Tris-HCl pH 7.6; 150 mM NaCl, 1% Nonidet P-40, 10 mM $MgCl_2$, 1mM PMSF y cóctel completo de inhibidores de proteasa (Roche Diagnostics. Barcelona. España)] utilizando una aguja de calibre 25G. Los lisados celulares se centrifugaron a 13.500 rpm durante 10 min a 4°C, y posteriormente, 1 mg de extractos de proteínas (medidos por la técnica de Bradford) se incubaron durante 1 h a 4°C con las perlas de glutatión-sefarosa previamente lavadas con tampón de lisis tres veces

para eliminar el exceso de proteína GST-RBD-PAK1. Las proteínas unidas a las perlas se lavaron tres veces, se resuspendieron en el tampón de muestra de 2×Laemmli y se analizaron mediante Western blot utilizando los anticuerpos apropiados.

Análisis de la captación de glucosa

La captación de glucosa se realizó en astrocitos control y *Epm2b-/-* siguiendo el procedimiento técnico descrito en el manual del ensayo de captación de glucosa-Glo™ (Promega #J1341. Manual técnico TM467). Se colocaron 30.000 células/pocillo en 100 µL de medio de cultivo en placas de 96 pocillos. La maduración de las células con dbcAMP se realizó en el mismo soporte durante 10 días. Cuando se indica, las células fueron tratadas durante 24 h con clorhidrato de 1,1-dimetilbiguanida 2 µM (metformina) (D150959, Sigma-Aldrich, Madrid, España) antes del ensayo. El día del ensayo, se retiraron los medios y las células se lavaron con 1xPBS (BE17516Q, Lonza, Madrid, España) dos veces. Se añadieron 50 µL de 2-desoxiglucosa (2-DG, concentración final del ensayo de 1 mM) a cada pocillo durante 10 min a temperatura ambiente. El ensayo se terminó con la adición de 25 µL de tampón de parada, mezclado brevemente en un agitador orbital, y neutralizado con 25 µL de tampón de neutralización. Finalmente, se agregaron 100 µL de reactivo de detección de 2-desoxiglucosa 6-fosfato (2DG6P) a cada pocillo, se mezclaron brevemente en un agitador orbital y se incubaron durante 1 h a temperatura ambiente. Los valores de luminiscencia se midieron con un lector de microplacas Tecan Spark. La captación de glucosa también se realizó en células en las que la expresión de P-Rex1 se silenció utilizando un siRNA P-Rex1 de ratón ON-TARGETplus (Dharmacon/Horizon Discovery Ltd. Madrid, España). Los astrocitos primarios de ratón se transfectaron con siRNAs SMARTpool P-Rex1 20 nM, o con siRNA control, utilizando Lipofectamine RNAiMAX (Thermo Fisher Scientific; Madrid, España), durante 48 h antes del ensayo de captación de glucosa.

Los siRNAs de SMARTpool de P-Rex1 incluyen:
siRNA J-053658-09 Secuencia objetivo: GGUCAUUAUUUCCGUGUUA
siRNA J-053658-10 Secuencia objetivo: GCACCAGCGUGGCGAAUGA
siRNA J-053658-11 Secuencia objetivo: GCUUCAAGGUGUCGGAGGA
siRNA J-053658-12 Secuencia objetivo: GUGAGAUCCAGGACGCAUA

Análisis de proteínas de la superficie celular por biotinilación

La biotinilación de la superficie celular en astrocitos primarios de ratón se realizó con el kit de aislamiento de proteínas de superficie celular de Pierce (89881. Thermo Fisher Scientific, Madrid, España), según protocolo del fabricante. Brevemente, se cultivaron $4x10^6$ células en matraces T75. La maduración de las células con dbcAMP se realizó en el mismo soporte durante 10 días y después se cultivaron durante 48 h en medios sin dbcAMP. El día del ensayo, las células se lavaron con PBS y se incubaron con EZ-LINK Sulfo-NHS-SS-biotina durante 1 h a 4 ° C, seguido de la adición de una solución de bloqueo. Las células se lisaron con el tampón de lisis (500 µL) proporcionado por el kit. Se guardó una alícuota (100 µL) del lisado para Western blot (fracción total). La fracción biotinilada se aisló con perlas NeutrAvidina, se eluyó con el tampón de muestra (400 µL) que contenía DTT, y se sometió a análisis de Western blot. Se utilizaron anticuerpos apropiados para detectar las proteínas biotiniladas a nivel de la membrana plasmática.

Preparación de muestras de hipocampo y corteza a partir de modelos de ratón LD.

Las muestras de hipocampo y corteza provenientes del cerebro de ratones se lisaron por separado en tampón RIPA [50 mM Tris-HCl, pH 8; 150 mM NaCl; 0.5% desoxicolato de sodio; 0.1% SDS; 1% Nonidet P40; 1 mM PMSF; y cóctel completo de inhibidores de proteasa (Roche, Barcelona,

España)] durante 30 min a 4 ºC con agitación ocasional. Los lisados se pasaron diez veces a través de una aguja de calibre 25G en una jeringa de 1 ml y se centrifugaron a 13.000 x g durante 15 min a 4 ºC. Se recogieron los sobrenadantes y un total de 30 µg de proteína, medidos mediante Micro BCA Protein Assay Kit (Thermo Scientific™ 23235), se resuspendieron en el tampón de muestra de 2×Laemmli, y fueron analizadas por Western blot utilizando los anticuerpos apropiados.

Análisis estadístico

Los resultados se muestran como medias +/- error estándar de la media (SEM) de al menos tres experimentos independientes. Las diferencias entre las muestras se analizaron mediante pruebas t de Student de dos colas no pareadas utilizando el software estadístico Graph Pad Prism versión 5.0 (La Jolla, USA). Los valores de p se han considerado significativos como *p<0,05, **p<0,01.

Conclusiones:

1. Se han identificado 88 sustratos candidatos diferencialmente ubiquitinados por malina mediante el uso de la estrategia bioUb.

2. Entre ellos, P-Rex1 se valida como un sustrato genuino de Malina.

3. Se sabe que P-Rex1 es un factor de intercambio de nucleótidos de guanina (GEF) de Rac1 que cambia su estado inactivo a uno activo. El complejo Laforina-Malina puede regular negativamente la actividad de P-Rex1 como GEF a través de su ubiquitinación.

4. Los astrocitos *Epm2b-/-* muestran una disminución en la tasa de degradación de P-Rex1 en comparación con los astrocitos silvestres, lo que sugiere un papel negativo de Malina en la estabilidad de P-Rex1.

5. Los astrocitos *Epm2b-/-* muestran un aumento en la captación de glucosa en comparación con los astrocitos silvestres. Este efecto está relacionado con la acción de P-Rex1.

6. El aumento en la captación de glucosa es causado por un aumento en la actividad de GLUT1 en lugar de un aumento en la cantidad de transportadores en la membrana plasmática.

7. Hsp90α y Hsp90β son sustratos genuinos de Malina.

8. Hsp90α interactúa con Malina pero no con Laforina.

9. En ausencia de Malina, no hay un cambio en la estabilidad de Hsp90α

ANNEX 3

Annex 3: Relación de publicaciones asociadas a la Tesis

TRIM32 and Malin in Neurological and Neuromuscular Rare Diseases.
Kumarasinghe L, Xiong L, Garcia-Gimeno MA, Lazzari E, Sanz P, Meroni G. Cells. 2021 Apr 6;10(4):820. doi: 10.3390/cells10040820. PMID:33917450

P-Rex1 is a novel substrate of the E3 ubiquitin ligase Malin associated with Lafora disease.
Kumarasinghe L, Garcia-Gimeno MA, Ramirez J, Mayor U, Zugaza JL, Sanz P. Neurobiol Dis. 2023 Feb;177:105998. doi: 10.1016/j.nbd.2023.105998. Epub 2023 Jan 10. PMID:36638890

Deciphering the Polyglucosan Accumulation Present in Lafora Disease Using an Astrocytic Cellular Model.
Moreno-Estellés M, Campos-Rodríguez Á, Rubio-Villena C, **Kumarasinghe L**, Garcia-Gimeno MA, Sanz P. Int J Mol Sci. 2023 Mar 23;24(7):6020. doi: 10.3390/ijms24076020. PMID:37046993